Equilibration Dynamics of Non-equilibrium Crystalline Systems

By

AMAL GIRI

PHYS04200904016

Variable Energy Cyclotron Centre

A thesis submitted to the

Board of Studies in Physical Sciences

In partial fulfillment of requirements
For the Degree of
DOCTOR OF PHILOSOPHY
of
HOMI BHABHA NATIONAL INSTITUTE

October, 2015

Homi Bhabha National Institute

Recommendations of the Viva Voce Board

As members of the Viva Voce Board, we certify that we have read the dissertation prepared by Amal Giri entitled **"Equilibration Dynamics of Non-equilibrium Crystalline Systems"** and recommend that it may be accepted as fulfilling the dissertation requirement for the Degree of Doctor of Philosophy.

Alok Chakrabarti Date: 14-10-2015

Chairman - Dr. Alok Chakrabarti

P. Barat Date: 14/10/2015

Guide/Convener - Dr. Parthasarathi Barat

Gayathri N. Date: 14/10/2015

Member 1 - Dr. Gayathri N. Banerjee

Date: 14/10/2015

Member 2 - Dr. Sangam Banerjee

P. Mandal Date: 14.10.15

Member 3 - Dr. Prabhat Mandal

S. Tarafdar Date: 14.10.2015

Dr. Sujata Tarafdar(External Examiner)

Final approval and acceptance of this dissertation is contingent upon the candidate's submission of the final copies of the dissertation to HBNI.

I hereby certify that I have read this dissertation prepared under my direction and recommend that it may be accepted as fulfilling the dissertation requirement.

Date: 14/10/2015

Place: VECC, Kolkata

P. Barat.

Guide

STATEMENT BY AUTHOR

This dissertation has been submitted in partial fulfillment of requirements for an advanced degree at Homi Bhabha National Institute (HBNI) and is deposited in the Library to be made available to borrowers under rules of the HBNI.

Brief quotations from this dissertation are allowable without special permission, provided that accurate acknowledgement of source is made. Requests for permission for extended quotation from or reproduction of this manuscript in whole or in part may be granted by the Competent Authority of HBNI when in his or her judgment the proposed use of the material is in the interests of scholarship. In all other instances, however, permission must be obtained from the author.

Date: 19·10·2015

Amal Giri

Amal Giri

DECLARATION

I, hereby declare that the investigation presented in the thesis has been carried out by me. The work is original and has not been submitted earlier as a whole or in part for a degree / diploma at this or any other Institution / University.

Amal Giri

Date: 19.10.2015

Amal Giri

DEDICATIONS

****

Dedicated to

My Parents and Siblings

****

ACKNOWLEDGEMENTS

This thesis would have not been possible without the help of so many individuals. I am privileged and lucky enough to come in the proximity of a lots of wonderful well wishers. The item 'Acknowledgment' would not be enough scope to acknowledge all of their help, support and wishes.

First of all, I am grateful to my mentor Dr. Parthasarathi Barat for his sincere guidance during the last four years of my doctoral tenure. His advice, teaching, approaches to deal with different branches of physics, interest in mathematics and punctuality not only helped me to accomplished my doctoral work but also will be the provision of my future academic and social life.

I thank all the members of material science section and physics group for their academic and technical support. I convey my regards to all teachers of Predoctoral course(2009-2010) what made my basic concepts of physics more stronger.

I am also grateful the Director Dr. D. K. Srivasatava and the technical and administrative authority of our institute, Variable Energy Cyclotron Centre, who have always extended their helping hand when I needed any sort of academic, technical and administrative assistance.

I convey my deep sense of gratitude to all the teachers of earlier days starting right from the dawn of my academic life. Especially, I offer my oblation to my higher secondary(class XI and XII) teacher Mr. Basudeb Paria of Banamali Chatta High School, Purba Medinipur, for his continuous inspirational talks and invaluable advices and to Dr. Subhash Chandra Samanta, former reader of Department of Physics, Midnapore College, for his assistances during my postgraduate days.

My doctoral batch mates Abhishek(Mishra), Subhash(Singha), Trambak(Bhattacharyya),

(Md)Nasim, Sukanya(Mitra) and Surasree(Mazumder) were fantastic through out the entire tenure. Thanks pals. My special thanks to my special friend Santu(Dey). Thanks to my seniors and juniors in VECC with whom I have spent quality time with academic and nonacademic discussions inside and outside the VECC campus.

Hearty thanks to my earlier friends Sushubhra(Das), Monalisa(Maity), shreyam(Jana), Rajsekhar (Manna) who were with me during my graduate and postgraduate days and shared my ups and downs alongside me.

I don't have words to express my gratitude and regards to my beloved parents and elder siblings to acknowledge their unconditional affection, faith, care and support. Undoubtedly I am indebted most to you people.

(Amal Giri)

Publications

a. Published:

In journals:

1. Universal Scaling property of system approaching equilibrium.

P. Barat, A. Giri, M. Bhattacharya, Nilangshu K. Das and A. Dutta, **Europhys. Lett., 104**(2013) 50003.

2. Oscillatory Shannon Entropy in the Process of Equilibration of Non-equilibrium systems.

A. Giri, Nilangshu K. Das,and P. Barat, **Chinese Physics B, 24** (2015) 088902.

In conference/ symposium proceedings:

1. Study of dislocation climb at nanovoids in bcc metal.

M. Bhattacharya, A. Dutta, A. Giri, N. Gayathri and P. Barat, **Conference: TMS Annual Meeting & Exhibition 2012, Volume: 2**

b. Communicated:

1. Modality of Equilibration in Non-equilibrium Systems.

P. Barat, A. Giri, Nilangshu K. Das, M. Bhattacharya and A. Dutta, arXiv: 1403.3237.

2. Effect of Temperature on the Complexity of Solid Argon System.

A. Giri, S. Dey, and P. Barat, arXiv:1409.2761.

3. Nature of the force that is responsible for the equilibration in non-equilibrium system (in preparation).

Homi Bhabha National Institute

SYNOPSIS OF Ph.D. THESIS

1.	**Name of the Student**:	Amal Giri
2.	**Name of the Constituent Institution:**	Variable Energy Cyclotron Centre
3.	**Enrolment No.:**	PHYS04200904016
4.	**Title of the Thesis:**	Equilibration Dynamics of Non-equilibrium Crystalline Systems
5.	**Board of Studies:**	Physical Sciences

SYNOPSIS

The non-uniqueness and ubiquity nature of non-equilibrium systems let an enormous scope for the researchers. Most of the systems we encounter and deal with in our practical life are non-equilibrium systems. A non-equilibrium system left of its own without any external perturbation, always tries to reach its stable equilibrium state. At equilibrium the system makes sure that the energy distribution among its constituents leads to maximum number of microstates. Equilibrium macrostate offers highest liberty to its constituents as per as their distribution among themselves at different energy eigen states is concerned [1]. Thus, the increasing freedom of the constituents in energy space propels the non-equilibrium system towards equilibrium macrostate and consequently makes the equilibrium state as the most probable macrostate. At equilibrium the highest probable macrostate remains unaffected over the time and hence the associated thermodynamic properties of equilibrium system are constant quantities of time. This idea enable us to represent a thermodynamically equilibrium state in terms of its uniquely defined thermodynamic parameters. Thus equilibrium physics is uniquely defined and can be handled relatively elegant way compared to its counterpart, the non-equilibrium physics. Comprehensive and rigorous experimental arrangements are required to maintain the equilibrium state of a system by isolating it from the environment. Similarly an isolated non-equilibrium state of a system cannot retain a particular non-equilibrium state without any experimental provision because of its continuous evolution towards the most probable macrostate. Thus equilibration should only be the path of an isolated non-equilibrium system.

Most of the works on non-equilibrium physics are primarily based on linear response theory [2]. In linear response regime the system is little away from its equilibrium state i.e. the applied perturbation on the system is very small and the system response is proportional to the perturbation. The governing physics in linear response regime are same as those in regression of microscopic spontaneous fluctuations in an equilibrium system [3, 4]. No generalized theoretical framework exists to calculate macroscopic thermodynamic properties of a system when it is far from equilibrium. In the last two decades, exact relations have been established relating thermodynamic parameters for systems irrespective of how far they are driven out of equilibrium. These studies are related to the path probabilities of the individual constituents of the non-equilibrium system [5]. Collective behavior of the constituents of non-equilibrium systems is poorly understood. In this context the studies of this thesis are focused on the dynamics of the equilibration process of a non-equilibrium system which is far away from equilibrium. A non-equilibrium system which is undergoing equilibration each and every constituent of the system participates in the equilibration process and their collective dynamics is responsible for the attainment of equilibrium distribution. Thus, the single particle dynamics and their collective behavior are complementary to each other to understand the equilibration process of a non-equilibrium system. As a whole the system dynamics and as well as the particle dynamics, during the process of equilibration, are studied in the scope of this work. Experimental methods deal with mere time average values of macroscopic properties. Analytical methods are not able to solve the equation of motion of the individual particles since they are connected with large number of particles in non-linear fashion. Like experiments analytic methods provides only the time average values of macroscopic quantities. This drawback of experiment and analytical methods can be solved by the use of molecular dynamics simulation technique. Molecular dynamics deals in the atomic level of the system under study in the time scale of the order of femtosecond. Thus molecular dynamics simulation technique is a useful tool for the study of individual particle dynamics of the system and in my entire study I have used this technique to generate non-equilibrium system which is far away from equilibrium. This thesis has the scope to discuss on the equilibration process of non-equilibrium systems of most possible simplest ensemble, the NVE ensemble (having constant number of constituents, constant volume of the system, and constant energy of the system) which does not interact with any source or sink to exchange any constituent particle or energy with them. The non-equilibrium systems taken for the analysis are composed of different crystalline materials having different crystalline structures (Si, Ge, solid Argon, Fe, Mo, Al and Cu) and they follow variety of potential functions in order to maintain the stability of their respective crystalline structures. In my entire study the adopted non-equilibrium systems are generated by making average kinetic energy and average potential energy of the system unequal. Each of these NVE systems has an identical environment in all the three directions of the simulation cell and it is maintained with the use of periodic boundary condition.

Atoms in the simulation cell, when brought to a non-equilibrium state by enhancing their kinetic energy, try to redistribute their excess kinetic energy by the process of diffusion. This process of redistribution of kinetic energy among the atoms changes their mean positions of vibration and consequently their potential energy. Here all the atoms in the cell participate together in the diffusion process. Thus by analyzing the variation of the kinetic energy with time for a single atom in the simulation cell one can account for the modality of this diffusion process and the nature of the equilibration. The time variations of the kinetic energy with time for each atom are found to be random since it is associated to the diffusion process. Whether there exist any self similarity property in this random time series data and whether the time series data is associated with a universality class, the answers of all these queries can be made by scaling analysis of the time series data. The scaling property of the time series of kinetic energy of individual particles are studied using two complementary scaling analysis methods: Diffusion Entropy Analysis (DEA) and Finite Variance Scaling Method (FVSM) [6, 7]. Application of these scaling analyses reveals that the fluctuations in the time series of kinetic energy follow similar kind of dynamics irrespective structures and non-equilibrium temperatures of the systems under study. Several crystal structures diamond cubic, face centered cubic and body centered cubic structure with suitable potential functions were used. The results of the scaling analyses conform that for all cases the time series of the kinetic energy of system particles exhibits an anomalous diffusion and it belongs to Levy walk process [8, 9]. In Levy walk a time series has a probability distribution function having a long tail. Most of the natural phenomena like food foraging in hungry animals, spreading of vector mediated disease in animals and human are examples of Levy walk with few but effective long hops. Thus the time series of kinetic energy of non-equilibrium system particles confirms the existence of a universality class.

Probability distribution function is the global representation of a system. Evolution of the probability distribution function of kinetic energy of the constituent atoms of the equilibrating system is oscillatory and subsequently the oscillation dies down after a long time(Fig. 1). Shannon entropy [10] is a measure of uncertainty or unpredictability of information contained in a probability distribution. The time variation of global information of the equilibrating system are studied by calculating the Shannon entropy from their time evolution of probability

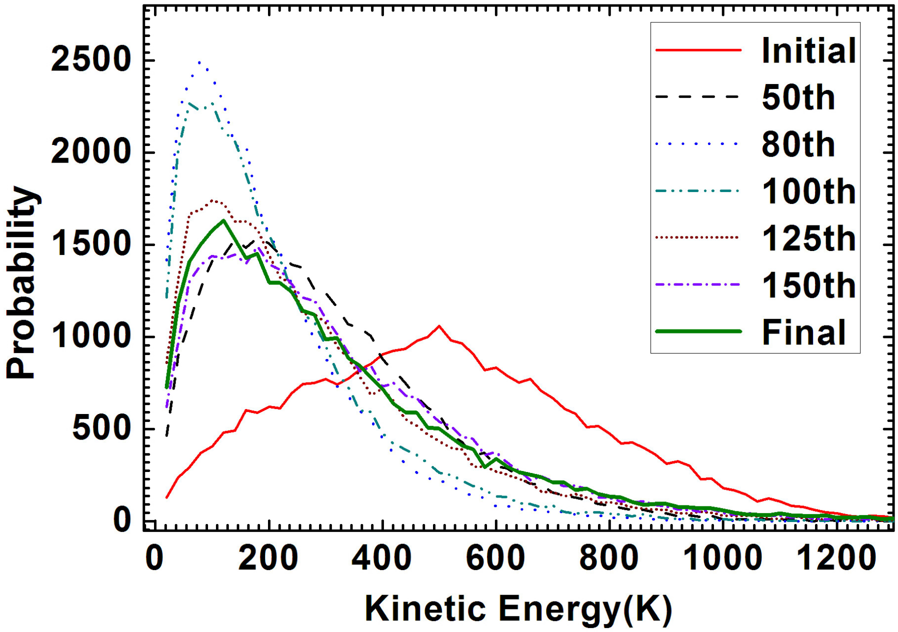

Figure 1: Probability distributions of kinetic energy of the Cu atoms equilibrated from non-equilibrium temperature 500K. Each time step is of 0.5fs and the total simulation time is 1.5 ps.

distribution. For more random information the uncertainty in its prediction is higher and the corresponding value of Shannon entropy will be more. In case of tossing coin or rolling n-sided die outcomes lead to maximum Shannon entropy given that that the coin or the die is fair. For unfair coin or die predictability of the outcomes becomes easy and value of Shannon entropy drops down. For a two headed/tailed coin or for a die with all the sides identical the outcomes become completely predictable and the entropy goes to zero. For a physical equilibrium/non-equilibrium system the distribution of constituent particles among energy eigen states is not as simple as the outcomes of tossing coin or rolling die. Except the combinations among particles occurrence of the energy eigen states follow some restriction in this case. Unlike the situation for fair coin or fair die where the all the outcomes are equally probable the equilibrium physical system does not generate a probability distribution with equal population in each energy eigen state. Thus the variation of Shannon entropy for completely unfair and partially unfair coin/die should be monotonically increasing and ultimately reaches a constant maximum value for fair coin/die. On the other hand due to adopted non-equilibrium nature of the system where the system kinetic energy and the system potential energy are not equal, in the initial phase of equilibration there will be transfer of kinetic energy into potential energy by changing the configuration of constituent atoms. Since this process is very fast the system cannot estimate exactly how much kinetic energy should be transferred into potential energy to make them equal. The inertia of the process transfers more kinetic energy and a reverse situation appears with potential energy more than the kinetic energy. This mechanism leads to an oscillatory transfer of energy during equilibration and the oscillation gradually dies down with time [11]. Such variation of energy and restriction in the energy states do not allow the Shannon entropy to follow monotonic increasing behavior but is oscillatory and at equilibrium it becomes constant of time.

The force field in crystalline system is the sum of deterministic part due to nearer atoms and random part due to distant atoms. The affects of these two parts of the force are reflected on the probability distribution function. The random part of the force introduces a noise component to the system response. Hence in the study of equilibration mechanism from the time variation of probability distribution function it is desirable to eliminate the noise part. Use of principal component analysis helps to eliminate the noise part and reduces the histograms of probability distribution functions into 2-3 principal dimensions and it becomes easier to study the evolution of probability distribution function in terms of those two or three components. The component which has highest egien value is most important (more than 75% of total eigen value except for solid Argon where it is around 60%) and is used for the analysis. The existence of 2-3 major eigen values ensure that the probability distribution functions are highly correlated. A statistical method called system identification technique [12] is used to analyze the evolution of most significant component. This method relates the system input and output by a rational function called transfer function. The analysis reveals that the dynamical process of equilibration takes place through two or three modes and the mode associated to lowest frequency which is very close to Debye frequency of the corresponding element [13, 14, 15]. These modes are calculated from the denominator of the transfer function of the system obtained from the system identification.

Another important aspect of non-equilibrium system is simultaneous impact of deterministic and random force together on the process of equilibration. I have tried to sort out in which region the total force field is most responsible for the equilibration process. How the process of equilibration depends on the magnitude of the force has been studied by changing the magnitude of the force slightly. For this study two separate crystalline solid Argon systems driven by original 12-6 Lennard Jones potential ($V_{12-6} = 4\epsilon[(\sigma/r)^{12} - (\sigma/r)^{6}]$) and the variant of original one, the 9-6 Lennard Jones potential ($V_{9-6} = 4\epsilon[(\sigma/r)^{9} - (\sigma/r)^{6}]$) [16] are taken. The nature of the non-equilibrium state is same as defined initially. It is seen that the force associated with 12-6 potential has the larger magnitude than that of 9-6 potential in the range between first nearest neighbor and forth nearest neighbor. The observed temperature profiles, leading to the equilibration for the two cases, indicate that the process of equilibration is significantly affected by the modified force. This observation concludes that force in the region between first nearest neighbor and fourth nearest neighbor is mostly responsible for equilibration. The system identification of the temperature profiles(Fig. 2) of the two equilibrating systems show that the equilibration driven by a force having larger magnitude (12-6 potential) is faster and the sharing of kinetic energy and potential energy occurs more frequently than those of the system driven by a force having smaller magnitude (9-6 potential).

A system which consists of a large number of parts and the parts are connected to each other in a non-linear fashion is a complex system. A crystalline system is composed of large number atoms and the constituent atoms interact with each other through a non-linear potential. The presence of non-linear interaction makes the crystalline system complex. Besides the non-linear behavior of the interaction if the system temperature is increased the constituent atoms vibrate about their mean positions with larger amplitudes making the system

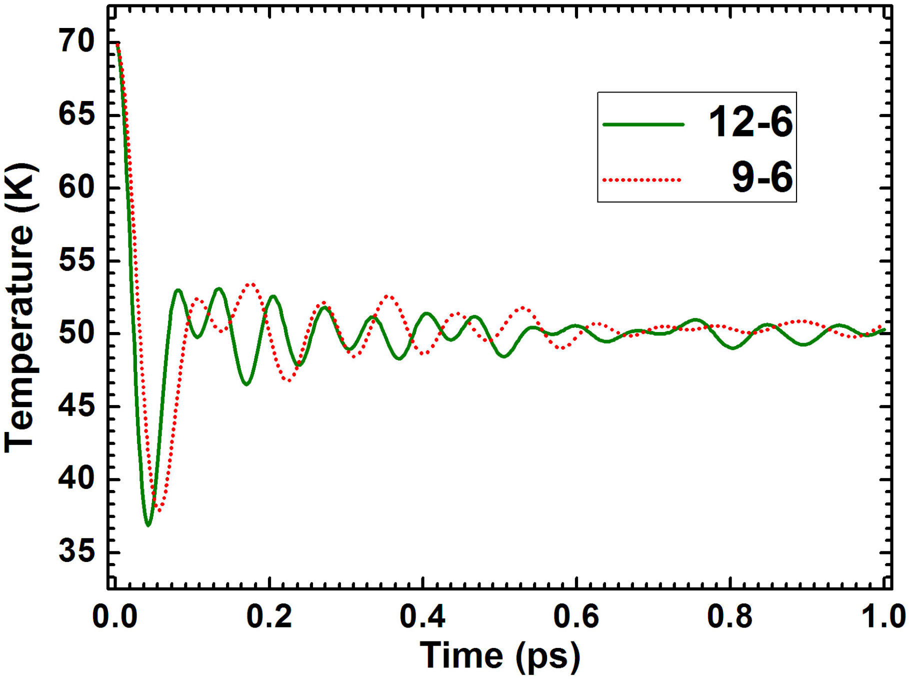

Figure 2: Time evolution of average temperature of the solid Argon systems driven by 12-6 and 9-6 potential during equilibration.

much more complex. Crystalline solid Argon systems at different equilibrium temperatures (10K, 30K, 50K and 70K) are generated from non-equilibrium state and temperature dependence of complex nature of the crystalline solid Argon are studied by measuring complexity at different equilibrium temperatures. Complexity of a system is associated with meaningful structural richness that gives an idea of correlation between the multiple spatio-temporal scales. Traditional entropy measurement of a time series data only quantifies the regularity and predictability of the time series. Complexity cannot be defined in a straightforward way from the regularity of the time series data. This is because neither completely predictable (e.g., periodic) data, which have minimum entropy, nor completely unpredictable (e.g., uncorrelated random) data, which have maximum entropy, are truly complex and they can be described very compactly. The time variations of the kinetic energy of single atoms at each equilibrium temperature are considered for complexity measurement. Sample entropy for increasing scale factors (multiscale entropy) [17, 18] are calculated from the time series data of the kinetic energy of individual constituent atoms instead of traditional entropy calculation. It is observed that with the increment of system temperature the complexity of the system also increases. The scale variation of complexity is found to follow the same nature as that of computer generated time series data of Levy process and Langevin solution. This result confirms that the diffusion kinetic energy among the constituent atoms is a Levy process and the atoms in crystal follow Langevin dynamics [19].

Bibliography

[1] David C. Schoepf, Am. J. Phys.70, 128(2002).

[2] L. Onsager, Phys. Rev. 37, 405(1931); 38, 2265(1931).

[3] M. S. Green, J. Chem. Phys. 19, 1036(1951).

[4] R. Kubo, J. Phys. Soc. Jpn. 12, 570 (1957).

[5] Udo Seifert, Rep. Prog. Phys. 75, 126001(2002) and the references therein.

[6] Nicola Scafetta and Paolo Grigolini, Phys. Rev. E66, 036130(2002).

[7] Nicola Scafetta and Bruce J. West, Phys. Rev. Lett.92, 138501(2004).

[8] B. V. Gnedenko and A. N. Kolmogorov, Limit Distributions for Sums of Independent Random Variables(Addison-Wesley, Reading, Mass.) 1954.

[9] P. Barat, A. Giri, M. Bhattacharya, Nilangshu K. Dasand A. Dutta, Europhys. Lett.104, 50003(2013).

[10] C. E. Shannon, The Bell System Technical Journal 27, 379(1948).

[11] A. Giri, Nilangshu K. Das,P. Barat, arXiv: 1401.8122.

[12] Lennart Ljung, System Identification: Theory for the User (second edition), Prentice Hall PTR (1999).

[13] C. Y. Ho, R. W. Powell, and P. E. Liley, Journal of Physical and Chemical Reference Data, Volume 3, Supplement no. 1 (1975).

[14] G. R. Stewart, Rev. Sci. Instrum. 54, 1(1983).

[15] P. Barat, A. Giri, Nilangshu K. Das,M. Bhattacharya and A. Dutta, arXiv: 1403.3237.

[16] A. Warshel and S. Lifson, J. Chem. Phys. 53, 582 (1970).

[17] Madalena Costa, Ary L. Goldberger, and C. K. Peng, Phys. Rev. E 71, 021906(2005).

[18] Madalena Costa, Ary L. Goldberger, and C. K. Peng, Phys. Rev. Lett. 89, 068102(2002).

[19] Hideo Hasegawa, Phys. Rev. E 83, 021104 (2011).

Publications in Refereed Journal:

a. Published:

1. Universal Scaling property of system approaching equilibrium.

P. Barat, A. Giri, M. Bhattacharya, Nilangshu K. Das and A. Dutta, **Europhys. Lett., 104**(2013) 50003.

b. Communicated:

1. Oscillatory Shannon Entropy in the Process of Equilibration of Non-equilibrium systems.

A. Giri, Nilangshu K. Das, P. Barat, arXiv: 1401.8122.

2. Modality of Equilibration in Non-equilibrium Systems.

P. Barat, A. Giri, Nilangshu K. Das, M. Bhattacharya and A. Dutta, arXiv: 1403.3237.

3. Complexity of the particle dynamics from the time series data of KE when the system brought to equilibrium (in preparation).

4. Nature of the force that is responsible for the equilibration in non-equilibrium system (in preparation).

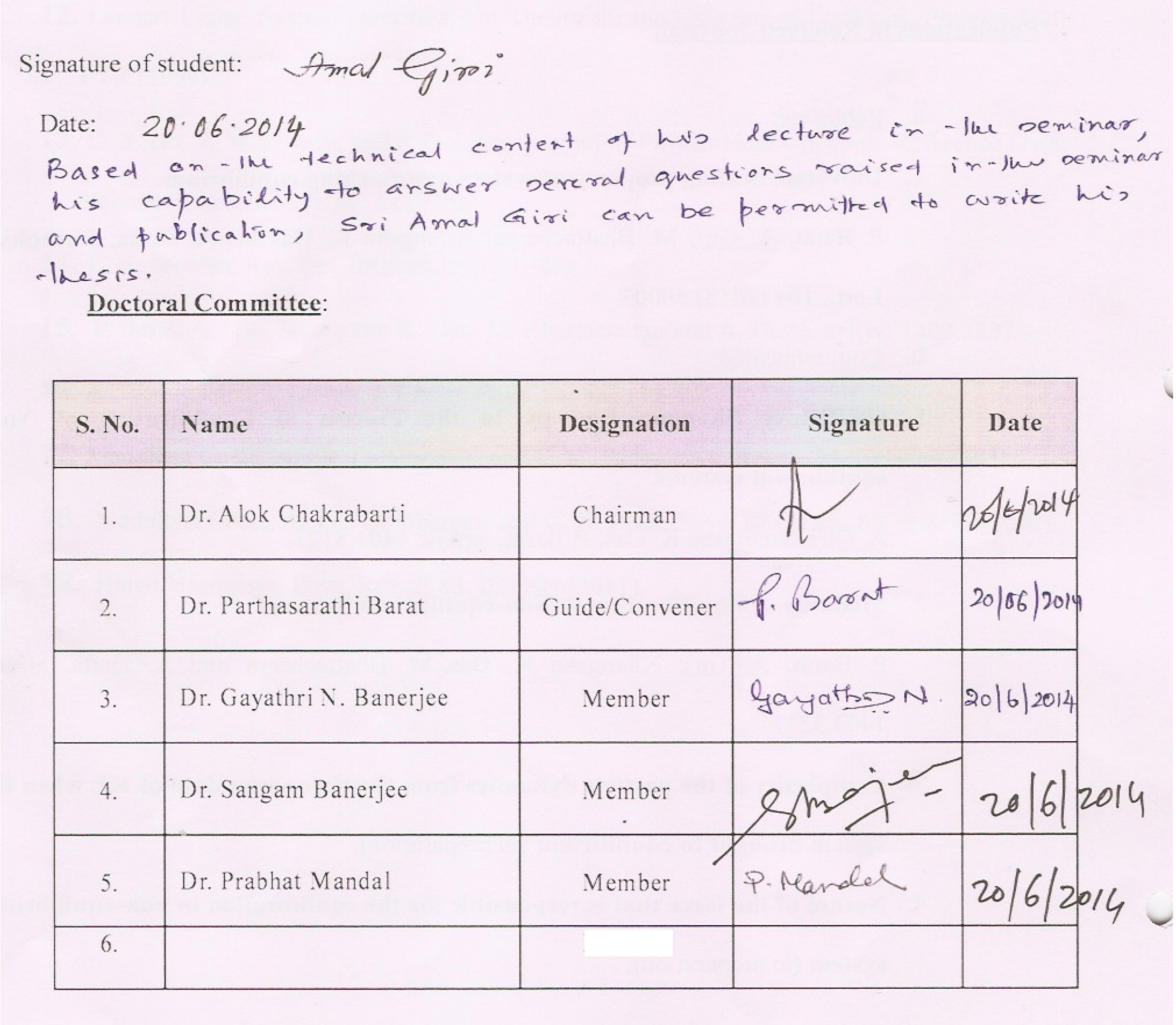

Signature of student: Amal Giri

Date: 20.06.2014

Based on the technical content of his lecture in the seminar, his capability to answer several questions raised in the seminar and publication, Sri Amal Giri can be permitted to write his thesis.

Doctoral Committee:

S. No.	Name	Designation	Signature	Date
1.	Dr. Alok Chakrabarti	Chairman		20/6/2014
2.	Dr. Parthasarathi Barat	Guide/Convener	P. Barat	20/06/2014
3.	Dr. Gayathri N. Banerjee	Member	Gayathri N.	20/6/2014
4.	Dr. Sangam Banerjee	Member		20/6/2014
5.	Dr. Prabhat Mandal	Member	P. Mandal	20/6/2014
6.				

Contents

List of Figures

List of Tables

Chapter 1

Introduction

The Concept of equilibrium state is ideal and delicate. It is utmost impossible to have and to maintain a system steadfastly in equilibrium. A system very close to equilibrium is immensely sensitive to a subtle perturbation and comes out of equilibrium. Since in nature thousands of events are simultaneously taking place, a particular thermodynamic process can not smoothly converge towards equilibrium unless a proper experimental arrangement is there to isolate the said thermodynamic system. Thus non-equilibrium state of a thermodynamic system is more probable compared to its very close-to-equilibrium condition and non-equilibrium phenomena are existing everywhere in Nature. Except their ubiquity, the non-equilibrium systems appear in different assorted flavors. At the same time, as a result of such huge phenomenology, a simple definition of the concept of non-equilibrium state is clearly a delicate issue and it necessarily requires deep exploration for its clarifications. From the perspective of text book knowledge let us see in the first section how are the equilibrium and non-equilibrium states affined to a thermodynamic system.

1.1 Equilibrium and non-equilibrium state

1.1.1 Equilibrium state

Modern statistical physics is highly rich and explored as per as the thermodynamic equilibrium is concerned. Ideally equilibrium systems are isolated from the environment and the macroscopic properties (pressure, temperature, energy etc) of such systems deal with most probable macrostate of the system particles among the possible energy states. The most probable distribution leads to maximum number of microstate and offers highest degree of freedom to the system constituents. The maximum number of microstates does not further dictate the macroscopic properties of the system. Rather, it ensures that the corresponding macrostate remains time invariant and makes the system stable and in equilibrium.

An isolated equilibrium system maintains a complete balanced state. It resists exchange of energy or matter, emission or absorption of radiation, presence of external force or unbalanced force and occurrence of phase change. Thermal, Mechanical and Chemical equilibrium, thus, accomplish the balanced condition of an thermodynamic equilibrium system. The time invariance of most probable macrostate defines an equilibrium system uniquely by an equation of state in terms of its thermodynamic parameters.

1.1.2 Non-equilibrium state

Absence of at least one of the three aforesaid equilibriums makes a system unbalanced and brings the system to non-equilibrium state. That means, having defined a system in (thermodynamic) equilibrium, a non-equilibrium system is anything else! Thus a system that is neither simply isolated from the rest of the universe, nor in contact with a constant temperature, and/or chemical potential bath, will be non-equilibrium. A system that is in the transient before reaching equilibrium is also non-equilibrium, for example a plasma with a non-Maxwellian velocity distribution. An interesting non-equilibrium situation that will arise in later examples is a system in contact with two constant temperature baths that are at different temperatures. The non-equilibrium state may also be maintained by external fields, such as the electric field driving an electric current around a conducting loop. Features that may be associated with non-equilibrium are dynamics (for example the transient relaxation towards equilibrium), and currents of the conserved quantities from one part of the system to another. Indeed we have seen that the lifetime of the non-equilibrium state is likely to be very short unless there are macroscopic disturbances in the conserved quantities away from the equilibrium distribution. Accompanying these disturbances will be macroscopic currents of the conserved quantities. A particularly interesting non-equilibrium situation is one in which there is no time dependence (*i.e.* a steady state situation), but one in which currents of the conserved variables are flowing, driven by injection at one boundary and subtraction at another. Since the dynamics of the system are dissipative, there will usually be an injection of energy, energy currents within the system, sometimes a transformation between different forms of energy (e.g. mechanical or chemical to heat), and then the subtraction of energy to maintain the steady state. For example the system in contact with two heat baths at different, but constant, temperatures, will exhibit energy currents transporting heat between the two baths. Such sustained non-equilibrium states provide the opportunity of accurate experimental and theoretical investigation. The example of transient relaxation is the charging of a capacitor in a RC circuit (Fig 1.1). Initially the capacitor voltage increases with time rapidly and the current through the circuit is very high. It is non-equilibrium variable state. After a long charging time ($t >> \frac{1}{RC}$) the current tends to zero and the capacitor voltage becomes a constant of time in the proximity of equilibrium. On the other hand an external condition may be imposed on a non-equilibrium system to retain its unbalance condition. An example here is continuous heating of a metallic bar at one end keeping the other end at lower temperature(Fig 1.2). Although after a long heating time the temperature profile of the bar remains constant of time, there will always be a temperature gradient along the bar which leads to a continuous heat flow from heating end

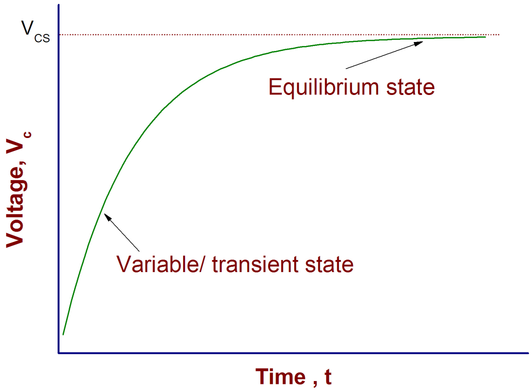

Figure 1.1: Charging of a capacitor in a RC circuit: non-equilibrium and equilibrium state

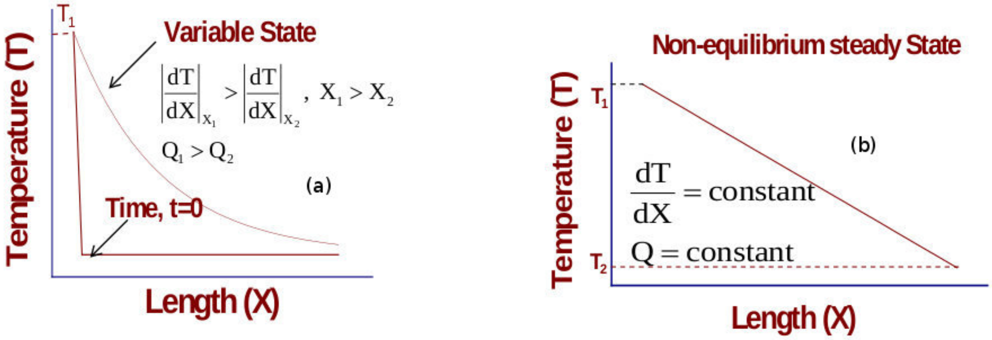

Figure 1.2: Temperature profiles along a metallic bar during its continuous heating Keeping its one end at constant source temperature T_1. (a) Initial and an intermediate non-equilibrium temperature profile and (b) a steady non-equilibrium temperature profiles are shown here

to other. This is also a non-equilibrium state but it is steady non-equilibrium state (heat entering at hot end and leaving at the cold end are equal and no accumulation of heat will be there). Due to unbalanced nature of such systems, thermodynamic parameters change with time and space and unlike the equilibrium state the thermodynamic parameters don't lead to a unique non-equilibrium state but depending on the unbalanced nature the a system can have different non-equilibrium flavor.

1.2 Consequence of non-equilibrium state: The equilibration process

A non-equilibrium state is associated to one or more constraints which don't allow the system constituents to distribute and rearrange themselves freely in their own way among different energy eigen states. Given a non-equilibrium state left its own, unlike the steady non-equilibrium state, the constraints are released then and constituent particles become free to generate new distribution with higher number of rearrangement. For a system of total N particles having total energy E, the constituents distribute themselves among the eigen states such that

$$N = \sum_{j=0}^{\infty} n_j, \tag{1.1}$$

and

$$E = \sum_{j=0}^{\infty} n_j E_j, \tag{1.2}$$

where n_j and E_j are the number particles and energy of a single particle in j_{th} eigen state respectively. An analytical expression for the number of microstates corresponding to a given macrostate can be deduced from a combinatorial argument. There are $N!$ ways of selecting the N particles to be placed in all the levels [the exclamation point (!) denotes a factorial product]. For each level, there are $n_j!$ ways of rearranging the particles within that level such that they yield the same microstate. Thus for each energy level we divide $N!$ by $n_j!$ to account for the number of repetitions of the same microstate. The result of this combinatorial analysis for the number of microstates W yields

$$W = \frac{N!}{n_0!n_1!n_2!n_3!...} \tag{1.3}$$

Actually a macrostate (a set of n_js *i.e.* $\{n_j\}$) specifies how many particles occupy each energy level, and a microstate specifies which particles occupy each energy level. Generally, macroscopic properties such as the pressure, temperature, and energy, are determined from the macrostate of the system. The microstates belonging to each macrostate are experimentally indistinguishable from one another because the macroscopic properties are the same for all the microstates. The significance of enumerating all the microstates is related to determining how likely it is for a given macrostate to occur. A fundamental postulate of statistical mechanics is that a system in equilibrium is equally likely to be in any of its allowed microstates. That is, all microstates are equally likely. For a discussion of the validity of this postulate, refer to the text by Reif[1]. Because not all macrostates are described by the same number of microstates, this postulate provides the foundation for attributing the likeliness of occurrence of a macrostate: the macrostate having the greatest number of microstates is the most likely macrostate. In other words, the distribution $\{n_0!n_1!n_2!n_3!...\}$ for which W in Eq.1.3 assumes its greatest value is the most likely distribution of particles among the energy levels. For a system in a macrostate that is not the most likely, the subsequent internal redistribution of the energy among the particles takes the system, on average, to macrostates that are more likely (that is, have larger values of W). This behavior is based on the interactions between random pairs of particles in which energy is transferred from one particle to the other[2].

1.3 Close-to-equilibrium

There exist several powerful ideas and tools for studying equilibrium systems. This is the topic covered in many textbooks kindred to the subject of thermodynamics and statistical mechanics. It might be thought that non-equilibrium systems that are near equilibrium, *i.e.* generated by small perturbations form equilibrium ones, are also amenable to treatment, and this is indeed the case. There may be very different time scales associated with the relaxation towards equilibrium. We will try to understand the slow relaxation processes occurring on time scales much longer than typical microscopic time scales. This idea goes under the general label of the Onsager[3] approach. The slowly relaxing degrees of freedom are the ones corresponding to the quantities of macroscopic subsystems that are the conserved variables of the isolated system. Let us first return to the previously mentioned simple example of a system divided into two subsystems by a partition that allows energy to flow weakly between the two subsystems, but no flow of the other conserved quantities. The equilibrium of the two subsystems is then given by the equality of the temperatures $T_1 = T_2$. Obviously, if a system is prepared with the two subsystems at different temperatures, this is a non-equilibrium state, and it is expected an energy current would flow between the subsystems moving the system towards equilibrium. The situation is particularly simple for small temperature differences $\Delta T = T_1 - T_2$ about a mean temperature $T1 \simeq T2 \simeq T$, because then the energy current J_E between the subsystems should be proportional to the small temperature difference by simple Taylor expansion (it is zero for no temperature difference)

$$J_E = K\Delta T, \tag{1.4}$$

Here K is a “kinetic coefficient that depends on the strength of the coupling of the two subsystems.

Eq.1.4 can then be used to describe the relaxation process. The energy current gives us the rate of increase of energy on one side, and the rate of decrease on the other side. Since other conserved densities are fixed, the temperatures of the subsystems will change at a rate proportional to the rate of change of energy

$$\dot{T}_1 = \dot{E}_1/C_1 \tag{1.5}$$

$$\dot{T}_2 = \dot{E}_2/C_2 \tag{1.6}$$

where C's are the thermal capacities of subsystems, the proportionality constant relating small changes of temperature to small changes of energy content. A key point is that since the relaxation between the systems is slow, each system may be taken as internally in equilibrium, so that the proportionality constant between changes of energy and temperature is the equilibrium value of the specific heat. Thus we find

$$\Delta\dot{T}_2 = -K/C\Delta T \tag{1.7}$$

with $C^{-1} = C_1^{-1} + C_2^{-1}$ giving an effective combined thermal capacity. This equation yields exponential relaxation with a time constant

$$\tau = K/C \tag{1.8}$$

given by macroscopic quantitieswe use the knowledge that ΔT is small to recognize that we may take C and K to be constants, equal to their values at the mean temperature T.

Since the energy current is the process of the approach to equilibrium, the entropy must increase in this relaxation. Using the thermodynamic identity we have

$$\dot{S} = \dot{S}_1(E_1) + \dot{S}_2(E_2) = \frac{\dot{E}_1}{T_1} + \frac{\dot{E}_2}{T_2} \simeq -J_E\Delta T/T^2 = K(\Delta T/T)^2 \tag{1.9}$$

where in the third step we have kept terms up to first order in ΔT . Thus the second law of thermodynamics, that the entropy increases as an isolated system returns to equilibrium, tells us that the kinetic coefficient Kmust be positive.

The results are readily generalized to study continuum dynamics. Considering only the temperature and energy variables, a macroscopic system is in equilibrium when the temperature is uniform in space. Correspondingly, a spatially varying temperature will lead to an energy flow, and for small, slowly varying, perturbations the energy current will be proportional to the gradients of the temperature. It is useful to introduce the energy density (energy per unit volume) e, and the energy current density $\mathbf{j_E}$ (so that the energy flow across a surface S is $\int_S \mathbf{j_E}.\mathbf{dS}$). The conservation of energy now takes the form

$$\frac{\partial e}{\partial t} = -\nabla.\mathbf{j_E}, \tag{1.10}$$

where the energy current is proportional to the spatial gradient of the temperature

$$\mathbf{j_E} = -K_T \nabla T, \tag{1.11}$$

with K_T the familiar thermal conductivity. Again the law of increase of entropy imposes constraints on the coefficient, namely that K must be positive. The equations of motion Eqs.(1.10,1.11) are closed if we know how the energy density depends on the temperature. This relationship is again taken to be the same one as in equilibrium, *i.e.* by the appropriate specific heat, since the dynamical equations already represent the leading order expansion in the deviation from equilibrium. The dynamical equations are linear, and for a given finite physical system the evolution will be the sum of exponentially decaying modes of the system. (Since an system of infinite size has an infinite number of modes, and the relaxation may then be non-exponential.)

Eq.1.11 is the familiar equation for the conduction of heat, and could easily be written down from phenomenological considerations. This allows us to make the obvious but important point that the familiar macroscopic equations of continuum mechanics, heat and particle diffusion etc. are fully consistent with the general principles of thermodynamics. In particular, in any solution to the macroscopic dynamical equations, a positive rate of entropy production is guaranteed by the formalism(which is not case for system away from equilibrium, Chapter 4). If we assume that the thermal conductivity K_T is independent of temperature over the range encountered in an experiment, and also relate changes in the energy density e to changes in temperature through the specific heat per unit volume C_T that may also be considered temperature independent, the two equations Eqs.1.10 and 1.11

can be combined into the single equation

$$\frac{\partial T}{\partial t} = k_T \nabla^2 T, \tag{1.12}$$

with $k_T = K_T / C_T$. This equation takes the form of a time dependent diffusion equation for the temperature, and the energy density e satisfies an identical equation. The coefficient k_T, with the dimensions of a diffusion constant, is known as the thermal diffusivity. Since equations like 1.10 and 1.11 are a direct consequence of a conservation law and a flux proportional to gradients, one can see diffusion equations, or diffusion terms supplemented by additional terms describing other physical phenomena, commonly appear as equations for pattern forming systems.

To summarize, we have learned from a simple example the following results:

- A state near equilibrium decays exponentially towards equilibrium.
- The dynamics is given by equations of motion that are on the one hand the usual phenomenological equations (in our simple example the heat current proportional to temperature difference) and on the other hand derivable from the fundamental laws of thermodynamics. Necessarily the equations of motion are consistent with the laws of thermodynamics.
- The law of the increase of entropy places constraints on the coefficients of the dynamical equations, not on the solutions to the equations. Any solution to the dynamical equations necessarily is consistent with the law of the increase in entropy, and we do not gain additional constraints on the solutions by applying this law.

These results may be extended to the general case of coupled equations for more than one conserved quantity. For example in a fluid we need to consider the thermodynamic consequences of the conservation of mass and momentum as well, leading to the familiar equations of fluid dynamics (including viscous dissipation etc.).

1.4 Far away from equilibrium and nonlinear response theory

The Onsager theory[3] of near equilibrium leads to perturbations that decay exponentially towards equilibrium. This result is derived simply from the assumption of small perturbations, so that only terms linear in the deviation from equilibrium are retained($Lt_{\to 0}\ e^x = 1 + x$)[4, 5, 6]. We may characterize a system as far from equilibrium when the linearization is no longer valid and deviations from the linearization lead to qualitatively new effects. A key feature of these systems is that the equations of motion will be nonlinear, since the linear expansion must necessarily break down. Thus we no longer have the useful tools of global thermodynamics and linearization, and the study of these systems correspondingly becomes much harder. We will concentrate almost entirely on systems that although far from equilibrium globally, are near equilibrium locally. This allows us to treat the systems using the equations derived from the Onsager approach to non-equilibrium thermodynamics, or equivalently the standard equations of fluid dynamics, chemical reaction and diffusion, etc. The appropriate systems are macroscopic ones in which for example the temperature deviations across the system are “large”, but the spatial gradients of the temperature are “small”. Temperature differences on a characteristic microscopic scale (*e.g.* the mean free path for collisions in a gas) will be small. We may then take pieces of the system that are small enough that the linearization procedure above is sufficiently accurate, but large enough that a macroscopic description is also sufficiently accurate. Thus locally the currents of the conserved quantities are proportional to the gradients of the conjugate fields, with the same coefficients as introduced above (maybe depending on the local values of the temperature etc.). Furthermore the conjugate variables vary only slightly across these subsystems, so that the relationship between changes in the conserved densities and the conjugate variables, such as the specific heat relating energy and temperature changes, may again be taken to be the equilibrium equation of state. Thus the equations of motion will again be given by Eq.1.10 and Eq.1.11, but with coefficients C_T and K_T that in general are functions of the local conjugate variables. Again these dynamical equations and the Onsager constraints on the kinetic coefficients guarantee positive entropy production in any solution of the dynamical equations.

In practice, rather than pursuing the formal Onsager approach, the equations of motion are often written down from phenomenological considerations. In some cases, motivated by the aim of simple tractable equations that perhaps capture specific aspects of a problem, grossly simplified "model" equations may be used, for which there is no direct connection to an underlying thermodynamic system. It is therefore useful to consider issues such as equilibrium versus non-equilibrium directly from the form of the dynamical equations. Here the important issue is whether the equations are dissipative or conservative. Dissipative macroscopic systems are associated with a relaxation towards a single state or a reduced set of states from a broad range of initial conditions. In the language of dynamical systems we expect phase space volumes to contract in time. These equations must display a sense of time, and so are not invariant under time reversal. Conservative macroscopic systems are invariant under time reversal, and so do not show a systematic trend towards a subset of states as time advances. Phase space volumes are preserved by the dynamics. Pattern formation is the spontaneous development of spatial structures from a wide range of initial conditions. In dissipative systems this tendency is expected to be more stronger.

1.5 Thermal fluctuations

The familiar macroscopic equations of fluid dynamics, thermal and particle diffusion etc. can be thought of as averages over the underlying microscopic molecular dynamics. At macroscopic length scales the rms fluctuations about the mean values are much smaller than the mean values by factors of order $N^{-1/2}$ where N is the number of molecular degrees of freedom in the averaging volume[1, 7, 8]. This is because the fluctuations tend to cancel in the summation to form the macroscopic variable. For most of the pattern forming systems with length scales of order mm, cm, or larger the size of the fluctuating corrections to the macroscopic deterministic equations are very small indeed.

There are some situations however where the residual fluctuations are important. One example is in answering how the growing perturbation about an unstable solution is initiated. In principle even an unstable solution may persist indefinitely if there is nothing to give an initial small kick away to establish a perturbation that then continues to grow. In almost all cases the small kick is supplied by experimental imperfections such as slight deviations of the geometry from the ideal, or an imperfectly controlled environment or initial condition-or from another point of view the idea that a precise solution exists but is unstable due to theoretical oversimplification, so that there is no issue of where an initial kick might come from. In some systems however very careful experiments can be done to eliminate these "external" sources driving the unstable mode, and uncover the intrinsic driving due to thermal fluctuations even on the mm length scale. In addition, for phenomena at smaller length scales, the residual effects of molecular fluctuations may be more apparent. One example is the formation of side branches in the dendritic growth of crystals apparent in the pictures of snowflakes. There is good evidence that side branches develop through the selective amplification of thermal noise at the tip of the dendrite[9]. Fortunately we do not have to revert to molecular theory to include these small fluctuation effects. The constraint that the fluctuating forces must yield a distribution of the thermodynamics variables given by the Boltzmann factor (*i.e.* probability proportional to $\exp(-\beta E)$ with $\beta = 1/k_B T$ with k_B the Boltzmann constant and E the energy, or more precisely the free energy, of the fluctuation), and the observation that the stochastic effects due to individual molecular collisions act on time scales very short compared to the macroscopic phenomenon of interest, are sufficient to pin down the strength and character of the fluctuating forces. A profound result of statistical mechanics known as the fluctuation-dissipation theorem[10] in fact directly relates the strength of the fluctuating forces to the dissipative kinetic coefficients in the macroscopic equations, and to the temperature. Examples people may be familiar with are the expression for the voltage noise source associated with any electrical resistance known as Johnson noise[11, 12, 13] and the random forces on a particle immersed in a fluid that lead to Brownian motion. The precise expression for the fluctuation corrections to the equations of fluid dynamics and heat flow can be found in Vol. 6 of the Landau and Lifshitz series on Theoretical Physics[14]. We emphasize again though, that it is only in very careful experiments designed specifically to seek out the phenomenon, or in a very small number of examples of patterns in nature that are at micron length scales, that these fluctuating forces arising from the tiny residual effects of molecular fluctuations not quite canceling in averages over macroscopic regions become evident.

1.6 Utility of molecular dynamics

Collective behavior of the constituents of non-equilibrium systems is poorly understood. In this context the studies of this thesis are focused on the dynamics of the equilibration process of a non-equilibrium system which is far away from equilibrium. A non-equilibrium system which is undergoing equilibration each and every constituent of the system participates in the equilibration process and their collective dynamics is responsible for the attainment of equilibrium distribution[15]. Thus, the single particle dynamics and their collective behavior are complementary to each other to understand the equilibration process of a non-equilibrium system. As a whole the system dynamics and as well as the particle dynamics, during the process of equilibration, are studied in the scope of this work. Experimental methods deal with mere time average values of macroscopic properties. Analytical methods are not able to solve the equation of motion of the individual particles since they are connected with large number of particles in non-linear fashion. Like experiments analytic methods provides only the time average values of macroscopic quantities. This drawback of experiment and analytical methods can be solved by the use of molecular dynamics simulation technique. Molecular dynamics deals in the atomic level of the system under study in the time scale of the order of femtosecond. Thus molecular dynamics simulation[16] technique is a useful tool for the study of individual particle dynamics of the system and in this entire dissertation this technique is used to generate non-equilibrium system which is far away from equilibrium.

1.7 Motivation behind the choice of non-equilibrium system and scopes of the thesis

Presently the topic of collective phenomena in equilibrium systems is a mature one. Extensive studies over the last six to seven decades have produced a clear understanding of the phenomenology as well as many rigorous mathematical results. On the other hand, systems that are not in thermodynamic equilibrium are more poorly understood. Indeed, a general theoretical framework for the study of non-equilibrium collective phenomena is lacking and our understanding to date has relied on the study of specific models. By "non-equilibrium system" it refers both to systems held far from thermal equilibrium by an external driving force and to the complementary situation of systems relaxing towards thermal equilibrium. Such systems display a broad range of phenomena, such as phase transitions and slow collective dynamics, which we should understand at a deeper level. The study of non-equilibrium systems arises in many different contexts such as reactiondiffusion processes, interacting particle systems, driven diffusive systems, and the slow dynamics of both ordered and disordered glassy systems. It is a major research area which is represented in many different scientific communities throughout the world. In recent years the study of specific model systems has led to important breakthroughs in a variety of areas. Mathematical tools have been developed and some rigorous results derived pertaining to specific systems. These developments bring us closer to the point where we can ask questions of generality, both of techniques and results. This dissertation has laid another new dimension to the diverse field of non-equilibrium physics.

This thesis has the scope to discuss on the equilibration process of non-equilibrium systems of most possible simplest ensemble, the NVE ensemble (having constant number of constituents, constant volume of the system, and constant energy of the system) which does not interact with any source or sink to exchange any constituent particle or energy with them. The non-equilibrium systems taken for the analysis are composed of different crystalline materials having different crystalline structures (Si, Ge, solid Argon, Fe, Mo, Al and Cu) and they follow variety of potential functions in order to maintain the stability of their respective crystalline structures. In my entire study the adopted non-equilibrium systems are generated by making average kinetic energy and average potential energy of the system unequal. It is notable that in such no-equilibrium state(when average kinetic energy and average potential energy of the system are not equal) the configuration of crystal atoms is different equilibrium atomic configuration. However, it does not affect the volume of the simulation cell since the simulation is performed in NVE environment. It is the pressure of the system which is affected because of continuous change of atomic configuration while the system is in NVE environment. Each of these NVE systems has an identical environment in all the three directions of the simulation cell and it is maintained with the use of periodic boundary condition. Here is the sort introduction of the studies covered in this dissertation:

- **Scaling property of the time series data of kinetic energy of individual constituent particles during the process of equilibration:** Atoms in the simulation cell, when brought to a non-equilibrium state by enhancing their kinetic energy, try to redistribute their excess kinetic energy by the process of diffusion. This process of redistribution of kinetic energy among the atoms changes their mean positions of vibration and consequently their potential energy. Here all the atoms in the cell participate together in the diffusion process. Thus by analyzing the variation of the kinetic energy with time for a single atom in the simulation cell one can account for the modality of this diffusion process and the nature of the equilibration. The time variations of the kinetic energy with time for each atom are found to be random since it is associated to the diffusion process. Whether there exist any self similarity property in this random time series data and whether the time series data is associated with a universality class, the answers of all these queries can be made by scaling analysis of the time series data. The scaling property of the time series of kinetic energy of individual particles are studied using two complementary scaling analysis methods: Diffusion Entropy Analysis (DEA) and Finite Variance Scaling Method (FVSM) [17, 18]. Application of these scaling analyses reveals that the fluctuations in the time series of kinetic energy follow similar kind of dynamics irrespective structures and non-equilibrium temperatures of the systems under study. Several crystal structures diamond cubic, face centered cubic and body centered cubic structure with suitable potential functions were used. The results of the scaling analyses conform that for all cases the time series of the kinetic energy of system particles exhibits an anomalous diffusion and it belongs to Levy walk process [19, 20]. In Levy walk a time series has a probability distribution function having a long tail. Most of the natural phenomena like food foraging in hungry animals, spreading of vector mediated disease in animals and human are examples of Levy walk with few but effective long hops. Thus the time series of kinetic energy of non-equilibrium system particles confirms the existence of a universality class.

• **Evolution Shannon entropy during equilibration:** Probability distribution function is the global representation of a system. Evolution of the probability distribution function of kinetic energy of the constituent atoms of the equilibrating system is oscillatory and subsequently the oscillation dies down after a long time. Shannon entropy [21] is a measure of uncertainty or unpredictability of information contained in a probability distribution. The time variation of global information of the equilibrating system are studied by calculating the Shannon entropy from their time evolution of probability distribution. For more random information the uncertainty in its prediction is higher and the corresponding value of Shannon entropy will be more. In case of tossing coin or rolling n-sided die outcomes lead to maximum Shannon entropy given that that the coin or the die is fair. For unfair coin or die predictability of the outcomes becomes easy and value of Shannon entropy drops down. For a two headed/tailed coin or for a die with all the sides identical the outcomes become completely predictable and the entropy goes to zero. For a physical equilibrium/non-equilibrium system the distribution of constituent particles among energy eigen states is not as simple as the outcomes of tossing coin or rolling die. Except the combinations among particles occurrence of the energy eigen states follow some restriction in this case. Unlike the situation for fair coin or fair die where the all the outcomes are equally probable the equilibrium physical system does not generate a probability distribution with equal population in each energy eigen state. Thus the variation of Shannon entropy for completely unfair and partially unfair coin/die should be monotonically increasing and ultimately reaches a constant maximum value for fair coin/die. On the other hand due to adopted non-equilibrium nature of the system where the system kinetic energy and the system potential energy are not equal, in the initial phase of equilibration there will be transfer of kinetic energy into potential energy by changing the configuration of constituent atoms. Since this process is very fast the system cannot estimate exactly how much kinetic energy should be transferred into potential energy to make them equal. The inertia of the process transfers more kinetic energy and a reverse situation appears with potential energy more than the kinetic energy. This mechanism leads to an oscillatory transfer of energy during equilibration and the oscillation gradually dies down with time [22]. Such variation of energy and restriction in the energy states do not allow the Shannon entropy to follow monotonic increasing behavior but is oscillatory and at equilibrium it becomes constant of time.

- **Modality of equilibration process:** The force field in crystalline system is the sum of deterministic part due to nearer atoms and random part due to distant atoms. The affects of these two parts of the force are reflected on the probability distribution function. The random part of the force introduces a noise component to the system response. Hence in the study of equilibration mechanism from the time variation of probability distribution function it is desirable to eliminate the noise part. Use of principal component analysis helps to eliminate the noise part and reduces the histograms of probability distribution functions into 2-3 principal dimensions and it becomes easier to study the evolution of probability distribution function in terms of those two or three components. The component which has highest egien value is most important (more than 75% of total eigen value except for solid Argon where it is around 60%) and is used for the analysis. The existence of 2-3 major eigen values ensure that the probability distribution functions are highly correlated. A statistical method called system identification technique [23] is used to analyze the evolution of most significant component. This method relates the system input and output by a rational function called transfer function. The analysis reveals that the dynamical process of equilibration takes place through two or three modes and the mode associated to lowest frequency which is very close to Debye frequency of the corresponding element [24, 25, 26]. These modes are calculated from the denominator of the transfer function of the system obtained from the system identification.

- **Dependence of the process of equilibration on the interaction potential:** Another important aspect of non-equilibrium system is simultaneous impact of deterministic and random force together on the process of equilibration. It is a exertion to sort out in which region the total force field is most responsible for the equilibration process. How the process of equilibration depends on the magnitude of the force has been studied by changing the magnitude of the force slightly. For this study two separate crystalline solid Argon systems driven by original 12-6 Lennard Jones potential ($V_{12-6} = 4\epsilon[(\sigma/r)^{12} - (\sigma/r)^{6}]$) and the variant of original one, the 9-6 Lennard Jones potential ($V_{9-6} = 4\epsilon[(\sigma/r)^{9} - (\sigma/r)^{6}]$) [27] are taken. The nature of the non-equilibrium state is same as defined initially. It is seen that the force associated with 12-6 potential has the larger magnitude than that of 9-6 potential in the range between first nearest neighbor and forth nearest neighbor. The observed temperature profiles, leading to the equilibration for the two cases, indicate that the process of equilibration is significantly affected by the modified force. This observation concludes that force in the region between first nearest neighbor and fourth nearest neighbor is mostly responsible for equilibration. The system identification of the temperature profiles of the two equilibrating systems show that the equilibration driven by a force having larger magnitude (12-6 potential) is faster and the sharing of kinetic energy and potential energy occurs more frequently than those of the system driven by a force having smaller magnitude (9-6 potential).

- **Complexity of a equilibrium system:** A system which consists of a large number of parts and the parts are connected to each other in a non-linear fashion is a complex system. A crystalline system is composed of large number atoms and the constituent atoms interact with each other through a non-linear potential. The presence of non-linear interaction makes the crystalline system complex. Besides the non-linear behavior of the interaction if the system temperature is increased the constituent atoms vibrate about their mean positions with larger amplitudes making the system much more complex. Crystalline solid Argon systems at different equilibrium temperatures (10K, 30K, 50K and 70K) are generated from non-equilibrium state and temperature dependence of complex nature of the crystalline solid Argon are studied by measuring complexity at different equilibrium temperatures. Complexity of a system is associated with meaningful structural richness that gives an idea of correlation between the multiple spatio-temporal scales. Traditional entropy measurement of a time series data only quantifies the regularity and predictability of the time series. Complexity cannot be defined in a straightforward way from the regularity of the time series data. This is because neither completely predictable (e.g., periodic) data, which have minimum entropy, nor completely unpredictable (e.g., uncorrelated random) data, which have maximum entropy, are truly complex and they can be described very compactly. The time variations of the kinetic energy of single atoms at each equilibrium temperature are considered for complexity measurement. Sample entropy for increasing scale factors (multiscale entropy) [28, 29] are calculated from the time series data of the kinetic energy of individual constituent atoms instead of traditional entropy calculation. It is observed that with the increment of system temperature the complexity of the system also increases. The scale variation of complexity is found to follow the same nature[30] as that of computer generated time series data of Levy process and Langevin solution. This result confirms that the diffusion kinetic energy among the constituent atoms is a Levy process and the atoms in crystal follow Langevin dynamics [31].

Bibliography

[1] Fundamentals of Statistical and Thermal Physics, Section A.12: The H theorem and the approach to equilibrium, F. Reif, 2008

[2] David C. Schoepf, Am. J. Phys.70 (2002) 128.

[3] L. Onsager, Phys. Rev. 37 (1931) 405; 38 (1931) 2265.

[4] M. S. Green, J. Chem. Phys. 19, 1036(1951).

[5] R. Kubo, J. Phys. Soc. Jpn. 12, 570 (1957).

[6] R. Kubo, J. Phys. Soc. Jpn. 12, 1203 (1957).

[7] Thermodynamics and Fluctuations far from Equilibrium, John Ross, Springer, 2008.

[8] Statistical Mechanics, R. K. Pathria, Paul D. Beale, 2011.

[9] T. Gonda, H Nakahara, Journal of Crystal Growth 160, 162 (1996).

[10] R. Kubo, Rep. Prog. Phys. 29, 255(1966)

[11] J. B. Johnson, Nature 119, 50(1927).

[12] J. B. Johnson, Phys. Rev. 29, 367(1927).

[13] J. B. Johnson, Phys. Rev. 32, 97(1928).

[14] Fluid Mechanics, L. D. Landau, E.M. Lifshitz, Second Edition: Volume 6 (Course of Theoretical Physics S), 1987.

[15] Udo Seifert, Rep. Prog. Phys. 75, 126001(2002) and the references therein.

[16] Handbook of Materials Modeling, S. Yip, Springer, 2005.

[17] Nicola Scafetta and Paolo Grigolini, Phys. Rev. E66, 036130(2002).

[18] Nicola Scafetta and Bruce J. West, Phys. Rev. Lett.92, 138501(2004).

[19] B. V. Gnedenko and A. N. Kolmogorov, Limit Distributions for Sums of Independent Random Variables(Addison-Wesley, Reading, Mass.) 1954.

[20] P. Barat, A. Giri, M. Bhattacharya, Nilangshu K. Dasand A. Dutta, Europhys. Lett.104, 50003(2013).

[21] C. E. Shannon, The Bell System Technical Journal 27, 379(1948).

[22] A. Giri, Nilangshu K. Das,P. Barat, arXiv: 1401.8122.

[23] Lennart Ljung, System Identification: Theory for the User (second edition), Prentice Hall PTR (1999).

[24] C. Y. Ho, R. W. Powell, and P. E. Liley, Journal of Physical and Chemical Reference Data, Volume 3, Supplement no. 1 (1975).

[25] G. R. Stewart, Rev. Sci. Instrum. 54, 1(1983).

[26] P. Barat, A. Giri, Nilangshu K. Das,M. Bhattacharya and A. Dutta, arXiv: 1403.3237.

[27] A. Warshel and S. Lifson, J. Chem. Phys. 53, 582 (1970).

[28] Madalena Costa, Ary L. Goldberger, and C. K. Peng, Phys. Rev. E 71, 021906(2005).

[29] Madalena Costa, Ary L. Goldberger, and C. K. Peng, Phys. Rev. Lett. 89, 068102(2002).

[30] A. Giri, S. Dey, and P. Barat, arXiv:1409.2761.

[31] Hideo Hasegawa, Phys. Rev. E 83, 021104 (2011).

Chapter 2

Classical Molecular Dynamics

2.1 Molecular dynamics: then and now

Introduction of the concept of classical Newtonian mechanics has laid the path to deal with many body processes in nature which were apparently indeterministic. This comes true when the associated momenta of the system particles are large enough and that makes the quantum effect insignificant. In this context although the electronic scale does not fulfill this restriction the molecular scale and even the atomic scale also suitable enough for the application of classical concepts over a wide range temperature. Thus, application this strength of classical mechanics would have been an exponent for the determination of the properties of solids. Till early 1950's, people had to wait for appropriate numerical methods,realistic interatomic potentials and powerful computer to deal with many body systems with realistic physical significance. Before this era, the only theoretical alternative for predicting the properties of matter was to employ the approximate physical models, e.g., the van-der Waals equation for the real gases or the Boltzmann's equation for transport properties of dilute gases.

In 1952 MANIAC computer was launched from Los Alamos National Laboratory and in 1953 it was first used for atomistic simulations of liquids followed by those of one-dimensional anharmonic crystals by Fermi and co-workers. The first unrealistic molecular dynamics simulation using hard-sphere model was performed by Alder and Wainwright in 1958 and in 1960 the first realistic molecular dynamics simulation on the radiation damage of copper was reported. Although with time we have seen the advancement of computer hardware and numerical methods but the basic algorithm of classical molecular dynamics are still same.

This power of classical mechanics remained unutilized in unfolding the properties of solids for centuries. The most crucial barrier to achieving this goal was the fact that in the relevant many body problems, the term ‘many’ actually meant ‘too many’. Clearly, mankind had to wait for a long time, till powerful digital computers and state of the art numerical methods started appearing. In the early 1950’s, the electronic computers became available for non-strategic applications. The most significant of them had been the MANIAC at the Los Alamos National Laboratory, which was commissioned in March, 1952. Before this era, the only theoretical alternative for predicting the properties of matter was to employ the approximate physical models, e.g., the van-der Waals equation for the real gases or the Boltzmann’s equation for transport properties of dilute gases. The researchers were striving to obtain the realistic interatomic potentials so that the new computers available to them could use those models and churn out the numbers with realistic physical significance. In such a scenario, the liquids were opted as the first system of choice for simulation in MANIAC, for the simple hard-sphere model was sufficient to yield many statistical features associated with them. Consequently, Metropolis and his colleagues were the first one to perform the atomistic simulations of liquids on the MANIAC computer[1]. These simulations were soon followed by those of one-dimensional anharmonic crystals by Fermi and his co-workers[2]. The first molecular dynamics (MD) simulation (using the unrealistic hard-sphere model) was performed by Alder and Wainwright[3], while the first realistic MD (of radiation damage in copper) was reported only in 1960[4]. Interestingly, the basic algorithm of atomistic simulation has remained the same since the era of 50’s, even though the development in computer hardware and numerical methods have taken place in leaps and bounds. Today, some of the most powerful computing machines performing at hundreds of Teraflops are regularly being utilized for carrying out the different flavors of atomistic simulations. Although the Monte Carlo simulations constitute a significant part of atomistic simulation, the studies covered in the subsequent chapters deal with molecular statics (MS)and dynamics (MD) simulations. Therefore, the nuts and bolts of MS and MD will be highlighted in the present chapter. These simulations are aimed at computing the stable minimum energy configurations and evolution of the system in time. The fundamental idea is actually quite simple. Here one conceives a material as a many-body system consisting of atoms and directly simulates the material's behavior by tracking the trajectories of the atoms under a set of given conditions. The first essential requirement for both MS and MD is a suitable interatomic potential, which is capable of modeling the interactions among the atoms with reasonable accuracy. Once the interatomic potential is chosen, we can compute the forces (and accelerations) experienced by the atoms as gradients of the system's potential energy. Thereafter, the system is either relaxed to a mechanically stable structure or allowed to exhibit a dynamic behavior through the integration of its equation of motion, depending upon whether the mode of simulation is MS or MD. The following sections detail the basic ingredients for performing these atomistic computations.

2.2 Potential models for interatomic interaction

Since periodicity of lattice points is the definition of a crystal and atoms or molecules are the building block of a crystal, so the simulation scheme of dynamics of a crystal is studied at atomic level and one of the most popular simulation technique at atomic level is 'Molecular Dynamics' which requires appropriate interatomic potential model and the statistical distribution of atomic parameters. If two atoms are closed to each other then they exert a force and consequently an interatomic potential is involved there. The nature of this potential can be precisely measured solving the Schroedinger equation of interacting electrons which is referred as *ab initio* theory(as used in density functional theory[5]). But as in this theory

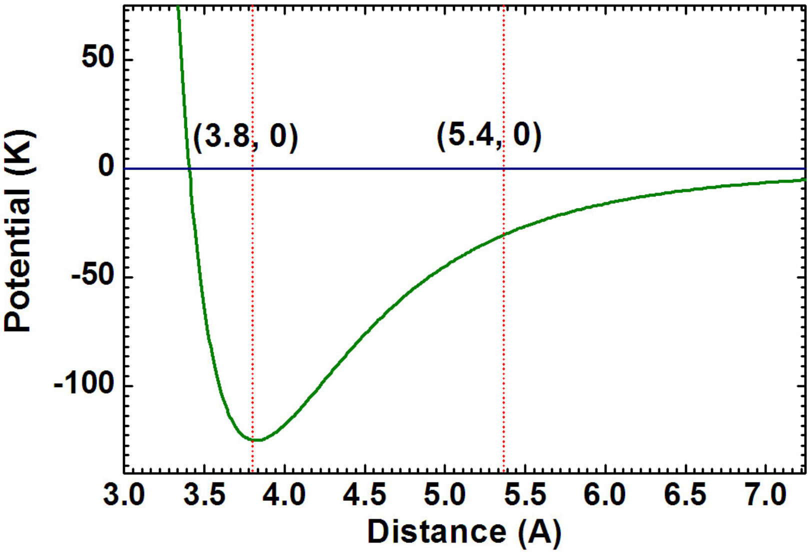

Figure 2.1: Lennard-Jones potential for solid Argon crystal with $r_m = 2^{1/6}\sigma_0 = 3.8$ Å, $\sigma_0 = 3.405$ Å, and $\epsilon = 124.84$ Kelvin.

the numerical calculation is based on electronic interaction so it is very expensive. For large crystal size the amount of calculation becomes too huge to be calculated even by a powerful computer.

Quantum mechanics suggests that two atoms can't be closed to each other infinitely as their potential energy increases then. Such type of potential model, similar to well known "Lennard-Jones" potential[6] (Fig .2.1), is given by

$$\begin{aligned} V_{LJ}(r) &= 4\epsilon\left[\left(\frac{r}{\sigma_0}\right)^{-12} - \left(\frac{r}{\sigma_0}\right)^{-6}\right] \\ &= \epsilon\left[\left(\frac{r}{r_m}\right)^{-12} - 2\left(\frac{r}{r_m}\right)^{-6}\right] \end{aligned} \tag{2.1}$$

For noble gas atoms the potential is two body. Otherwise the potential energy is many body and for N-body system it is

$$V(\{r_i\}) = \sum_{i<j} \Phi(|r_i - r_j|) + \sum_{i<j<k} \Phi_3(r_i, r_j, r_k) + \sum_{i<j<k<l} \Phi_4(r_i, r_j, r_k, r_l) + ...$$

, where the $1st$ term introduces the potential for noble gas. If the higher order terms converge then this model is very similar to "Stillinger-Weber" potential[7]. For a metal the ions are considered immersed in the sea of electrons and the potential model used is "Embedded-Atom Model" (EAM)[8, 9] with form

$$V_{EAM}(\{r_i\}) = \sum_{i<j} \Phi(|r_i - r_j|) + F(\rho_i)$$

, where $(\{r_i\}) = (r_1, r_2, .., r_N)$ and $\rho_i = \rho(\{r_i\}) = \sum_{i<j} f(|r_i - r_j|)$ is local density of bonding electrons contributed by the atoms around i_{th} atom with $f(|r_i - r_j|)$ is the contribution of an atom to the electron density . $F(\rho_i)$ is an embedding function with special form $F(\rho_i) = -A\sqrt{\rho_i}$ leads to 'Finnis-Sinclair'(FS) potential[10, 11]. The square root form of the FS potential is very similar to the second moment approximation of the tight binding (TB) theory[12], where the cohesive energy of a solid varies as square root of the coordination number. Although the FS potential works well with some pure metals, particularly the b.c.c structures, they are not so popular for simulating alloys. Still there are some potentials for the noble metal alloys which have been designed in the FS framework[13, 14, 15].

2.2.1 Stillinger Weber potential

$$V = \sum_{i<j} V_2(r_{ij}) + \sum_{i<j<k} V_3(r_{ij}, r_{jk}, r_{ik})$$

$$V_2 = \epsilon f_2(r_{ij}/\sigma)$$

$$V_3 = \epsilon f_3(r_{ij}/\sigma, r_{ij}/\sigma, r_{ij}/\sigma)$$

$$f_2(r) = A(Br^{-p} - r^{-q})e^{\frac{1}{r-a}}, r < a$$

$$= 0, r > a$$

and

$$f_3 = h(r_{ij}, r_{ik}, \theta_{jik}) + h(r_{ij}, r_{jk}, \theta_{ijk}) + h(r_{ik}, r_{jk}, \theta_{ikj})$$

$$h(r_{ij}, r_{ik}, \theta_{jik}) = \lambda \left(\cos\theta_{jik} + \frac{1}{3} \right)^2 e^{\left(\frac{\gamma}{r_{ij}-a}\right)} e^{\left(\frac{\gamma}{r_{ik}-a}\right)}, r_{ij} < a \text{ and } r_{ik} < a$$

$$= 0, r_{ij} \geq a \text{ and } r_{ik} \geq a$$

r_{ij} is the distance between i_{th} and j_{th} particle. σ and ϵ being characteristic length and energy parameter respectively. θ_{jik} is the bond angle centered on i_{th} atom and bordered by individual bond r_{ij} and r_{ik}.

2.3 Periodic boundary condition

While a bulk material contains atoms of the order of Avogadro number or more than that, a supercomputer can work with at most billion atoms and a desktop is able to deal with not more than million of atoms. This reality restricts the simulation methodologies applicable only for the systems of atomic clusters i.e. for the systems having nanosized volume. The feasibility of simulation methodologies can be extended above the limitation of simulation domain size by the introduction of periodic boundary condition(PBC). In Fig. 2.2 the concept of PBC has been illustrated. It assumes, as the name suggests, that the primary simulation supercell is repeated *ad infinitum* such that at any instant of time, an image cell is essentially an exact replica of the primary supercell. Only a very small portion of an infinite crystal is considered as the primary supercell for molecular dynamics simulation because the atoms in remaining part are image of the atoms of selected portion and a translation of the primary supercell, as shown in Fig .2.2(b), can alter the enclosed atomistic

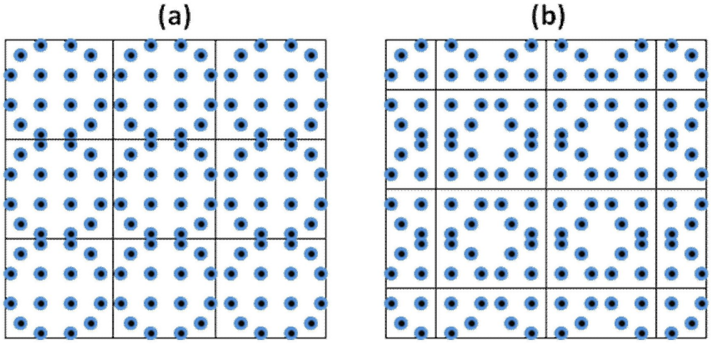

Figure 2.2: The periodic boundary condition: both the adjacent figures (a) and (b) generate, in effect, the same tiling even though the primary cell in (b) is obtained by horizontally translating the boundaries of the primary cell of (a).

configuration, yet the whole system consisting of the primary plus the image cells remains invariant. Thus, the apparent boundaries of primary supercell are not effective interfaces and unlike the simulations for nanostructures, in bulk simulations the surface effect can be avoided using the trick of PBC. Actually in the simulations of nanostructures, PBC is not used and the surface effect comes into play to exhibit the properties of nanomaterials. By the introduction of PBC, computational scheme always considers the infinite system as a whole and there is no hierarchy of preference among the primary and image cells. For the calculation of the force between two atoms a sphere is selected such that it contains only one closest image of each kind. Thus image convention method suggests that the radius of cut off sphere is less than half width of simulation cell. This technique, known as the 'minimum image convention', ensures that when an atom exits the primary cell and enters an adjacent image cell, another atom must enter the primary cell from the opposite boundary[16].

2.4 Molecular statics, energy minimization and stable atomic configuration

For the determination of the equilibrated atomic configuration of a material molecular statics(MS) calculations are introduced .The primary concept is to start from a given initial mechanically unstable structure and varying the atomic position coordinates until the resulting structure is in mechanical equilibrium. In this case, the restriction is that the net force in the final equilibrium system is zero although equilibration can be done both in the presence or absence of external forces. In the second case, the system is in the local minimum of the total potential energy. Molecular statics is an essential part of molecular mechanics. In most of the molecular dynamics simulations, the system is initially relaxed to its minimum energy structure using the MS algorithm. The minimum energy condition is also essential for calculations of free energy and different Monte Carlo simulations[16, 17]. Usually, the MS algorithms help a given system to relax to its nearest local minimum and can not cross any energy barrier during the entire process. For the search of global minimum, the methods like simulated annealing[18] and genetic algorithm[19] might be employed. However, these methods are only meant for better optimization but an algorithm, which can ensure the attainment of actual global optimum, does not exist so far. The work presented in this report has extensively used the local optimization of material structures and hence, some of the widely used algorithms employed for this purpose have been discussed in detail.

2.4.1 Steepest-descent method

It is called also as the 'Gradient descent' and is based upon the fact that a function, $f(\mathbf{r})$, always tends to decrease along the direction of $-\vec{\nabla} f$. Therefore, in every successive step, the function argument, $\mathbf{r}$, is updated so as to shift it along the direction of $-\vec{\nabla} f$ in small steps. Accordingly, we can use the following algorithm[16].

Step 1: Obtain the potential energy, $V(\mathbf{r})$, at the initial atomic coordinates given by the vector, $\mathbf{r}_0$, using some suitable empirical potential model or *ab initio* method.

Step 2: Compute the norm of the force vector, $-\vec{\nabla}\ V(\mathbf{r})$. If it does not exceed the maximum tolerance, terminate the algorithm.

Step 3: Obtain the unit vector $\hat{d} = \frac{-\vec{\nabla} f}{|-\vec{\nabla} f|}$.

Step 4: $\mathbf{r} \rightarrow \mathbf{r} + \chi\hat{d}$, where χ is a small step size.

Step 5: Continue from step 2.

Steepest descent is not a preferable choice for large number of atoms or when a high precision is required in the result. This is due to the fact that as the algorithm takes the system nearer to the optimum point, the convergence usually becomes increasingly slow. Therefore, we would use a more intelligent strategy as discussed below.

2.4.2 Conjugate-gradient relaxation

Alike the Steepest-descent this method also uses the atomic forces to obtain the local energy minimum. But unlike the Steepest-descent method, instead of searching along the direction of maximum gradient throughout the iterations, it follows a more innovative strategy. This algorithm is based upon the idea that faster convergence is possible if each search direction is conjugate to all the other search directions. For atomistic simulations, a nonlinear version of this algorithm is usually employed. In principle, this algorithm would be most efficient if the optimized function is quadratic, *i.e.*, $V(\mathbf{r}) = \frac{1}{2}\mathbf{r}^T.\mathbf{G}.\mathbf{r}$, where $\mathbf{r}$ if the coordinate vector and $(\mathbf{G})$ is a symmetric matrix. But in many practical cases, this algorithm converges fast enough. This method can use the following algorithm for energy minimization.

Step 1: Compute the atomic force vector, $\mathbf{F}$, as the negative gradient of potential. Exit if its magnitude is within the maximum tolerance.

Step 2: At the first iteration, set the search direction $\mathbf{s}^{[1]} \rightarrow \mathbf{F}^{[1]}$. Otherwise, for n^{th} iteration, calculate $k = \frac{\mathbf{F}^{[n]}.\mathbf{F}^{[n]}}{\mathbf{F}^{[n-1]}.\mathbf{F}^{[n-1]}}$, $\mathbf{s}^{[n]} \rightarrow \mathbf{F}^{[n]} + k\mathbf{s}^{[n-1]}$.

Step 3: Relax the system to its minimum energy only along the direction of $\mathbf{s}^{[n]}$.

Step 4: Continue from step 1.

Determination of the search direction, $\mathbf{s}$, is done here by the so called Polak-Ribiere formula[20]. It ensures that each search direction is conjugate to the previous one. Then it can be proven[21] that it would be conjugate to all the previous search directions as well.

2.4.3 Fast inertial relaxation engine

In contrast to the other two methods described above, the FIRE algorithm is an inertial (mass-dependent) technique based upon the methods of MD. This is a new method devised by Bitzek *et al.*[22]. In cases where the energy landscapes are too complicated, some other well known methods are found to have failed in converging fast enough. The present algorithm eliminates this drawback. It suggests to integrate the following equation of motion:

$$\frac{d\hat{\mathbf{v}}}{dt} = \frac{\hat{\mathbf{F}}(t)}{m} - \gamma(t)|\mathbf{v}(t)|[\hat{\mathbf{v}}(t) - \hat{\mathbf{F}}(t)] \tag{2.2}$$

where the hats ($\hat{}$) denote the unit vectors in the directions of the corresponding velocity and force vectors. The above equation says that to the usual Newtonian equation of motion, an addition acceleration is provided in a direction which is steeper that the equation of motion. With a time step, Δt, and an initial parameter, α_0, the Euler discretization of Eq. 2.2 yields the following algorithm:

Step 1: Initialize the velocity vector,$\mathbf{v} \rightarrow 0$.

Step 2: Calculate the force vector, $\mathbf{F}$, and integrate the equation of motion. Even a crude integration is satisfactory.

Step 3: Evaluate the power, $P = \mathbf{F}.\mathbf{v}$

Step 4: If $P > 0$ and the number of steps since P was negative is larger than N_{min}, $\Delta t \rightarrow$

$min(\Delta t f_{inc}, \Delta t_{max})$ and $\alpha \to f\alpha$.

Step 5: If $P \leq 0$, $\Delta t \to \Delta t f_{dec}$, $\mathbf{v} \to 0$ and $\alpha \to \alpha_0$.

Step 6: Continue from step 2 until the algorithm converges.

The parameter N_{min} is an integer. All other parameters accept f_{inc} are smaller than 1. FIRE is quite robust in the sense that the convergence is always good regardless of the choice of the initial parameters.

2.5 Molecular dynamics

From its heart, the molecular dynamics simulation is the tool for solving the following second order differential equation for a many body system:

$$\frac{d^2\mathbf{r}}{dt^2} = \frac{\mathbf{F}(\mathbf{r},t)}{m} \tag{2.3}$$

Generally, the net force, $\mathbf{F}$, is the sum of internal and external forces. When the net force is derivable from a time independent potential function, $V(\mathbf{r})$, the Hamiltonian of the system given by $H(\mathbf{r};\mathbf{p}) = \frac{|\mathbf{p}|^2}{2m} + V$, where $\mathbf{p}$ is the momentum vector, remains invariant in time. Using this Hamiltonian form, the classical equations of motion can be rewritten as

$$\frac{d\mathbf{r}}{dt} = \frac{\delta H}{\delta \mathbf{p}} \tag{2.4}$$

$$\frac{d\mathbf{p}}{dt} = -\frac{\delta H}{\delta \mathbf{r}} \tag{2.5}$$

2.5.1 Numerical integration of the equations of motion

It is now clear that in principle MD involves the solutions of Eq. 2.3 or Eq. 2.4 and 2.5. Although the idea is very simple, the actual numerical implementation is nontrivial. This is primarily due to the fact that most of the systems we simulate consist of a large number of atoms; even a small system of 10,000 atoms are associated to 60,000 variables of coordinates and momenta. So we are compelled to use the digital computers to solve such many body problems numerically. On the other hand, digital computers, albeit precise, can only solve discretized problems. However, discretizing an otherwise continuous mathematical form always yields some errors. Adding more precision by taking the accuracy to higher orders enhances the computational complexity and thus the CPU time. Hence, it is a challenging task to design an algorithmic solver, which gives optimized trade-off between accuracy and speed under the particular requirements of a given study. Here we shall discuss some of the well known numerical solvers for MD simulations[17].

2.5.1.1 Basic verlet algorithm

From Taylor series expansion we have

$$\vec{r}\,(t+\Delta t) = \vec{r}\,(t) + \vec{v}\,(t)\,\Delta t + \vec{a}\,(t)\,\frac{\Delta t^2}{2!} + O(\Delta t^3)$$

and

$$\vec{r}\,(t-\Delta t) = \vec{r}\,(t) - \vec{v}\,(t)\,\Delta t + \vec{a}\,(t)\,\frac{\Delta t^2}{2!} + O(\Delta t^3)$$

$\vec{r}(t)$, $\vec{v}(t)$ and $\vec{a}(t)$ are position, velocity and acceleration of an arbitrary atom at time t. Δt is the length of each time step.

Adding the above two equation

$$\vec{r}\,(t+\Delta t) = 2\vec{r}\,(t) - \vec{r}\,(t-\Delta t) + 2\vec{a}\,(t)\,\frac{\Delta t^2}{2!} + O(\Delta t^4). \tag{2.6}$$

And subtracting the 1st two equations

$$\vec{v}\,(t) = \frac{\vec{r}\,(t+\Delta t) - \vec{r}\,(t-\Delta t)}{2\Delta t} + O(\Delta t^2). \tag{2.7}$$

Limitations:

Verlet algorithm is not self-starting, since it requires the positions at two previous times (t and $t - \Delta t$) to get the position at the next time, $t + \Delta t$. Here velocity is not explicit and one step behind position and to get velocity, position of three consecutive steps are required[17].

2.5.1.2 Verlet leapfrog algorithm

Taylor series expansion generates

$$\vec{v}\left(t+\frac{\Delta t}{2}\right) = \vec{v}\,(t) + \vec{a}\,(t)\,\frac{\Delta t}{2} + \frac{\dot{\vec{a}}\,(t)}{2!}\left(\frac{\Delta t}{2}\right)^2 + O(\Delta t^3)$$

$$= \vec{v}\,(t) - \vec{a}\,(t)\,\frac{\Delta t}{2} + \vec{a}\,(t)\,\Delta t + \frac{\dot{\vec{a}}\,(t)}{2!}\left(\frac{\Delta t}{2}\right)^2 + O(\Delta t^3)$$

$$= \vec{v}\,(t) - \vec{a}\,(t)\,\frac{\Delta t}{2} + \frac{\dot{\vec{a}}\,(t)}{2!}\left(\frac{\Delta t}{2}\right)^2 + \vec{a}\,(t)\,\Delta t + O(\Delta t^3)$$

$$= \vec{v}\left(t-\frac{\Delta t}{2}\right) + \vec{a}\,(t)\,\Delta t + O(\Delta t^3). \tag{2.8}$$

$$\vec{r}\,(t+\Delta t) = \vec{r}\,(t) + \vec{v}\,(t)\,\Delta t + \vec{a}\,(t)\,\frac{\Delta t^2}{2!} + O(\Delta t^3)$$

$$= \vec{r}\,(t) + \left\{\vec{v}\,(t) + \vec{a}\,(t)\,\frac{\Delta t}{2}\right\}\Delta t + O(\Delta t^3)$$

$$= \vec{r}\,(t) + \vec{v}\left(t+\frac{\Delta t}{2}\right)\Delta t + O(\Delta t^3). \tag{2.9}$$

Limitations:

Although velocities are explicitly calculated, however, the disadvantage is that they are not calculated at the same time as the positions. The velocities are first calculated at time $t{+}1/2\Delta t$; these are used to calculate the positions, r, at time $t{+}\Delta t$. In this way, the velocities leap over the positions, then the positions leap over the velocities[17]. The velocities at time t can be approximated by the following way:

$$\vec{v}\left(t+\frac{\Delta t}{2}\right)=\vec{v}\left(t\right)+\vec{a}\left(t\right)\frac{\Delta t}{2}+\frac{\dot{\vec{a}}\left(t\right)}{2!}\left(\frac{\Delta t}{2}\right)^{2}+O(\Delta t^{3}),$$

$$\vec{v}\left(t-\frac{\Delta t}{2}\right)=\vec{v}\left(t\right)-\vec{a}\left(t\right)\frac{\Delta t}{2}+\frac{\dot{\vec{a}}\left(t\right)}{2!}\left(\frac{\Delta t}{2}\right)^{2}-O(\Delta t^{3}).$$

Adding last two equations

$$\vec{v}\left(t\right)=\frac{\vec{v}\left(t+\frac{\Delta t}{2}\right)+\vec{v}\left(t-\frac{\Delta t}{2}\right)}{2}+O(\Delta t^{2}).$$

2.5.1.3 Velocity verlet algorithm

Once again using Taylor series expansion

$$\begin{aligned}\vec{r}\left(t+\Delta t\right)&=\vec{r}\left(t\right)+\vec{v}\left(t\right)\Delta t+\vec{a}\left(t\right)\frac{\Delta t^{2}}{2!}+O(\Delta t^{3})\\&=\vec{r}\left(t\right)+\left\{\vec{v}\left(t\right)+\vec{a}\left(t\right)\frac{\Delta t}{2}\right\}\Delta t+O(\Delta t^{3})\\&=\vec{r}\left(t\right)+\vec{v}\left(t+\frac{\Delta t}{2}\right)\Delta t+O(\Delta t^{3}),\end{aligned}\tag{2.10}$$

Where,

$$\vec{v}\left(t+\frac{\Delta t}{2}\right)=\vec{v}\left(t\right)+\vec{a}\left(t\right)\frac{\Delta t}{2}+\frac{\vec{a}\left(t\right)}{2!}\left(\frac{\Delta t}{2}\right)^{2}+O(\Delta t^{3})$$

and

$$\begin{aligned}\vec{v}\left(t+\Delta t\right)&=\vec{v}\left(t\right)+\vec{a}\left(t\right)\Delta t+\dot{\vec{a}}\left(t\right)\frac{\Delta t^{2}}{2!}+O(\Delta t^{3})\\&=\vec{v}\left(t\right)+\vec{a}\left(t\right)\frac{\Delta t}{2}+\frac{\Delta t}{2}\left[\vec{a}\left(t\right)+\dot{\vec{a}}\left(t\right)\Delta t\right]+O(\Delta t^{3})\\&=\vec{v}\left(t\right)+\vec{a}\left(t\right)\frac{\Delta t}{2}+\vec{a}\left(t+\Delta t\right)\frac{\Delta t}{2}+O(\Delta t^{3})\\&=\vec{v}\left(t\right)+\frac{\Delta t}{2}\left[\vec{a}\left(t\right)+\vec{a}\left(t+\Delta t\right)\right]+O(\Delta t^{3}).\end{aligned}\tag{2.11}$$

This algorithm is free from all shortcomings which appear in the first two algorithms and has been used in simulation[17].

2.5.2 Statistical distribution at equilibrium

The total energy of a system, containing N atoms each of mass m and total interacting potential $V(\{r_i\})$, is the Hamiltonian of the system and is given by

$$H(\{p_i, r_i\}) = \sum_{i=1}^{N} \frac{|p_i|^2}{2m} + V(\{r_i\}),$$

where, p_i and r_i are momenta and position of i_{th} particle and $(\{p_i, r_i\}) = (p_1, p_2, .., p_i, .., p_N; r_1, r_2, .., r_i, .., r_N)$. Now the probability density of the system at absolute equilibrium temperature T with microstate$\{p_i, r_i\}$ is given by Boltzmann distribution[23]

$$f(\{p_i, r_i\}) = \frac{1}{Z} \exp\left[-\frac{H(\{p_i, r_i\})}{k_B T}\right],$$

where,

$$Z = \int \prod_{i=1}^{N} dr_i dp_i \exp\left[-\frac{H(\{p_i, r_i\})}{k_B T}\right]$$

with $k_B = 1.38 \times 10^{-23}$Joule/K, the Boltzmann's constant and Z is the partition function. Thus the ensemble average of a macroscopic quantity A is average over all possible microstates and is given by

$$\langle A \rangle = \frac{1}{Z} \int \prod_{i=1}^{N} dr_i dp_i A(\{p_i, r_i\}) \exp\left[-\frac{H(\{p_i, r_i\})}{k_B T}\right].$$

The average potential energy of the system is

$$U = \langle V(\{r_i\}) \rangle = \langle A \rangle = \frac{1}{Z} \int \prod_{i=1}^{N} dr_i dp_i V(\{r_i\}) \exp\left[-\frac{H(\{p_i, r_i\})}{k_B T}\right]$$

$$= \frac{\int \prod_{i=1}^{N} dr_i V(\{r_i\}) \exp\left[-\frac{V(\{r_i\})}{k_B T}\right]}{\int \prod_{i=1}^{N} dr_i \exp\left[-\frac{V(\{r_i\})}{k_B T}\right]}.$$

Similarly kinetic energy of j_{th} atom is

$$\langle E_{K.E}, j \rangle = \frac{\int dp_j \frac{|p_j|^2}{2m} \exp\left[-\frac{|p_j|^2}{2mk_B T}\right]}{\int dp_j \exp\left[-\frac{|p_j|^2}{2mk_B T}\right]} = \frac{3}{2} k_B T.$$

If $V(\{r_i\})$ is quadratic function then $U = \langle V(r_i) \rangle = \frac{3}{2} N k_B T$ and total average energy of the system is 3N$k_B T$.

2.5.3 Temperature initialization and its maintenance

The symplectic integrator like Velocity-Verlet inherently simulate an isolated system with conserved total energy if no explicit provision is made. However, one can seldom be interested in simulating an isolated system and instead, the canonical (constant temperature) ensemble needs to be simulated more often. In molecular dynamics, the thermostat algorithms are used to maintain a system at a constant desired temperature. Following is the detailed descriptions of three of the most commonly employed thermostats in MD.

2.5.3.1 Velocity scaling

The instantaneous temperature, $T(t)$, of the N atom system is defined as

$$T(t) = \frac{\sum_{i=1}^{n} m_i v_i^2}{3Nk}. \tag{2.12}$$

The velocity scaling[24] algorithm maintains the desired object temperature, T_{obj}, simply by scaling the instantaneous velocities with the multiplication factor, λ, as $v(t) \rightarrow \lambda v(t)$, where $\lambda = \sqrt{\frac{T_{obj}}{T(t)}}$. The obvious disadvantage of this method is that the system's temperature remains precisely constant throughout the simulation and no thermal fluctuation is observed, which renders this method unrealistic. Moreover, the scaling can take the system away from the initial Boltzmann's distribution.

2.5.3.2 Berendsen thermostat

This method implements a differential negative feedback to maintain the temperature. In this case, a virtual heat bath acts as the source or sink of thermal energy and exchanges heat with the system to either increase or decrease the temperature. Here the extent of coupling between the system and the heat bath is tunable in terms of a relaxation constant, τ , which further determines the velocity scaling factor, λ. The following relation is employed for this purpose[25],

$$\frac{dT(t)}{dt} = \frac{T_{obj} - T(t)}{\tau}. \tag{2.13}$$

Here τ is typically specified in the unit of picoseconds and the scaling factor is given by

$$\lambda = \sqrt{1 + \frac{\delta t}{\tau}\left\{\frac{T_{obj}}{T(t - \frac{\delta t}{2})} - 1\right\}}. \tag{2.14}$$

The change in the temperature in one time step is now

$$\delta T = \delta t \left\{\frac{T_{obj} - T(t)}{\tau}\right\}. \tag{2.15}$$

Unlike the velocity scaling method, the temperature fluctuations are present in the Berendsen algorithm. A small value of τ reduces the fluctuations, whereas a large value increases them. At $\tau = \delta t$, this algorithm reduces to the velocity scaling method. Berendsen algorithm also fails to maintain the statistical distribution of the canonical ensemble.

2.5.3.3 Nose-Hoover thermostat

Similar to the Berendsen method, the Nose-Hoover thermostat also considers a constant temperature heat reservoir as a part of the system. In this case, the thermal mass, Q, dictates the extent of coupling with the heat bath and thus controls the thermal fluctuations. Here a details of this thermostat is presented in detail. In its original form, S. Nose[26, 27] introduced an extra degree of freedom, s, and proposed a modified Lagrangian,

$$L(\mathbf{r}, \dot{\mathbf{r}}, s, \dot{s}) = \sum_i \frac{1}{2} m_i s^2 \dot{\mathbf{r}}_i^2 - V(\mathbf{r}) + \frac{1}{2} Q \dot{s}^2 - gKT_{obj} \ln s, \tag{2.16}$$

where $g = 3N + 1$ is the total number of degrees of freedom for the 3D simulation including the extra degree, s. Nose proposed that this extra degree of freedom can be perceived as a scaling factor relating the real time step, say $\delta t'$, to the scaled time step, δt, as

$$\delta t' = \frac{\delta t}{s}. \tag{2.17}$$

Similarly, the other scaled quantities are also related to their corresponding real counterparts and accordingly, $\dot{\mathbf{r}}_i' = s\dot{\mathbf{r}}_i$. The real momentum of particle i, $\mathbf{p}_i'$, is related to the scaled value, $\mathbf{p}_i$, as $\dot{\mathbf{p}}_i' = \dot{\mathbf{p}}_i / s$. Clearly, Eq. 2.16 expresses the Lagrangian in the scaled time frame. Nose proved that if the Lagrangian in Eq. 2.16 is used to generate the equation of motion, the potential term, $gkT_{obj} \ln s$, forces the system to sample the canonical ensemble.

Using the Lagrangian in Eq. 2.16, we obtain the following partial derivatives,

$$\frac{\partial L}{\partial \dot{\mathbf{r}}_i} = m_i s^2 \dot{\mathbf{r}}_i, \tag{2.18}$$

$$\frac{\partial L}{\partial \dot{s}} = Q\dot{s}, \tag{2.19}$$

$$\frac{\partial L}{\partial \mathbf{r}_i} = -\frac{\partial V}{\partial \mathbf{r}_i}, \tag{2.20}$$

$$\frac{\partial L}{\partial s} = \sum_i m s \dot{\mathbf{r}}_i^2 - \frac{g}{\beta s}, \tag{2.21}$$

where $\beta = \frac{1}{kT}$. We can now form the Lagrange's equation of motion as

$$\frac{d}{dt}\left(\frac{\partial L}{\partial \dot{\mathbf{r}}_i}\right) - \frac{\partial L}{\partial \mathbf{r}_i} = 0, \tag{2.22}$$

which yields the equation of motion

$$\ddot{\mathbf{r}}_i = -\frac{2\dot{\mathbf{r}}_i \dot{s}}{s} - \frac{1}{m_i s^2}\frac{\partial V}{\partial \mathbf{r}_i}. \tag{2.23}$$

Equation Eq. 2.23 can be rescaled to the real time axis as

$$\ddot{\mathbf{r}}_i' = -\frac{2}{s}\frac{ds}{dt'}\dot{\mathbf{r}}_i' - \frac{1}{m_i}\frac{\partial V}{\partial \mathbf{r}_i}. \tag{2.24}$$

In the same way, the Lagrange's equation for the degree of freedom, s, can be written as

$$\frac{d}{dt}\left(\frac{\partial L}{\partial \dot{s}_i}\right) - \frac{\partial L}{\partial s_i} = 0, \tag{2.25}$$

which gives the solution,

$$Q\ddot{s} = \sum_i m s \dot{\mathbf{r}}_i^2 - \frac{g}{\beta s}. \tag{2.26}$$

Similar to Eq. 2.24, Eq. 2.26 is also re-scalable to the real time domain as

$$\frac{\partial^2 s}{\partial t^2} = \frac{1}{Q}\left(\sum_i m s \dot{\mathbf{r}}_i'^2 - \frac{gs}{\beta}\right). \tag{2.27}$$

Using Eq. 2.16, we obtain the conjugate momenta

$$\mathbf{p}_i = \frac{\partial L}{\partial \dot{\mathbf{r}}_i} = m_i s^2 \dot{\mathbf{r}}_i, \tag{2.28}$$

$$p_s = \frac{\partial L}{\partial \dot{s}} = Q\dot{s}. \tag{2.29}$$

The Nose Hamiltonian is accordingly given by

$$\begin{aligned} H &= \sum_i \mathbf{p}_i \dot{\mathbf{r}}_i + p_s \dot{s} - L \\ &= \frac{1}{2} \sum_i \frac{p_i^2}{m_i s^2} + V(\mathbf{r}_i) + \frac{p_s^2}{2Q} + \frac{g \ln s}{\beta}. \end{aligned} \tag{2.30}$$

Hamilton's equations become

$$\dot{\mathbf{p}}_i = -\frac{\partial H}{\partial \mathbf{r}_i} = -\frac{\partial U}{\partial \mathbf{r}_i}, \tag{2.31}$$

$$\dot{\mathbf{r}}_i = \frac{\partial H}{\partial \mathbf{p}_i} = \frac{\mathbf{p}_i}{m_i s^2}, \tag{2.32}$$

$$\dot{p}_s = -\frac{\partial H}{\partial s} = \sum_i \frac{p_i^2}{m_i s^3} - \frac{g}{\beta s}, \tag{2.33}$$

$$\dot{s} = \frac{\partial H}{\partial p_s} = \frac{p_s}{Q}. \tag{2.34}$$

In real time frame, the conjugate equations are

$$\mathbf{p}'_i = \frac{\partial L'}{\partial \mathbf{r}'_i} = m_i \dot{\mathbf{r}}'_i = \frac{\mathbf{p}_i}{s}, \tag{2.35}$$

$$p'_s = \frac{\partial L'}{\partial \dot{s}'} = \frac{Q}{s^2} \frac{ds}{dt'} = \frac{p_s}{s}. \tag{2.36}$$

Now, the time derivatives of the real time quantities can be obtained using the Eqs. 2.31-2.34 as

$$\frac{d\mathbf{p}'_i}{dt'} = -\frac{\mathbf{p}'_i s p'_s}{Q} - \frac{\partial V}{\partial \mathbf{r}_i}, \tag{2.37}$$

$$\frac{d\mathbf{r}_i}{dt'} = \frac{\mathbf{p}'_i}{m_i}, \tag{2.38}$$

$$\frac{dp'_s}{dt'} = \frac{1}{s} \left(\sum_i \frac{p_i'^2}{m_i} - \frac{g}{\beta} \right) - \frac{s p_s'^2}{Q}, \tag{2.39}$$

$$\frac{ds}{dt'} = \frac{s^2 p'_s}{Q}. \tag{2.40}$$

Similarly the Hamiltonian given in Eq. 2.30 is expressed in terms of the real time variables as

$$H' = \sum_i \frac{p_i'^2}{2m_i} + V(\mathbf{r}_i) + \frac{s^2 p_s'^2}{2Q} + \frac{g \ln s}{\beta}. \tag{2.41}$$

In spite of being a conserved quantity, H' is not a Hamiltonian in true sense, for it does not provide the equations of motion, e.g.,

$$\frac{\partial \mathbf{p}_i'}{\partial t'} \neq -\frac{\partial H'}{\partial \mathbf{r}_i}. \tag{2.42}$$

To further simplify the mathematical structure of the thermostat, Hoover[28] defined the new variable

$$\zeta \equiv \frac{p_s}{Q} = \frac{s p_s'}{Q} = \dot{s} = \frac{d \ln s}{dt'}. \tag{2.43}$$

Thus, the Eqs. 2.37-2.40 can be rewritten as

$$\frac{d\mathbf{p}_i'}{dt'} = -\zeta \mathbf{p}_i' - \frac{\partial V}{\partial \mathbf{r}_i}, \tag{2.44}$$

$$\frac{d\mathbf{r}_i}{dt'} = \frac{\mathbf{p}_i'}{m_i}, \tag{2.45}$$

$$\frac{d\zeta}{dt'} = \frac{1}{Q}\left(\sum_i \frac{p_i'^2}{m_i} - \frac{g}{\beta}\right), \tag{2.46}$$

$$\frac{d \ln s}{dt'} = \zeta. \tag{2.47}$$

Using Eqs. 2.44 and 2.45, we obtain

$$\ddot{\mathbf{r}}_i' = -\frac{1}{m_i}\frac{\partial V}{\partial \mathbf{r}_i} - \zeta \dot{\mathbf{r}}_i, \tag{2.48}$$

$$\dot{\zeta}' = \frac{1}{Q}\left(m_i |\mathbf{r}_i'|^2 - \frac{g}{\beta}\right). \tag{2.49}$$

Defining the instantaneous temperature, T_{inst}, as

$$\frac{1}{2}gk_BT_{inst} = \frac{1}{2}\sum_i m_i|\mathbf{r}'|^2, \tag{2.50}$$

we get from Eq. 2.49,

$$\dot{\zeta}' = \frac{gk_B}{Q}(T_{inst} - T_{obj}), \tag{2.51}$$

where T_{obj} is the object temperature. The above equation indicates a differential feedback system. If $T_{inst} > T_{obj}$, ζ increases until it becomes positive. Once it becomes positive, it starts exerting a drag force on the atoms to reduce the velocities and hence, reduces the temperature. Due to the Nose-Hoover thermostat, the instantaneous temperature always fluctuates around the object temperature.

2.6 Summary

In this chapter several essential concepts associated to the atomistic simulations of materials are discussed. The concept of molecular dynamics simulations is articulated and the relevant algorithms are also presented. In particular, various inter atomic potentials, the periodic boundary condition, structural relaxation, and integration algorithms for the constant temperature simulation have been elaborated. In the subsequent chapters, we will face with these issues frequently, when the simulation methods will be employed to solve the objective problems of this thesis.

Bibliography

[1] N. Metropolis *et al.*, J. Chem. Phys. 21 (1953) 1087 .

[2] E. Fermi, J. G. Pasta and S. M. Ulam, Studies of non-linear problems. LASL Report, LA-1940 (1955).

[3] B. J. Alder and T.E. Wainwright, in Proc. of the Int. Symp. on stat. mech. theory of transport processes (Brussels, 1956), (Interscience, Wiley, New York, 1958).

[4] J. B. Gibson, A. N. Goland, M. Milgram and G.-H. Vineyard, Phys. Rev. 120 (1960) 1229.

[5] D. S. Sholl and J. A. Steckel, Density functional theory: A practical introduction, (John Wiley and Sons, New Jersy, 2009).

[6] J. E. Lennard-Jones, Proc. R. Soc. Lond. A, 106 (1924) 463.

[7] F. Stillinger and T. A. Weber, Phys. Rev. B, 31 (1985) 5262.

[8] M. S. Daw and M. I. Baskes, Phys. Rev. B, 29 (1984) 6443.

[9] M. S. Daw, S. M. Foiles, and M. I. Baskes, Mat. Sci. Rep., 9 (1993) 251.

[10] M. W. Finnis and J. E. Sinclair, Phil. Mag. A 50 (1984) 45, ibidem 53 (1986) 161.

[11] M. W. Finnis and J. E. Sinclair, Phil. Mag. A 53 (1986) 161.

[12] G. J. Ackland , M. W. Finnis and V. Vitek, J. Phys. F: Met. Phys. 18 (1988) L153.

[13] G. J. Ackland and V. Vitek, Phys. Rev. B 41 (1990) 10324 .

[14] H. R.-Tabar and A. P. Sutton, Phil. Mag. Lett. 63 (1991) 217.

[15] X. D. Dai, Y. Kong, J. H. Li and B. X. Liu, J. Phys.: Cond. Mat. 18 (2006) 4527.

[16] V. V. Bulatov and W. Cai, Computer Simulations of Dislocations (Oxford University Press, Oxford, 2006).

[17] Handbook of materials modeling, edited by S. Yip (Springer, Netherlands, 2006).

[18] P. Salamon, P. Sibani and R. Frost, Facts, conjectures, and improvements for simulated annealing (Society for industrial and applied mathematics, Philadelphia, 2002).

[19] D. E. Goldberg, Genetic Algorithms (Pearson Education, New Delhi, 2009).

[20] E. Polak and G. Ribiere, Revue Francaise Inf. Rech, Oper. 16 RI (1969) 35. 60

[21] W. H. Press, B. P. Flannery, S. A. Tukolsky and W. T. Vetterling, Numerical Recipes in C: The Art of Scientific Computing (Cambridge University Press, Cambridge, 1992).

[22] E. Bitzek, P. Koskinen, F. Ghler, M. Moseler and P. Gumbsch, Phys. Rev. Lett. 97 (2006) 170201.

[23] D. ter Haar, Elements of statistical mechanics (Butterworth-Heinemann Ltd., Oxford, 1995).

[24] R. J. Sadus, Molecular Simulation of Fluids (Elsevier, Amsterdam, 1999).

[25] H. J. C. Berendsen et al., J. Chem. Phys. 81 (1984) 3684.

[26] S. Nose, Mol. Phys. 52 (1984) 255.

[27] S. Nose, J. Chem. Phys. 81 (1984) 511.

[28] W. G. Hoover, Phys. Rev. A 31 (1985) 1695.

Chapter 3

Scaling Property of Kinetic Energy

3.1 Introduction

Scaling as a manifestation of underlying dynamics of dynamical systems is familiar throughout the physics fraternity. It has been instrumental in helping scientific community to gain deeper insights into problems ranging across the entire spectrum of science and technology. Scaling laws typically reflects the underlying generic features and the physical principles which are independent of detailed dynamics or characteristics of a particular model. Scale invariance has been found to hold empirically for a number of complex systems, and the correct evaluation of the scaling exponents is of fundamental importance in assessing if any universal class exists [1]. Scale invariance seems to be widespread in natural systems. Numerous examples of scale invariance properties are found in literatures in the fields like rainfall, econophysics, fractal, network, cloud earthquakes etc.[2, 3, 4, 5, 6, 7, 8, 9, 10].

Scaling analysis searches for property which describes the self-similarity of time series. Actually the fractal nature of an object leads to the idea of the statistical self-similar property. The statistical self-similarity property resemble the structure of an object by composing its sub-unit and sub-sub-unit in successive levels. Theoretically and mathematically this property should maintained in all possible scales. Practically, however, there exists a limit of upper and lower value of scale where self-similarity property is observed. For a curve in two dimension, its self-similarity can be determined by taking a part of the curve as the subset of the original and enlarging the subset with the help of rescaling such that its size is equal to that of the original curve both along height and width. The statistical property of enlarged subset and the original curve are then compared to test the self-similarity. As already mentioned the idea of fractal structure is extendable to the analysis of complex temporal processes. But the challenge in the determination and quantification of self-similarity of temporal process is that unlike the fractal although the present data is also two dimensional in nature yet the time series is associated to different physical variable. Whereas the horizontal axis represents the 'time', the vertical axis may show the variation of some other physical or biophysical variables like kinetic energy, momentum, stress, strain, heartbeat etc. Thus two the axes have two different unit (in this case unit of time and kinetic energy). On the contrary, geometrical curves the situation is different, where both axes have unit of length(for two dimension). Thus for proper comparison of original and magnified data associated to complex temporal processes we need two different magnification factor. One for time axis and other one for the physical quantity, the time variation of which is the focus of this work.

In terms of mathematics, in the light of above discussed paragraph, the self-similarity of a temporal process can be represented as

$$y(t) \overset{d}{\equiv} a^{\alpha} \, y\left(\frac{t}{a}\right)$$

where $\overset{d}{\equiv}$ implies equivalence of the statistical properties of both side of the equation are identic. In alternative words a self-similar statistical process, y(t), has the the similar probability distribution as that of a rescaled process, $a^{\alpha} \, y\left(\frac{t}{a}\right)$. That means if the time scale is rescaled by a factor $a(t \to t/a)$ then the variable y is rescaled by factor a^{α}, with α as scaling exponent or self-similarity parameter.

For two distributions to be identical, they should maintain this criteria for all the moments similar and then the two associated processes will be self-similar. This is practically a difficult practice and we limit ourselves this criteria up to only variance of the distributions. Lets consider a time series, for example, and a sub-set of it. The x axis and y axis of the sub-set are rescaled by factors M_x and M_y respectively in order to retrieve the original series. The scaling exponent α is then

$$\alpha = \frac{\ln a^{\alpha}}{\ln a} = \frac{\ln M_y}{\ln M_x}$$

If the lengths of time windows of original series and sub-set series are n_1 n_2 respectively then $M_x = \frac{n_1}{n_2}$. Magnification factor associated to the y axis is determined by calculating the standard deviations(s_1 and s_2) of y variable for time windows n_1 and n_2. This method results in $M_y = \frac{s_1}{s_2}$. Hence

$$\alpha = \frac{\ln a^{\alpha}}{\ln a} = \frac{\ln M_y}{\ln M_x} = \frac{\ln \frac{s1}{s_2}}{\ln \frac{n1}{n_2}} = \frac{\ln s1 - \ln s_2}{\ln n1 - \ln n_2}$$

Thus the scaling exponent is nothing but the slope the straight line obtained from the $\log - \log$ plot of standard deviation(s) against length of time window(n). In doing so, for each time window, a number of sub-sets of equal size are considered to calculate average standard deviation(s). The averaging procedure enable us to get more accurate and reliable scaling exponent(α).

3.2 Self-Similar Process, time series and their mapping

The Previous section clearly signifies that if $\alpha > 0$ then with the length of time window the fluctuation(which is equivalent to the standard deviation, s) increases and the time series is unbounded one. On the contrary, in reality whatever be the length of time window the fluctuation and hence the corresponding standard deviation of the series is finite i.e. practical time series are restricted to bounded one. For heart rate time series it is seen that only if x axis of a sub-set is rescaled then automatically the y axis becomes self-similar.

This implies $M_y = 0$ and hence $\alpha = 0$. By randomizing the original heart rate time series if completely uncorrelated white noise time series is generated then also the scaling exponent remain unchanged($\alpha = 0$). Then the issue is what is the difference between the $\alpha(= 0)$ of complex correlated time series and $\alpha(= 0)$ of randomized and uncorrelated time series. An innovative idea to dodge this issue of times series analysis is to consider the fractal property of integrated time series of the temporal process instead of the original time series of the complex temporal process. Alike physiological time series, the random noise acting on a Brownian particle is bounded in nature. However, its trajectory is the result of all earlier random forces and is a unbounded time series having fractal property with a scaling exponent. Similarly application of fractal scaling analysis to the integrated time series of previously discussed original and randomized heart rate time series produces two different similarity parameter α. In the present chapter, it is the fractal scaling analysis which is going to be used on integrated time series.

3.3 What is Levy distribution?

Usually in traditional scaling analysis people study pick up the variance for the test of scaling behavior. This is possible if the time series possesses a finite variance. However, Paul Levy observed an exceptional case where the central limit theory does not hold good and the variance and the other higher moments of the series diverge [11]. In terms of Fourier Transform the Levy distribution can be represented by

$$f(k) = \exp(-a|k|^{\alpha}) \quad 0 \leq \alpha \leq 2$$

and for asymptotic case, $k \to \infty$ the distribution is

$$f(k) = |k|^{-1-\alpha}$$

Since Practically, in scaling analysis, finite time series is taken hence we can use variance method given that the variance of the series is finite. Otherwise the variance would turn into a erroneous method. In order to get escape from this serious issue Scafetta *et al.* [12, 13] came with a new method of scaling analysis which study the scaling nature of probability distribution in place of its variance. This method is familiar as diffusion entropy analysis(DEA) in the field of scaling analysis of time series and it is based on the calculation Shannon entropy. In the scaling analysis of time series data of kinetic energy individual constituent particles of non-equilibrium crystalline systems we use two methods: DEA method and Finite variance scaling method(FVSM). Simultaneous use of these two methods is necessary to draw a conclusion whether the said process shows Gaussian or Levy nature. In the next three sections we would discuss about the formulation DEA and FVSM methods.

3.4 Introduction to diffusion trajectory

The process of equilibration is a sort of diffusion of kinetic energy and potential energy. For scaling analysis of a diffusion process it is required to generate diffusion trajectories for different time windows. Lets consider a time series data $\{\xi_i : 1 \leq i \leq N\}$ and consider the following representation

$$\xi_i^s = \xi_{i+s}$$

Total N number of diffusion trajectories are possible and the width of the time window varies from 1 to N. For time window t, the diffusion trajectory can be represented in terms of $N - t + 1$ subsequences. The s_{th} subsequence of diffusion trajectory corresponds to time window t is

$$x^s(t) = \sum_{i=1}^{t} \xi_i^s = \sum_{i=1}^{t} \xi_{i+s}, 0 \leq s \leq N - t$$

3.5 Diffusion entropy analysis

Dynamical systems arising from diversified disciplines of science can be quantified in a unified way from their scale invariance properties. Scafetta *et al.* introduced two complementary scaling analysis methods: the diffusion entropy analysis and the finite variance scaling method (FVSM) to evaluate correct scaling that prevails in complex dynamical systems.

For time window t the subsequences of the diffusion trajectory probability distribution function is calculated. The Shannon entropy associated to each trajectory can be expressed as

$$S(t) = -\int_{-\infty}^{+\infty} p(x,t) \ln[p(x,t)]\, dx$$

where, $p(x,t)$'s are the probabilities of the probability distribution function of the concerned diffusion trajectory.

Considering the scaling condition $p(x,t) = t^{-\delta} F(xt^{-\delta})$ holds appropriately, the Shannon entropy can be easily represented as

$$S(t) = A + \delta \ln t$$

where, A is a constant given by $A = \int_{-\infty}^{+\infty} F(y) \ln F(y)\, dy$ and δ is scaling exponent. A semi-log plot of Shannon entropy $S(t)$ against t is a straight line with exponent δ as its slope.

3.6 Standard deviation analysis

The other methodology (FVSM) introduced by Scafetta *et al*. uses the second moment of the diffusion trajectory to examine the scaling property. Standard deviation analysis is one version of FVSM. The evolution of standard deviation $D(t)$ of variable $x^s(t)$ for different

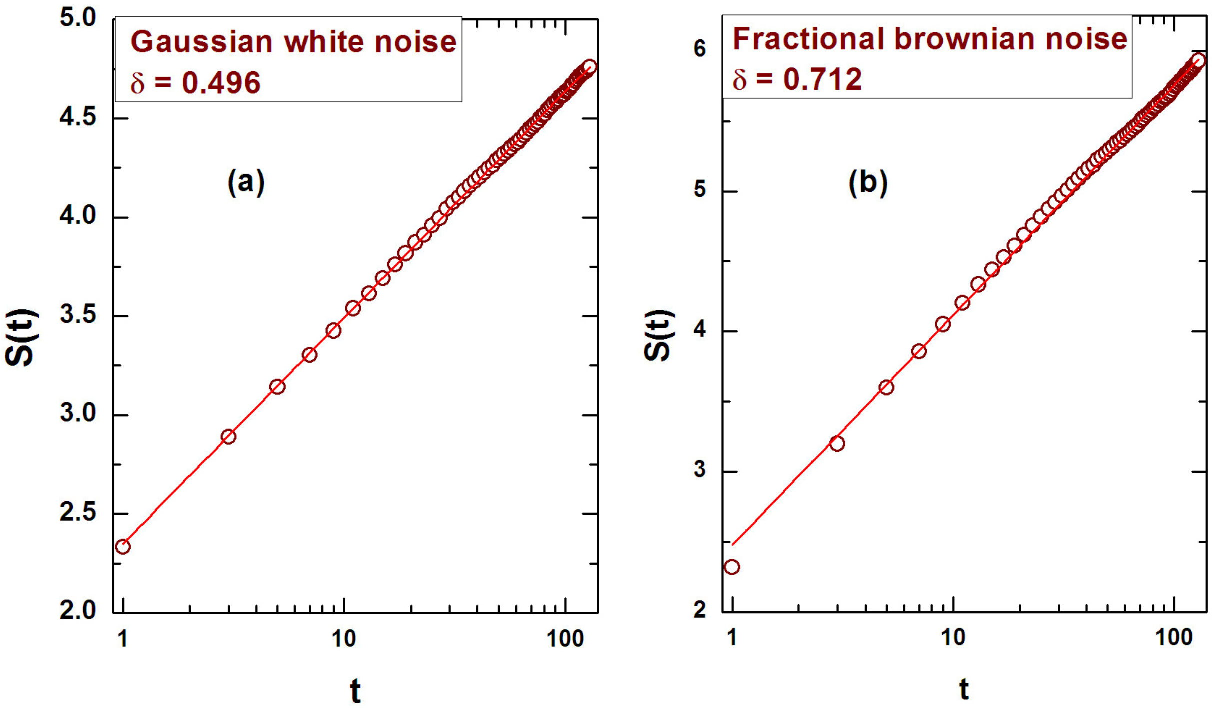

Figure 3.1: Scaling exponents of (a) Gaussian white noise and (b) fractional Brownian noise from diffusion entropy analysis

time windows are used to test the scaling property. The standard deviation $D(t)$ of the diffusion trajectory having time window t is given by

$$D(t) = \sqrt{\frac{\sum_0^{N-t}[x^s(t) - \bar{x}^s(t)]^2}{N-t}}$$

where, $\bar{x}^s(t)$ is the average of the all subsequences of diffusion trajectory of time window t.

According to the traditional wisdom of the methods based on variance, the existence of scaling is assessed by observing, with numerical methods, the following property:

$$D(t) \propto t^H$$

$$\ln D(t) = \text{constant } + H \ln t$$

The exponent H is interpreted as scaling exponent of the diffusion process. The slope of

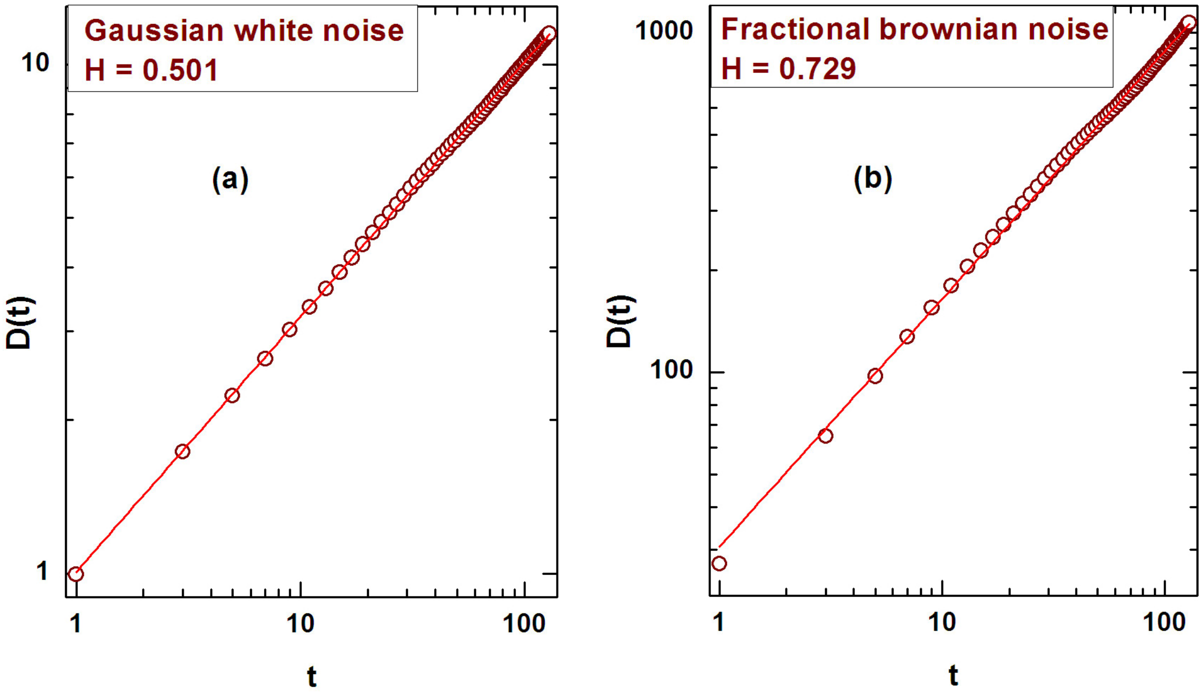

Figure 3.2: Scaling exponents of (a) Gaussian white noise and (b) fractional Brownian noise from standard deviation analysis

straight line obtained from log-log plot of $D(t)$ against t provides the scaling exponent.

3.6.1 Scaling exponents for various kind of time series data

For random noise with finite variance, the diffusion distribution $p(x,t)$ will converge, according to the central limit theorem, to a Gaussian distribution with $H = \delta = 0.5$. If $H \neq \delta$, the scaling represents anomalous behavior. Levy-walk is a kind of anomalous diffusion which is obtained by generalizing the central limit theorem [14]. In this particular kind of diffusion process the scaling exponents H and δ are found to obey the relation $\delta = (3-2H)^{-1}$ instead of being equal [13].

Gaussian white noise : $\delta = H = 0.5$ (Fig. 3.1(a) and Fig. 3.2(a))

Fractional Brownian noise : $\delta = H = 0.7$ (Fig. 3.1(b) and Fig. 3.2(b))

Levy flight : scaling exponent can not be defined properly by these two methods. Because of long tail of the distribution of such and as a result we can not define the standard deviation of the time series.

Levy walk : $\delta = \frac{1}{3-2H}$

When each step of a Levy motion takes the same time regardless of length, the process is usually called a Levy flight. A Levy motion is called a Levy walk when the time taken for each step is proportional to its length. Levy flights and walks have very different scaling behaviors: the former are characterized by memoryless jumps governed by a heavy-tail, while the latter, now having a fixed step size, have attained serial correlations within each huge jump [15].

3.7 Scaling analysis and equilibrium process

Since non-equilibrium systems are ubiquitous in nature and equilibrium systems are ideal and can only be achieved in the laboratory. Attempts have been made to understand the dynamics of non-equilibrium systems by linear response theory [16] albeit its domains of validity are restricted to the linear response regime. There exists no general formalism to deal with systems that are far from equilibrium. For a system out of equilibrium, the probability of a given microstate evolves continuously with time. In the long time limit the system reaches a stationary state in which the probability measure over the configuration space converges to a constant distribution. Non-equilibrium systems display fluctuations which are less sensitive to the conditions of the surroundings and carry information about the dynamics of its present state. In the last decade certain general relations have been discovered which are valid for non-equilibrium systems and are independent of how far the system is driven out of equilibrium. These results include the Jarzynski equality [17, 18] and the fluctuation theorems [19, 20, 21, 22, 23, 24, 25, 26, 27]. They have been verified for a variety of systems theoretically as well as experimentally [28, 29, 30, 31, 32]. After the work by Crooks [22] and Seifert [23], it is now understood that many of these relations are closely related to the path probability of the systems trajectory. In the absence of any general theory to understand the dynamics of a system far from equilibrium, one approach will be to take a simple but nontrivial model system and try to understand its dynamics when it approaches equilibrium from its non-equilibrium state. The general dynamical behavior of a non-equilibrium system will consist of superposition of various dynamics on well speared time scales which compel several thermodynamic parameters of the system like heat, work, internal energy, kinetic energy of the particles of the system to fluctuate. To understand the general features of the dynamics one has to apply statistical analysis to these fluctuations. In this chapter an attempt has been made to study a universal scaling relation for systems driven far from equilibrium by analyzing its fluctuation properties. Application of two aforesaid complementary scaling analysis methods(DEA and SDA)[12, 13] produce the universal scaling relation for the non-equilibrium systems. The non-equilibrium systems of study are generated by molecular dynamics simulation[33] technique.

3.8 Simulation procedure

To generate the non-equilibrium model system molecular dynamics (MD) simulation technique has been utilized the in an innovative way. Depending on the interaction potential model, a typical MD simulation computes the trajectories of atoms in a system by solving Newtons equations of motion numerically. In this chapter, the simulations have been performed for elements having different crystal structures like Silicon (Si) and Germanium (Ge) with diamond cubic structure, Iron (Fe) and Molybdenum (Mo) with body centered cubic structure and Copper (Cu), Aluminium (Al) and solid Argon (Ar) having face centered cubic structure. Thus, a variety of interaction potential models have been employed (refer Table 3.1) in the simulations. For all these elements, periodic boundary conditions are imposed along three directions (x,y,z) in the simulation cell. Initially, all the systems are equilibrated using constant energy and volume ensemble (NVE) at 100 K for 2.5 ps except for Ar, where the equilibration run is performed at 30K for 10 ps. The kinetic energy in the equilibrium state will follow Boltzmann distribution. The period of time for equilibration is chosen to be sufficient to bring the total energy of the system to divide approximately equally between kinetic energy (KE) and potential energy (PE). Details of the parameters used in the simulations like simulation cell size, number of atoms taken in the simulation cell, the time steps after which simulation data are recorded and the nature of the inter-atomic potentials used for the elements under study are given in Table I. To generate the non-equilibrium state, the three components of velocities of individual atom in the simulation cell were changed to random values such that the instantaneous KE of the atom increases however the average temperature of the system corresponds to T = 500 K (T = 70 K for Ar). The atoms in the simulation cell are then allowed to equilibrate. After sufficiently long period of time, the system is observed to attain equilibrium temperature of 300 K (50 K for Ar) and the average kinetic energy becomes equal to the average potential energy of the respective systems. The variations of temperature (equivalent to KE) with time of the systems of Al and Cu leading to equilibration are shown in Fig. 3.3. Atomistic simulation data are recorded for each time step for the entire equilibration time to study the dynamic nature of the equilibration process.

3.9 Result of scaling analysis

Few atoms in the simulation cell are identified in a sphere of radius ‘r’ whose centre is chosen to be almost at the middle of the cell, far away from the surface. The values of ‘r’ and the number of atoms in the sphere for each simulation are given in Table 3.1. The KE in the consecutive time steps for the atoms in the sphere are used for further analysis. In these simulations the atoms in the simulation cell are kept isolated from the environment and hence there was no dissipation of energy, only there is a redistribution of KE and PE among

Table 3.1: The parameters used for the MD simulations.

Material	**Si**	**Ge**	**Cu**	**Solid Ar**	**Mo**	**Fe**	**Al**
Simulation cell size (in unit cell)	25^3	15^3	20^3	20^3	25^3	25^3	20^3
Number of atoms in simulation cell	125000	27000	32000	32000	31250	31250	32000
Simulation time step (fs)	0.25	0.5	0.5	2.0	0.5	0.5	0.5
Nature of inter-atomic potential used	SW[a]	SW	EAM[b]	LJ[c]	FS[d]	FS	GLUE
Total number of data taken	6000	3000	3000	10000	3000	3000	3000
Radius 'r' (Å)	8.8250	9.0809	5.4766	7.9952	6.2944	5.7330	6.1566
No of atoms in the sphere of radius 'r'	150	147	55	55	63	63	55

---

[a] SW (Stillinger-Weber)
[b] EAM (Embedded Atom Model)
[c] LJ (Lennard-Jones)
[d] FS (Finnis-Sinclair)

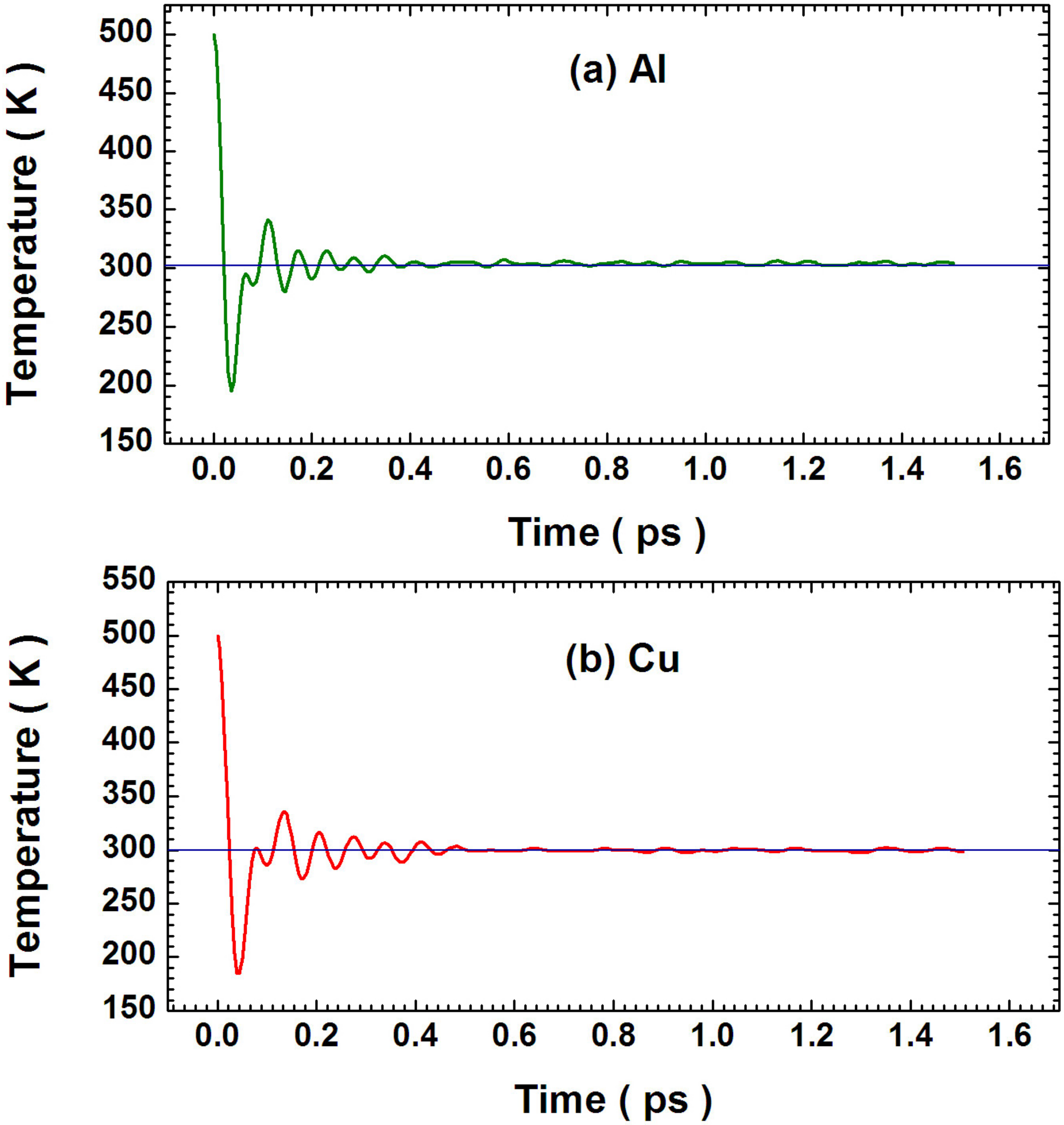

Figure 3.3: Variations of temperature (equivalent to KE) with time of the systems of (a) Al and (b) Cu leading to the equilibration

the atoms. DEA and SDA analyses [34] are performed for the time series data (Fig. 3.4) of the KE for an individual atom. Typical plots of DEA and SDA analysis from which δ and H are calculated for a Copper atom are shown in Fig. 3.5.

The slopes of the curves evaluate δ and H. DEA and SDA analyses were performed

Table 3.2: Mean values of the scaling exponents δ and H obtained from ten atoms chosen randomly in the shell of radius 'r'. Exponents δ and H are evaluated from the time series of the evolution of KE for a single atom.

Material	**Non-equilibrium Temperature(K)**	δ	H	$\left[\left(\delta - \frac{1}{3-2H}\right)/\delta\right] \times 100$
Si	500	0.953±0.016	0.968±0.008	1.380
Si	800	0.898±0.025	0.901±0.025	7.046
Si (single atom)	500	0.943	0.970	0.042
Ge	500	0.930±0.021	0.953±0.026	1.712
Ge	800	0.930±0.020	0.960±0.015	0.438
Ar	70	0.968±0.010	0.968±0.005	2.908
Ar (single atom)	70	0.963	0.972	1.665
Cu	500	0.920±0.020	0.955±0.022	0.279
Cu (single atom)	500	0.935	0.978	2.444
Fe	500	0.925±0.018	0.964±0.022	0.847
Fe (single atom)	500	0.959	0.974	0.879
Mo	500	0.935±0.016	0.964±0.021	0.231
Al	500	0.935±0.008	0.966±0.013	0.142

for ten atoms randomly chosen from the atoms confined in the sphere of radius 'r' and the average of values of δ and H are given in Table 3.2. Simulation cell sizes, number of atoms in the cell, sampling time, the crystal structure, and the nature of the interaction potential

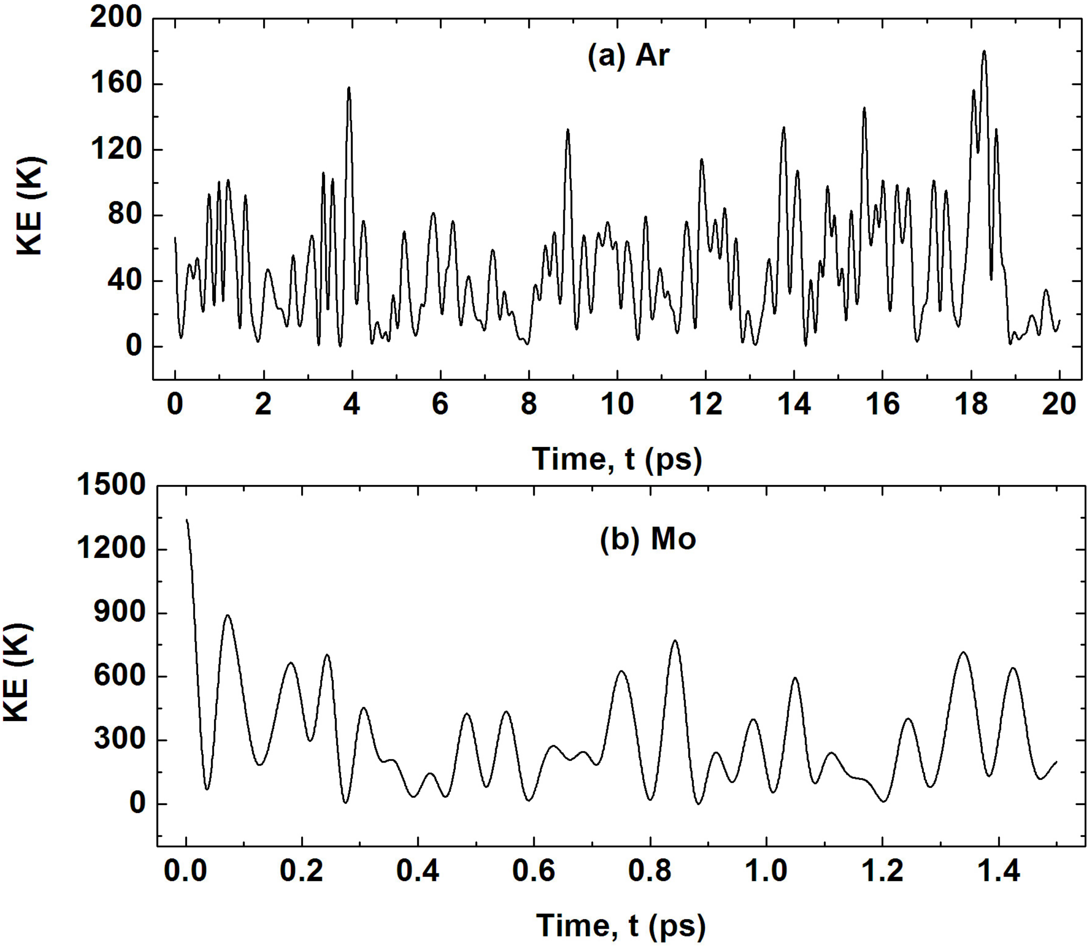

Figure 3.4: Time series data of KE of an arbitrary (a) Ar atom and a (b) Mo atom during the course of equilibration

were varied to find the exact nature of the scaling.

To understand the process of equilibration when a single excited atom interacts with an ensemble of atoms that are in equilibrium, another kind of exercise was performed by MD simulation. In this case from the equilibrated ensembles of Si, Cu, Fe at 300 K and solid Ar at 50 K one atom in the middle of the cell was excited to a KE corresponding to 500 K and 70 K respectively. The excited atom is then allowed to equilibrate and the KE possesses by the atom at different time steps was monitored. In these simulations the energy of the simulation cells was also a constant of motion. All the equilibrated atoms in the cell form

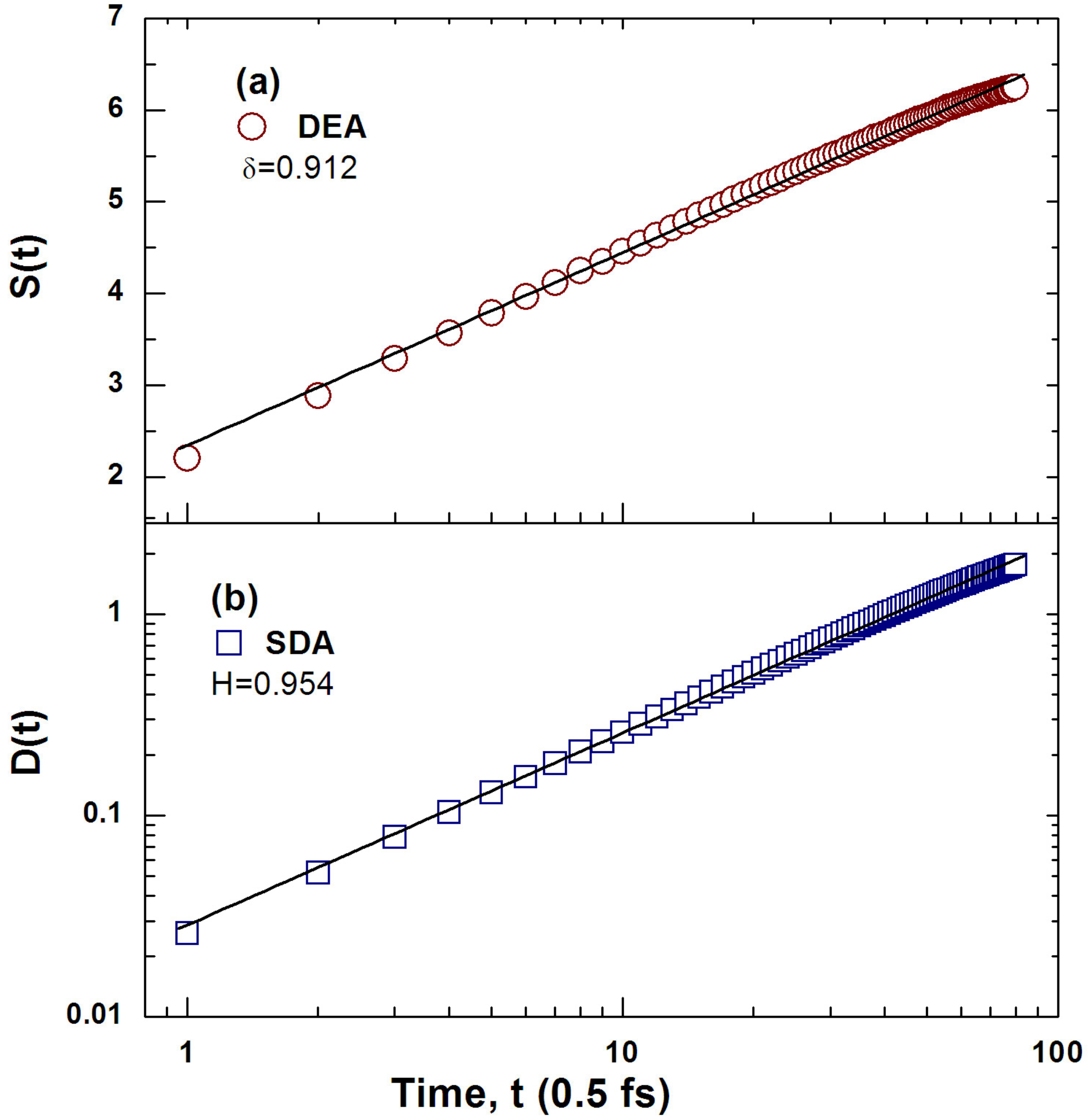

Figure 3.5: (a) DEA and (b) SDA of the variation of kinetic energy against time data obtained from a Cu atom in an ensemble when brought to a non-equilibrium state at 500K from 100K and allowed to equilibrate at 300K

a heat bath and the excited atom equilibrate by interacting with this heat bath by sharing its excess KE. The time series of KE of the excited atom between consecutive time steps are used to understand the diffusion process of KE and the nature of the dynamical process responsible to bring the atom to the equilibrium state. The values of δ and H obtained by DEA and SDA analysis from the time series are given in Table 3.2.

Atoms in the simulation cell, when brought to a non-equilibrium state by enhancing their KE, try to redistribute their excess KE by the process of diffusion. This process of redistribution of KE among the atoms changes their mean positions of vibration and consequently their PE. Here all the atoms in the cell participate together in the diffusion process. Thus by analyzing the variation of the KE with time for a single atom in the cell one can account for the modality of this diffusion process and the nature of the equilibration. The change in the KE for an atom in the i^{th} time step is given by $\Delta E = \left(\frac{2E_i}{m}\right)^{\frac{1}{2}} F_i \Delta t$ where F_i is force on the atom at the i^{th} time step. The force field experience by an atom in the cell will consist of three parts. The deterministic force, arising from the nearest neighbor interaction potential, and it plays the role of the external force $F(t)$ acting on the atom. There will be energy exchange between the atom and the surrounding atoms in a result of which the atom loses a part of its KE for exciting various degrees of freedom of the atoms in the ensemble as well there will be increase in the PE in the cost of KE of the atom. This can be described with help of a frictional force $F_f(t)$ acting on the atom. Besides loosing KE due to frictional effect there is a possibility of gaining KE in the form of random movement of the atom due to interactions from all other atoms in the cell and can be modeled by a random force $\Gamma(t)$ acting on the atom. $\Gamma(t)$ will have the property as $\langle \Gamma(t) \rangle = 0$ and $\langle \Gamma(t_1)\Gamma(t_2) \rangle = Ag(\Delta t)$ where $\Delta t = (t_2 - t_1)$, the function $g(t)$ dies down rapidly with t and A is the strength of the random force and is a function of temperature T. Thus the dynamics of the atoms will follow Langevin type equation [35]. To see the effect of this random force field on the scaling behavior, the ensembles of Si and Ge atoms were exited to a higher temperature i.e. at 800 K and allowed to equilibrate at 450 K. The δ and H values for the time series of the KE for these cases are given in Table 3.2. As the systems were allowed to equilibrate of its own without any defined protocol, forces acting on the atoms are time dependent through the dynamical process of equilibration. The force field experienced by an atom in the simulation cell in the i^{th} time step is calculated from its velocities, at $i-1$, i, $i+1^{th}$ time steps. Typical mean values of these forces are 1.011654×10^{-10} N and

24.7088×10^{-10} N for solid Argon and Si respectively. The fluctuating part of the force field at different time steps was obtained by subtracting the mean values. Typical probability distributions for the fluctuating part of the force field in case of solid Ar and Si atoms are shown in Fig. 3.6. The distributions are Gaussian with center -6.69×10^{-12} N and width 9.59×10^{-11} N for Ar and the corresponding values for Si are -4.98×10^{-11} N and 1.95×10^{-9} N respectively. To understand the correlation of the fluctuating force field, vectors $\{|X_i\rangle\}$ are generated from the time series data of the fluctuating force field by taking consecutive n time steps for constructing each vector. The eigen value spectrum of the covariance matrix Σ_x of these vectors are calculated to establish the nature of the correlation. Fig. 3.7 shows typical eigen value spectra for Ar and Si cases. The flatness of the spectra confirms that the fluctuating force fields are uncorrelated.

The motion of the atoms in the simulation cell is thus governed by these forces and dictates the variation of KE of the atoms. The memory effect of the initial velocity will die down with time. In the long time limit the system equilibrates leading to equipartition of energy. The characteristic of the variation of KE in terms of time series indicates the evolution of the non-equilibrium state. To understand the universality of this evolution for different dynamical processes as generated by MD simulations, the Shannon entropy of the diffusion process of KE of an atom in the cell was obtained by calculating the PDF from the sub trajectories of this time series. The high values of δ and H as given in Table 3.2 signifies a strong persistence in the fluctuations of the KE of the atoms. The values of H are always larger than that of δ for all cases studied and are seen to fulfill the Levy-walk diffusion relation within the error bar as shown in Table 3.2. In the work of P. Barat *et al.*[36] the Portevin-Le Chatelier effect in an Al-2.5%Mg alloy also exhibits similar scaling behavior having scaling exponent between 0.98 and 0.88.

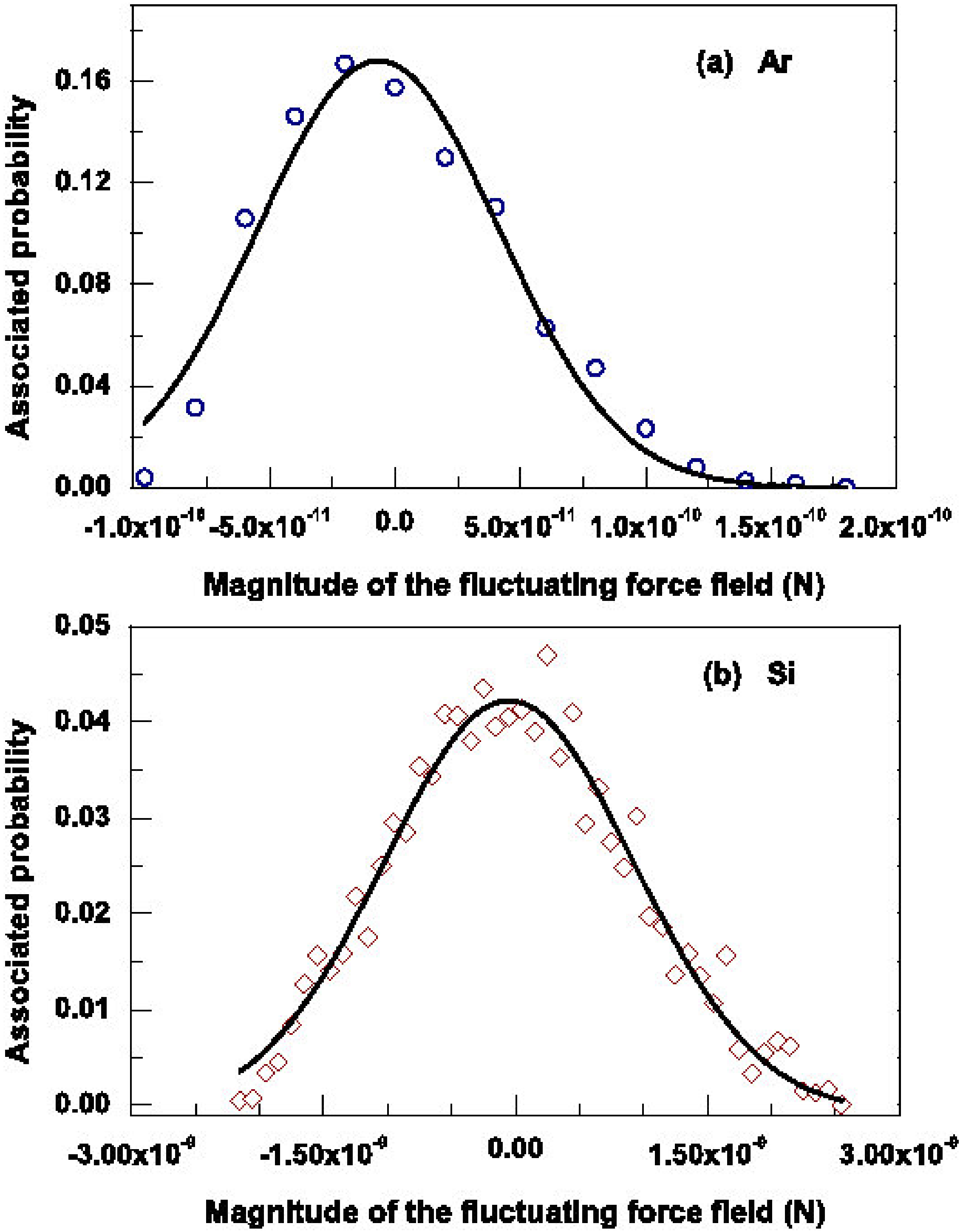

Figure 3.6: Probability distributions of the fluctuating forced fields experienced by (a) an Argon and (b) a Silicon atom when brought to a non-equilibrium state at 500 K from 100 K and allowed to equilibrate at 300 K

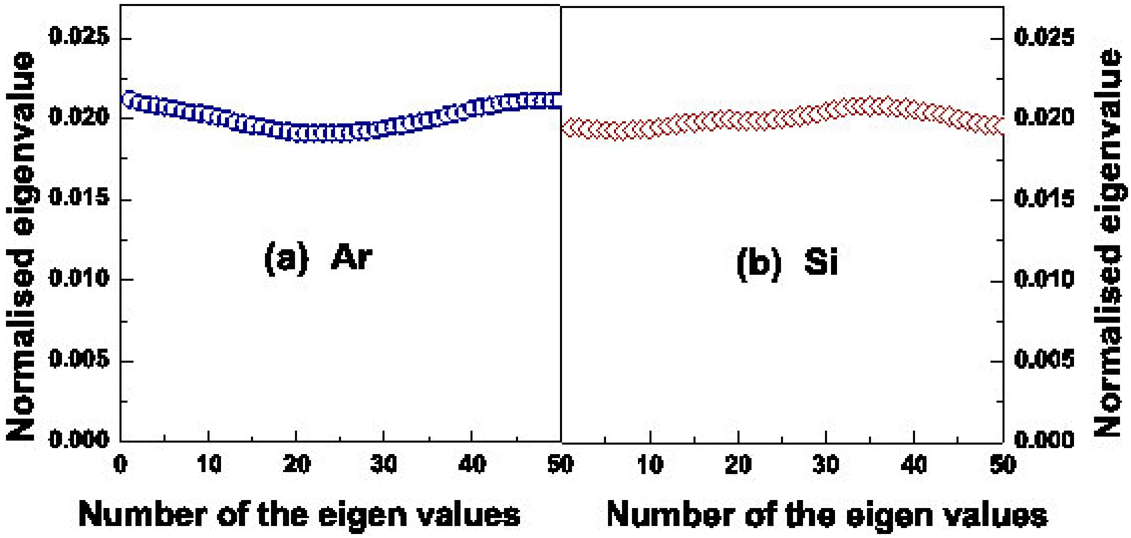

Figure 3.7: Eigen value spectra of the covariance matrices constructed from the time series of the fluctuating forced fields experienced by (a) an Argon and (b) a Silicon atom when brought to a non-equilibrium state at 500 K from 100 K and allowed to equilibrate at 300 K

3.10 Conclusions

The exact inherent dynamics of the process of transmitting excess KE of an atom to its surroundings could not be revealed from this analysis. However, this analysis reflected the underlying generic features and physical principles that are independent of the detailed dynamics or characteristics of particular model. The diffusion of KE of an atom to its surroundings is a continuous stationary stochastic process as the probability of the diffusion trajectories follows a scaling relation. As the exponent H is greater than 0.5 for all cases, the diffusion is anomalous super diffusion. Any diffusion is a kind of random walk and the Levy-walk is a mathematical model to describe anomalous super diffusion where the scaling exponent of variance against time is greater than one. Levy-walks have coupled space-time probability distributions and are characterized by a cluster of smaller variations of the random variable with a few large variations between them. This pattern repeats for all scales. As the process of equilibration of KE of an atom in the ensemble from its non-equilibrium state has to be very rapid, it cannot be Brownian type and it should be Levy-walk type as

Levy-walk will outperform Brownian walk during the process of equilibration. The Levy-walk type of diffusion of KE among the atoms may be due to the following reason. Excess KE of an atom should disburse locally however there is a finite probability to transport its excess KE to a distant atom and consequently this atom again redistributes its KE in the same process. This process is much faster than normal diffusion when the mean squared value of fluctuation depends on t only. Mostly three dimensional systems show normal diffusion except in glassy systems [37]. The anomalous or super-diffusion and Levy-walks have been observed in various real-life phenomena like fluid flow in rotating annulus [38], low dimensional heat transport [39], light scattering in porous media [40] etc. However the present findings show that the diffusion of KE for a single atom in its non-equilibrium state, when embedded in an environment of atoms that are either in equilibrium or in non-equilibrium state, show super-diffusion and Levy-walk properties throughout the process of equilibration. In the case when a single atom interacts with the ensemble of atoms that are in equilibrium it may be assumed that the atom is interacting with a thermal bath by absorbing or releasing KE without appreciable change in the bath state. In this case also the diffusion of KE of the atom is found to fallow the Levy-walk process.

Atoms of crystals when brought to a non-equilibrium state, try to redistribute its energy amongst them to converge to an equilibrium distribution. Such fundamental process is governed by the increase in entropy of the trajectories of the individual atom and should be identical in nature for all types of elemental atoms and will be independent of the nature of interactions between the atoms and the perturbation which brought them to non-equilibrium state. The calculation of Shannon entropy of the diffusion process was made for one atom. However, the concept of entropy in statistical mechanics is for an ensemble. But the entropy production for a single trajectory has been addressed in the literature [23] concerning fluctuation theorems.

Atoms in a lattice possessing KE different from its equilibrium values at any instant of time try to transport or accept from the nearest neighbors and arrive at a new value.

The time series of this KE were translated in to a diffusion process in the form of diffusion trajectories and PDF of these trajectories were estimated. The estimated Shannon entropy production of this dynamical process with time is found to obey a universal scaling relation. This scaling relation is exact and valid for systems no matter how far they are driven out of equilibrium and is independent of the strength of perturbation that brought the system out of equilibrium. In equilibrium the same scaling property of KE of constituent particles has been studied. The result once again shows the Levy-walk nature of constituent particles in KE space. Thus the randomness in the energy possessing of the individual constituent particles is irrespective of the nature of the system whether it is in equilibrium or in non-equilibrium. The only difference is that in equilibrium they jump into different energy states keeping envelope of the probability distribution intact. Intuitively it seems that in non-equilibrium system the randomness in the values of KE of a particle could be different because of the low occurrence probability of the non-equilibrium state. However, this is for the first time it is noticed that the randomness of KE of a system particle is the same regardless of the state of the system.

Bibliography

[1] H. E. Stanley,L.A.N Amaral, P. Gopikrishnan,P. C. Ivanov, PC, T. H. Keitt, V. Plerou, Physica A 281 (2000) 60.

[2] A. Sarkar, P. Barat,Physica A, 364 (2006) 362.

[3] A. Sarkar, P. Barat, Fractals 14 (2007) 289.

[4] A. P. Siebesma and H. J. J. Jonker,Phys. Rev. Lett. 85 (2000) 214.

[5] S. N. Dorogovtsev and J. F. F. Mendes, Phys. Rev. E 63 (2000) 056125.

[6] P. Bak, K. Christensen, L. Danon, and T. Scanlon, Phys. Rev. Lett. 88,(2002)178501.

[7] Y. Gazit, D. A. Berk, M. Leunig, L. T. Baxter, and R. K. Jain, Phys. Rev. Lett. 75 (1995) 2428.

[8] K. Fraedrich and R. Blender, Phys. Rev. Lett. 90 (2003) 108501.

[9] R. C. Hwa and T, C. Ferree, Phys. Rev. E 66 (2002) 021901.

[10] A. Kiraly and I. M. Janosi, Phys. Rev. E 65 (2002) 051102.

[11] P. Levy, Bull. Soc. Math. France 52, (1924) 49.

[12] N. Scafetta, P. Hamilton and P. Grigolini, Fractals 9 (2001) 193.

[13] N. Scafetta and P. Grigolini, Phys. Rev. E 66 (2002) 036130, N. Scafetta and B.J.West, Phys. Rev. Lett. 92 (2004) 138501.

[14] B.V. Gnedenko, A.N. Kolmogorov, Limit Distributions for Sums of Independent Random Variables (Addison-Wesley, Reading, MA) 1954.

[15] J. Gao, Y. Cao, W. Tung, J. Hu, Multiscale Analysis of Complex Time Series (John Wiley & Sons. Inc.. Hoboken. New Jersey)2007.

[16] L. Onsager, Phys. Rev. 37 (1931) 405 ; 38 (1931) 2265 .

[17] C. Jarzynski, Annu. Rev. Condens. Matter Phys. 2 (2011) 329 .

[18] C. Jarzynski, Phys. Rev. Lett. 78 (1997) 2690 .

[19] D. J. Evans, E G. D. Cohen, and G. P. Morriss, Phys. Rev. Lett. 71 (1993) 2401 .

[20] D. J. Evans and D. J. Searles, Phys. Rev. E 50 (1994) 1645 .

[21] G. Gallavotti and E. G. D. Cohen, Phys. Rev. Lett. 74 (1995) 2694 .

[22] G. E. Crooks, Phys. Rev. E 60 (1999) 2721 .

[23] Udo Seifert, Phys. Rev. Lett. 95 (2005) 040602 .

[24] J. Kurchan, J. Phys. A: Math. Gen. 31 (1998) 3719 .

[25] J. L. Lebowitz and H. Spohn, J. Stat. Phys. 95 (1999) 333 .

[26] C. Maes, Sem. Poincare 2 (2003) 29 .

[27] P. Gaspard, J. Chem. Phys. 120 (2004) 8898 .

[28] J. Liphardt, S. Dumont, S.B.Smith, I. Tinoco Jr, and C. Bustamante, Science 296 (2002) 1832 .

[29] G. M. Wang, E.M.Sevick, Emil Mittag, Debra J. Searles and Denis J. Evans, Phys. Rev. Lett. 89 (2002) 050601 .

[30] K. Feitosa and N. Menon, Phys. Rev. Lett. 92 (2004) 164301.

[31] W. I. Goldburg, Y. Y. Goldschmidt and H. Kellay, Phys. Rev. Lett. 87 (2001) 245502.

[32] N. Garnier and S. Ciliberto, Phys. Rev E 71 (2005) 060101(R).

[33] http//micro.stanford.edu

[34] The programme for calculating DEA and SDA for the time series data was initially tested for synthetic time series like Gaussian White Noise generated by Box-Muller algorithm, Fractional Gaussian Noise generated based on the reference, Methodology and Computing in Applied Probability 1 (1999) 445 and Levy Noise generated based on the reference Phys. Rev. E 49 (1994) 4677.

[35] G.W. Ford, M. Kac and P. Mazur, J. Math. Phys. 6 (1965) 504.

[36] P. Barat, A. Sarkar, P. Mukherjee, and S. K. Bandyopadhyay, Phys. Rev. Lett. 94 (2005) 055502.

[37] L. Cipelletti and L. Ramos, J. Phys. : Condens. Matter 17 (2005) R253 and the references therein.

[38] T. H. Solomon, E. R. Weeks and H. L. Swinney, Phys. Rev. Lett. 71 (1993) 3975.

[39] A. Dhar, K.Saito and B. Derrida, Phys. Rev. E 87 (2013) 010103 (R) and the references therein.

[40] P. Barthelemy, J. Bertolotti and D. S. Wiersma, Nature 453 (2008) 495.

3.11 Appendix: Matlab programs used for noise data

3.11.1 Gaussian white noise :

```
% Box-Muller algorithm to generate Gaussian white noise
function[x] = boxmuller(n, sd)
x = zeros(n,1);
len = ceil(n/2);
rand(‘seed’, sd);
for i=1:len
u1 = rand(1,1);
u2 = rand(1,1);
x(i) = sqrt(-2*log(u1))*cos(2*pi*u2);
if(i+len¡=n)
x(i+len) = sqrt(-2*log(u1))*sin(2*pi*u2);
end
end
```

3.11.2 Fractional Brownian motion :

```
function f = fftfgn(sigma, H, n, N, M, force, varargin)


    if H==1/2,
f = sigma*randn(n,N);
elseif and((H>1/2),H<=1)
t=[-M:M];
co =0.5*sigma^2*(abs(t+1).^(2*H) + abs(t-1).^(2*H) - 2*abs(t).^(2*H));
if force,
```

```
nM = 2^(fix(log2(2*M+1))+1);
else
nM = 2*M+1;
end;
co_hat =fft(co,nM);
ft = real(ifft(abs(co_hat).^0.5, nM));
ft = [ft(fix(nM/2)+1:nM), ft(1:fix(nM/2))];
R = randn(n,2*M+N);
if ∼isempty(varargin),
fprintf(‘Generating n = %d paths’,n);
end;
f = [ ];
for i=1:n,
fi = fftconv(R(i,:),ft,force);
f = [f; fi(2*M:2*M+N-1)];
if ∼isempty(varargin),
fprintf(‘.’);
end;
end;
if ∼isempty(varargin),
fprintf(‘ done.\n’);
end;
elseif and((H<1/2),H>0)
G1=randn(n,N-1);
G2=randn(n,N-1);
G = (G1+sqrt(-1)*G2)/sqrt(2);
GN = randn(n,1);
```

```
G0 = zeros(n,1);
H2=2*H;
R=(1-((1:N-1)/N).^H2);
R=[1 R 0 R(N-1:-1:1)];
S=ones(n,1)*(abs(fft(R,2*N)).^0.5);
X=[zeros(n,1) G, GN, conj(G(:,N-1:-1:1)) ].*S;
x=ifft(X’,2*N)’;
y=sqrt(N)*real((x(:,1:N)-x(:,1)*ones(1,N)));
f = sigma*N^H*[y(:,1), diff(y‘)’];
else
error(‘The value of the Hurst parameter H is out of the range (0,1]’);
end;
```

3.11.3 Levy noise

```
function [z] = levy(alpha, c, n, N)
if (alpha < 0.3 | alpha > 1.99)
disp(‘Valid trange for alpha[0.3;1.99].’);
z = NaN * zeros(1,N);
return
end
if (c<=0)
disp(‘c must be positive.’)
z = NaN * zeros(1,N);
return
end
if (n<1)
```

```
disp(‘n must be positive.’)
z = NaN * zeros(1,N);
return
end
if nargin<4
N = 1;
end
if (N<=0)
disp(‘N must be positive’)
z = NaN;
return
end
invalpha = 1/alpha;
sigx = ((gamma(1+alpha)*sin(pi*alpha/2))/(gamma((1+alpha)/2)...
alpha*2^((alpha-1)/2)))^invalpha;
v = sigx*randn(n,N)./abs(randn(n,N)).^invalpha;
kappa = (alpha*gamma((alpha+1)/(2*alpha)))/gamma(invalpha)*....
((alpha*gamma((alpha+1)/2))/(gamma(1+alpha)*sin(pi*alpha/2)))^invalpha;
p = [-17.7767 113.3855 -281.5879 337.5439 -193.5494 44.8754];
c = polyval(p, alpha);
w = ((kappa-1)*exp(-abs(v)/c)+1).*v;
if(n>1)
z = (1/n^invalpha)*sum(w);
else
z=w;
end
z=c^invalpha*z;
```

Chapter 4

Evolution of Shannon Entropy in Kinetic Energy Domain

4.1 Introduction

Most of the systems observed in nature or in the laboratories are of non-equilibrium disposition. Physical properties of systems are measured by bringing them in their non-equilibrium state by applying external perturbations. In last two decades there was lot of impetus to understand the process of equilibration of non-equilibrium system, far from equilibrium, by studying the dynamical evolution of the individual constituents of the system [1]. In order to understand the collective behavior of a non-equilibrium system, it is important to study the behavior of the constituent atoms of the non-equilibrium system together during the passage of equilibration. This can be achieved by studying the variation of the probability distribution function (PDF) of the energy of the associated atoms in the system during equilibration. The global dynamics of equilibrium systems are studied by statistical mechanics forging the fundamental link between the interactions of the constituents and the macroscopic behavior of the interacting many body systems. Boltzmann established a general framework to evaluate the associate probability of an ensemble of an equilibrium system to achieve a particular energy state. Equilibrium distribution of a system is derived by maximizing the entropy. Thus, whenever an non-equilibrium system reaches an equilibrium state it has to follow the path of steepest entropy ascent compatible with the constraints of the system concerned. This observation is in consistent with Onsager theory of reciprocity [2] and fluctuation-dissipation theory [3].

A non-equilibrium system continuously undergoes transitions from one state to the other to maximize the entropy measure. Thus it is imperative to study the evolution process of equilibration of a non-equilibrium system one has to calculate the time dependent PDF, $p(E,t)$ and the corresponding measure of entropy. This chapter presents the time variation of the Shannon entropy [4] of non-equilibrium systems defined by the relation $S(t) = -\int p(E,t)\, \log p(E,t)\, dE$, where $p(E,t)$ is obtained by molecular dynamics (MD) simulation technique.

4.2 Simulation in details

A variety of materials having different crystal structures with widely employed empirical interaction potentials are used to carry out the MD simulations [5]. Depending on the potential function, the trajectories of the atoms are calculated at each time step of simulation by solving Newton's laws of motion. Copper (Cu), Aluminium (Al) and solid Argon (Ar) with face centered cubic (FCC) structure, and iron (Fe) with body centered cubic (BCC) structure are the elements considered in this study. The simulations are performed using MD++ [6] code. The empirical potentials used are Embedded Atom Method[7][8], Aluminum Glue[9], Lennard Jones[10] and Finnis-Sinclair[11] for Cu, Al, solid Ar and Fe respectively. Cubic cells of size $20 \times 20 \times 20$ unit cell (uc) containing 32000 Cu, Al and solid Ar atoms, and $25 \times 25 \times 25$ uc containing 31250 Fe atoms are considered as the simulation systems. Number of atoms in the simulations are much larger than that recommended in reference [12] to avoid the size effect. In all the cases, initially, the systems are relaxed at 100K (30K for solid Ar) temperature for 2.5ps (10ps for solid Ar) using periodic boundary condition in all three directions under constant number of atoms, volume and total energy (NVE) ensemble. The number of time steps used for relaxations was 5000 with each time step of 0.5fs (2fs for solid Ar). To set up the non-equilibrium state the velocity components of the atoms are redefined such that the average KE of the atoms becomes 500K (70K for solid Ar). The systems are then released for equilibration. Consequently the systems gradually proceed towards equilibrium.

During the equilibration process the position and velocity components of each atom are recorded at every time steps of 0.5fs (2fs for solid Ar). The total equilibration time was 1.5ps (20ps for solid Ar). The variation of the average system temperature for Aluminium and copper are shown in Fig. 4.1. The figure exhibits larger fluctuation of average temperature when the system is far away from the equilibrium temperature. The standard deviation of this fluctuation is tabulated in Table 4.1 for all the materials.

4.3 Formulation of probability distribution function in kinetic energy domain

An easy way to compute Shannon entropy is the construction of probability distribution (Fig. 4.2.) and subsequently with the help of binning of probability distribution the conventional formula computes the Shannon entropy. Since the quantity, Shannon entropy, provides the information of the system, the selection of bin is an important aspect of this work. If the bin size is not closed to the standard deviation average system temperature, information may be lost for larger bin size and for smaller bin size larger computation time has to be spent. Thus, in order to compromise with no loss of information value and the smaller computation time the bin size has been chosen around the standard deviation of the average system temperature. At each time step the KE spectrum of the atoms are divided into 200

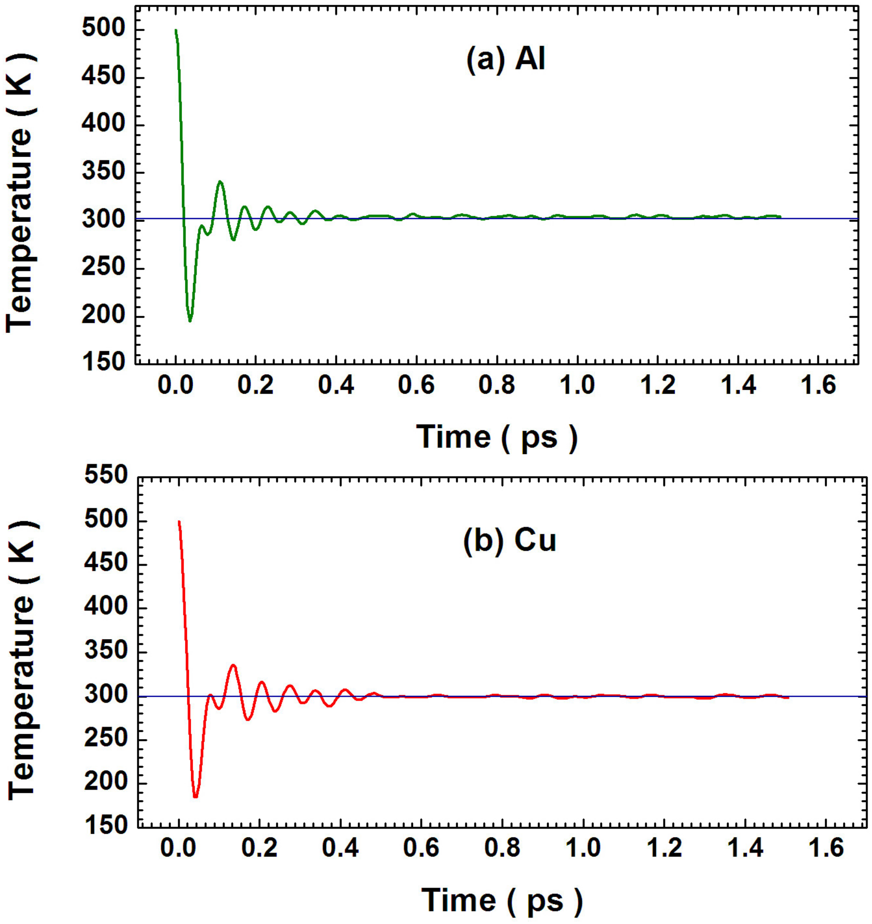

Figure 4.1: Variations of temperature (equivalent to KE) with time of the systems of (a) Al and (b) Cu leading to the equilibration.

bins (130 bins for slid Ar) with each bin corresponds to KE of 20K (5K for solid Ar) in oder to get the histogram of the KE spectrum. The normalized probability distribution of KE of Cu atoms expressed in terms of temperature during the process of equilibration are shown in Fig. 4.2. After making the normalization $\sum_{i=1}^{N} p_i(t) = 1$ (N = number of bins and $p_i(t)$'s are the discrete bin values of the probability $p(E,t)$ defined earlier) of the KE spectrum the values of the Shannon entropy $S(t) = -\sum_{i=1}^{N} p_i(t) \log p_i(t)$ at different instants of time are calculated. The variations of S(t) with time for Ar and Cu are shown in Fig. 4.3.

Ensemble of atoms in a crystal when brought to non-equilibrium state by enhancing the

Table 4.1: Table showing the standard deviation of the average temperature variation of solid argon, copper, iron, and Aluminium during the equilibration from their respective initial to final temperature.

Material	Initial average temperature(K)	Final average temperature(K)	Standard Deviation of average temperature(K)
Solid Argon	70	50	3.07
Copper	500	300	23.02
Iron	500	300	25.08
Aluminium	500	300	20.39

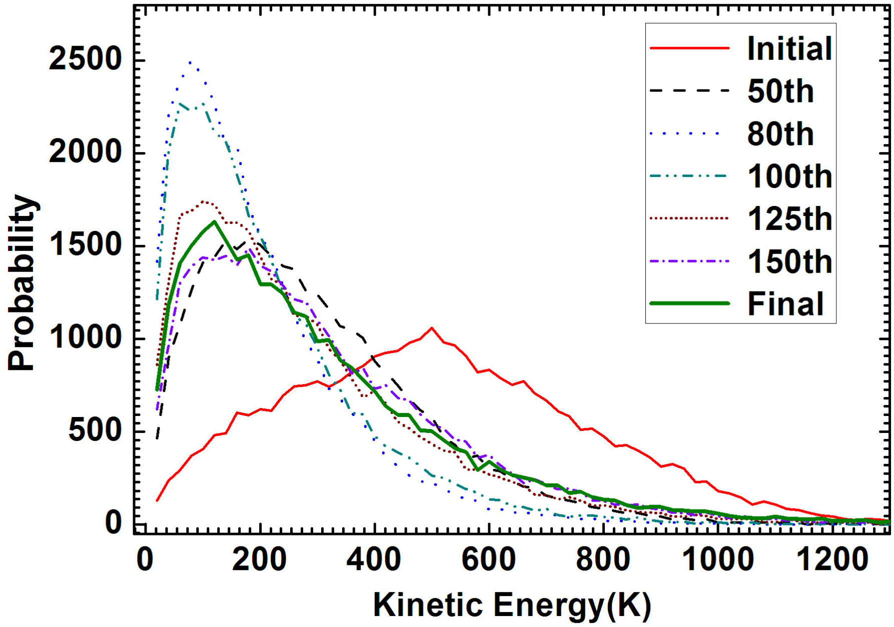

Figure 4.2: The probability distribution function of the kinetic energy (expressed in terms of temperature) of Cu atoms at initial, final and at five different time steps.

KE of the atoms from their equilibrium values, equilibrate by diffusing its excess KE. This diffusion process is governed by the various forces acting on the atoms. The force arising from the nearest neighbor interaction potential plays the role of the external force on the atom. There will be energy exchange between the atom and surrounding atoms in a result of

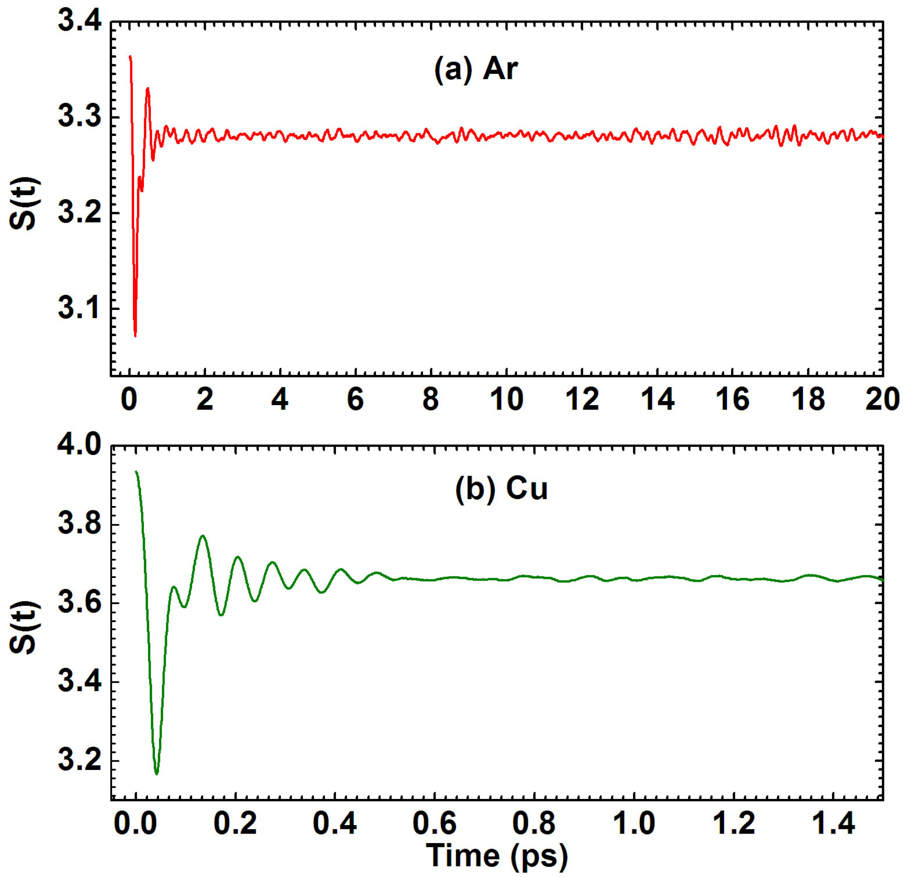

Figure 4.3: Variation of the Shannon entropy with time of (a) Ar and (b) Cu during the course of equilibration.

which the atom may lose a part of its KE. Loss of KE also occurs because of its conversion to PE in the ensemble of atoms. There will be a force acting on the atom arising from the interactions from all other atoms in the cell. Because of their thermal vibrations the net force will be random. Effect of these forces results in a change in the KE of the atoms and consequently in the PDF. The PDF changes with time and ultimately equilibrates to the stable time invariant distribution. The variation of the PDF of KE can be a measure of the dynamical process of equilibration. In this regard Shannon entropy $S(t)$ is evoked and it has been calculated at each time step.

The Shannon entropy oscillates (Fig. 4.3) around the equilibrium value during the pro-

Table 4.2: Frequencies of the first peak observed from the Fast Fourier Transform of Shannon entropy of the elements and their respective Debye frequencies.

Material	**1st peak from FFT**	**Debye frequency at 298K[13]**
Solid Argon	1.93 THz	1.77 THz(at 0K[14])
Copper	7.14 THz	7.16 THz
Iron	9.74 THz	9.79 THz
Aluminium	7.81 THz	8.21 THz

cess of equilibration. Thus high and low values of the Shannon entropy does not necessarily signify any stable state of the system but the invariance of the Shannon entropy with time suggests the attainment of equilibrium. Thus in equilibrium of any dynamical system Shannon entropy is a constant of motion. Fast Fourier Transformation (FFT) of the time evolution of the Shannon entropy shows a frequency spectrum having two major peaks as shown in Fig. 4.4. The first peak is closed to the Debye frequency of the element concerned as shown in Table 4.2.

4.4 Result and discussions

In the study of the statistical interpretation of the relaxation process of non-equilibrium systems, Boltzmann entropy plays the most important role and it attains the maximum value at equilibrium. However, Boltzmann entropy can not be estimated based on the concept of probabilities as defined in the field of statistics and as well difficult to measure in numerical studies. Thermodynamic probabilities or the statistical weight of a micro-state that reflects the Boltzmann entropy is not a probability as defined in the conventional statistics [15]. Hence, in this numerical studies of the relaxation process it is essential to evoke the Shannon entropy to understand the dynamics. Shannon entropy is a measure of uncertainty [4] and

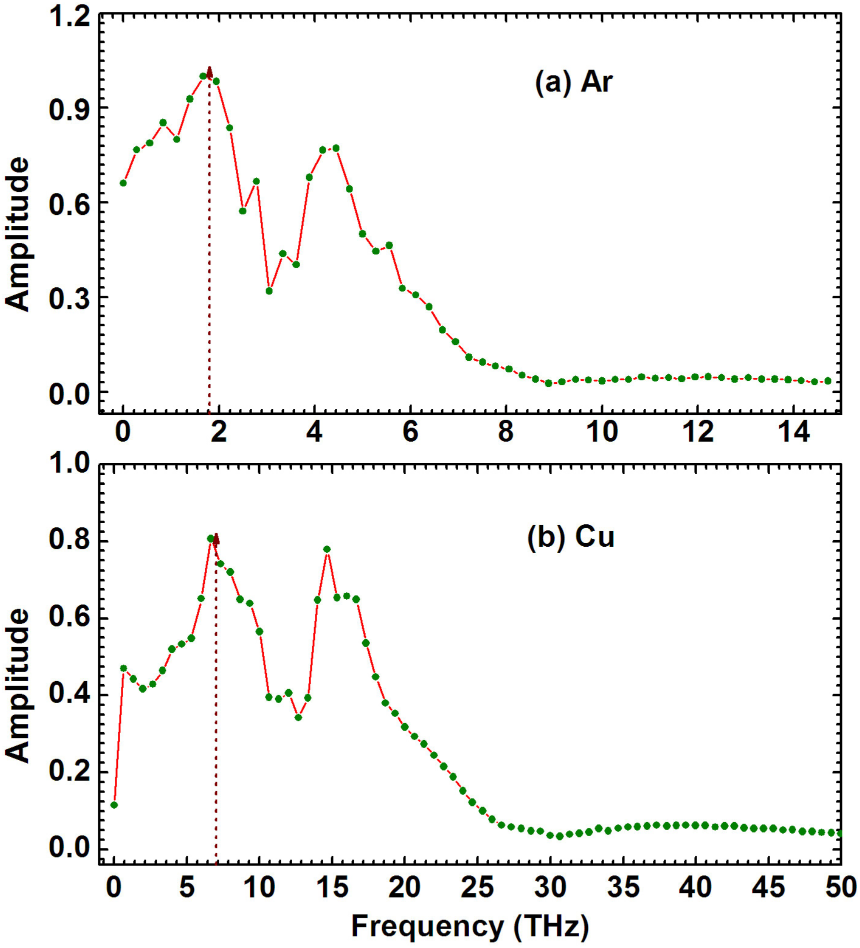

Figure 4.4: FFT of Shannon entropy of (a) Ar and (b) Cu.

is a positive function of p_is. Its extreme values are for the cases when all p_is are equal with $S = \log N$ and $S = 0$ when the system is uniquely defined with sharped peak at one of the p_is equal to 1.

When the system is far away from the equilibrium normalized values of probability in the respective bins are much different from the equilibrium values (Fig. 4.2). When the system is allowed to relax the values of probabilities start oscillating in such a way that these coupled oscillators reach the final destination correspond to the equilibrium distribution. The behavior of the PDF at different time steps (Fig. 4.2) shows that, initially the distribution starts peaking at the low temperature side in an attempt to approach the equilibrium distribution.

At 80th time step (for Cu) it peaked maximum and the corresponding Shannon entropy goes to minimum. However, as the coupled oscillating probabilities in the bins do not reach the equilibrium distribution it again starts flattening making the Shannon entropy to increase. This cumulative oscillation among the bins persists but its amplitude decays with time so long it reaches the equilibrium distribution making the Shannon entropy as a constant of motion. This is the dynamics of these equilibrium processes.

In this micro-canonical ensemble whenever the KE is exchanged between the atoms it generates a different micro-state for a given macro-state. This energy exchange is also responsible for the oscillations of the probabilities in the bins. These oscillators when coupled together generate higher modes of oscillations along with their fundamental frequency. Because of these coupled oscillators a frequency spectrum associated to the time dependence of the Shannon entropy is expected. It is presumed that the observed first peak in the frequency spectrum is the Debye frequency and is one of the primary frequencies responsible for the transfer of probabilities between the bins.

One of the characteristics of the non-equilibrium systems is that the PDF associated with the systems are necessarily time dependent. Because of this time dependence it is difficult to find any general analytical formalism to deal with its dynamics. The time evolution of p_is is governed by the master equation. However, it is extremely difficult to solve it numerically because of associated large degrees of freedom. In this attempt, the evolution dynamics of non-equilibrium systems could be justified by studying their time evolution of the Shannon entropy and a conclusion can be drawn describing the time variation is primarily dictated by two frequencies and one of them is the Debye frequency.

4.5 Conclusion

The motivating significance of this chapter is the oscillating nature of Shannon entropy. The common idea about an isolated system is that it is not in equilibrium when any quantity, and in particular the quantity $\int p(E,t)\,\log p(E,t)\,dE$ changes systematically with time [16]. Irrespective of the initial values of the probabilities of the bins the quantity $\int p(E,t)\,\log p(E,t)\,dE$ tends to decrease as long as the probability distribution acquire a form to achieve a minimum $\int p(E,t)\,\log p(E,t)\,dE$ value. The final distribution is most probable one and leads to the equilibrium of the system. Application of a little disturbance perturbs the probability distribution having occurrence probability much smaller than the most probable one and the value of the quantity $\int p(E,t)\,\log p(E,t)\,dE$ again increases. The small occurrence of the probability ensures the non-equilibrium state of the system after the introduction of disturbance. This study, for the first time, observes a contradictory property of non-equilibrium system which establishes that Shannon entropy does not always monotonically increase during the equilibration process.

Bibliography

[1] Udo Seifert, Rep. Prog. Phys., 75 (2012) 126001 and the references therein.

[2] Giovanni Gallavotti, Phys. Rev. Lett., 77 (1996) 4334.

[3] R. Kubo, Rep. Prog. Phys., 29 (1966) 255 and the references therein.

[4] C. E. Shannon, The Bell System Technical Journal, 27 (1948) 379.

[5] P. Barat, A. Giri, M. Bhattacharya, Nilangshu K. Das and A. Dutta, Europhys. Lett., 104 (2013) 50003.

[6] http://micro.stanford.edu/caiwei/Forum/2004-12-12-MD++/.

[7] M. S. Daw, M. I. Baskes, Phys. Rev. B, 29 (1984) 6443.

[8] M. S. Daw, S. M. Foiles, M. I. Baskes, Mat. Sci. Rep., 9 (1993) 251.

[9] F. Ercolessi and J. B. Adams, Europhys. Lett., 26 (1994) 583.

[10] J. E. Lennard-Jones, Proc. R. Soc. Lond. A, 106 (1924) 463.

[11] M. Finnis and E. Sinclair, Phil. Mag. A., 50 (1984) 45.

[12] David Sands, Jeremy Dunning-Davies, arXiv:1301.1364.

[13] C. Y. Ho, R. W. Powell, and P. E. Liley, Journal of Physical and Chemical Reference Data, Volume 3, Supplement no. 1 (1975).

[14] G. R. Stewart, Rev. Sci. Instrum., 54 (1983) 1.

[15] C. G. Chakrabarti and I. Chakrabarty, Mod. Phys. Lett., 20 (2006) 1471.

[16] Fundamentals of Statistical and Thermal Physics, Section A.12: The H theorem and the approach to equilibrium, F. Reif

Chapter 5

Modality of Equilibration

5.1 Introduction

For equilibrium systems, the probability distribution function (PDF) of energy is the well known Boltzmann distribution. Dynamic evolution of an equilibrium system through a sequence of equilibrium states is infinitesimally slow as it evolves in a quasi static manner retaining the Boltzmann distribution at every stage. Practical systems are usually in the non-equilibrium state and try to reach its equilibrium state. Thermodynamic entities of equilibrium systems are studied by equilibrium statistical physics from the knowledge of the interaction of the microscopic constituents of the system. Small deviation of the equilibrium state by external perturbation in the linear response regime is analytically handled through equilibrium correlation function[1, 2, 3]. No generalized theoretical framework exists to calculate macroscopic thermodynamic properties of a system when it is far from equilibrium. In the last two decades, exact relations have been established relating thermodynamic parameters for systems irrespective of how far they are driven out of equilibrium. These studies are related to the path probabilities of the individual constituents of the non-equilibrium system[4]. Collective behavior of the constituents of non-equilibrium systems is also to be understood. Probably this can be studied from the time evolution of the PDF of energy of non-equilibrium systems as they approach equilibrium.

It is easy to bring a system to its non-equilibrium state experimentally by the application of external perturbations like magnetic field, electric field, heat flux etc. However it is almost impossible to estimate the PDF of energy of the non-equilibrium system and its variation with time experimentally as one has to measure the energy of all the atoms in the system at different instant of time. On the other hand it is quite easy to study the evolution of the PDF of energy for a non-equilibrium system and its approach to equilibrium by molecular dynamics (MD) simulation technique. In MD simulation, it is possible to calculate all the attributes of an individual atom at a finer time steps. Hence, it is necessary to study the modality of the equilibration process globally of a non-equilibrium state of a system, MD simulation is possibly the only way. This chapter reports the mechanism of equilibration of the PDF of energy of several prototype crystalline systems by system identification technique [5] when they are brought to non-equilibrium state using MD simulation and allowed to equilibrate of its own without any interaction with bath or sink.

5.2 System identification technique

Every dynamical system responses while an excitation is imposed to the system. The dynamical characteristics of the system are reflected in the response of the system. Thus, there should be a fixed rule in the excitation-response characteristics for a particular system. For a well described dynamical system it is very easy to find out the output of the system from its description and from the input. On the other hand many times we may not know the system description, and we may need to figure out a description of the system from the known sample of input and output. In this chapter, as we will see later, the dynamical system is solid Argon crystal which is far away from its equilibrium state. Left of its own, the system gradually proceeds towards the most probable unique equilibrium state. At each step of the equilibration the output of the previous step acts as input to the system and the response of system to this input is its output. Thus, it seems that we have a time series of input and output but dont have any idea about the details of input output relationship. No description of the system, no dynamical characteristics of the system are available from this information in a straight forward manner. For a simple system it is possible to formulate a differential equation of the system and relate the input and output by an equation. Unfortunately, the studied system is not a simple one and consists of a large number of interacting particles. It is impossible to formulate the differential equation of that kind of complex system. The modality of the equilibration can be looked as a self control of the system to reach the unique equilibrium point. Thus, the process of equilibration is a self controlled attractor, although the initial states are man-made and countless. We are looking for an indirect methodology which can relate the input and output of the system and can provides us substantial information about its dynamical characteristics. Transfer function of the system can play this role significantly. The art of building this mathematical model of the response characteristics of a dynamical system from the input-output data is the system identification technique. The transfer function of a dynamical system is the ratio of the output and input in Laplace domain and is given by $H(s) = \frac{Y(s)}{X(s)}$. $X(s)$ and $Y(s)$ are the Laplace transformations of input $x(t)$ and output $y(t)$ respectively. For a practical system the transfer function is rational function in real or complex variable and its general form is

$$H(s) = \frac{N(s)}{D(s)} = \frac{b_m s^m + b_{m-1} s^{m-1} + ... + b_1 s + b_0}{a_n s^n + a_{n-1} s^{n-1} + ... + a_1 s + a_0} = \beta \frac{\prod_{i=1}^{m}(s - z_i)}{\prod_{j=1}^{n}(s - p_j)} \tag{5.1}$$

Where, all the coefficients b's and a's are real values and $\beta = b_m/a_n$ is gain constant. z_i's and p_j's are the poles and zeros of the transfer function. z_i's and p_j's occur either in purely real form $z_i = \sigma_i$, $p_j = \sigma_j$ or occur in complex conjugate pairs z_i, $z_{i+1} = \sigma_i \pm j\omega_i$; p_j, $p_{j+1} = \sigma_j \pm j\omega_j$(Fig. 5.1). The values of poles and zeros provide qualitative insights into the response characteristics of the system and together with gain constant they provide complete description of the system.

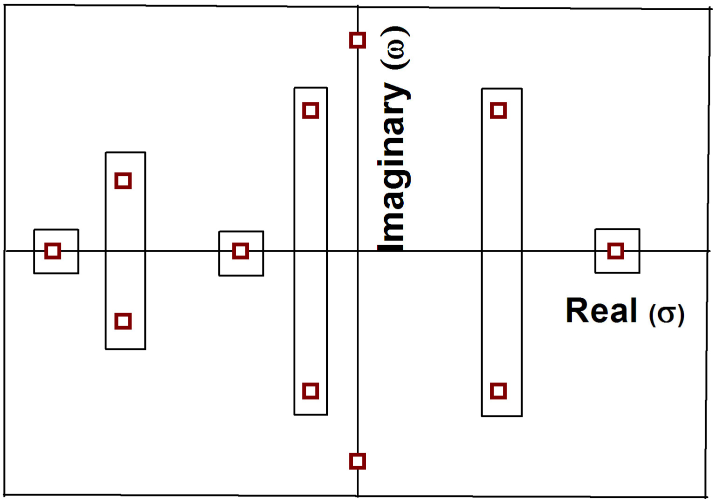

Figure 5.1: Nature of zeros and poles occurring in a transfer function.

5.3 Significance of poles and zeros

The significance of poles and zeros is schematically explained by Fig. 5.2. A complex zero represents the natural frequency associated with the energy-storage characteristic of a sub-portion of the system. It is lower than the natural frequency of the system, and it corresponds to the frequency at which the system behaves as an energy sink, such that the energy-storage elements of a sub-portion of the original system completely trap the energy that the input applies. Thus, no output can ever be detected at the point of measurement. The locations of the poles and the zeros of a transfer function are the result of design decisions and can make control easy or difficult. A complex-conjugate pole pair represents the natural frequency associated with the energy-storage characteristics, including kinetic and potential energy, of the physical system. At a frequency of the complex pole, energy can freely transfer back and forth between the kinetic and the potential energy, and the system behaves as an energy reservoir. The roots of denominator $D(s)$ i.e. the poles of transfer function determine whether a system is stable or not. Denominator $D(s)$ is characteristic polynomial of the system. A real pole $p_j = \sigma_j$ is associated with exponential response. The exponential response is diverging when σ_j is positive and converging when σ_j is negative. A complex pole

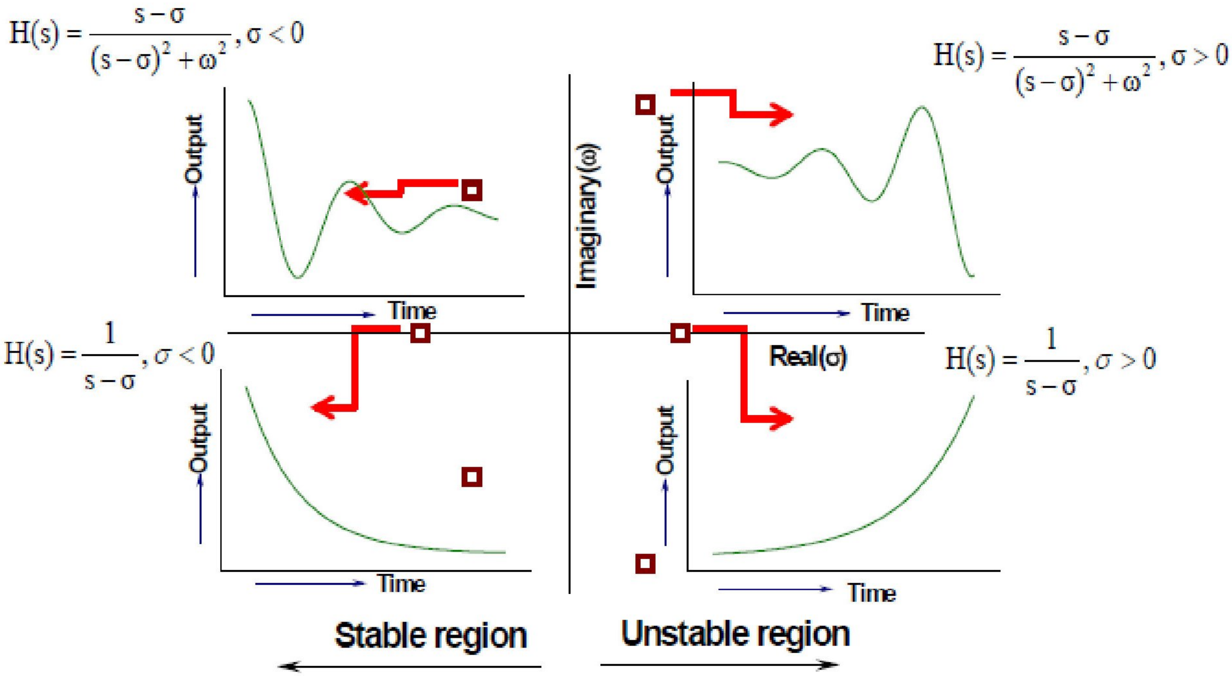

Figure 5.2: Stability representation of systems from different kind of transfer functions.

$p_j = \sigma_j \pm j\omega_j$ is associated with oscillatory exponential response. It is diverging oscillatory when σ_j is positive and decaying oscillatory when σ_j is negative. Equilibrium state at which the dynamical system is trying to reach from its non-equilibrium state is most probable and is most stable one. Thus, in equilibration process the real part of the poles of transfer function must be negative and the poles occupy the left side of s-plane.

5.4 Simulation Procedure

In MD[6] simulation technique the dynamics of an individual atom is governed by the Newton's laws of motion. The interaction potentials among the atoms are calculated by various techniques from which the interaction force field is calculated. Newton's equations of motion are then integrated based on these derived force field to understand the dynamics of individual atoms. The simulations have been performed for elements having different crystal structures like Silicon (Si), Germanium (Ge) having diamond cubic structure, Iron (Fe), Molybdenum (Mo) having body centered cubic structure and solid Argon (Ar), Copper (Cu) and Aluminum (Al) having face centered cubic structure. Various interaction potentials for different elements have been used for the calculation. In each simulation adopted periodic boundary condition has been adopted in three directions (x, y, z) in the simulation cell. Initially all the systems are equilibrated in the NVE (constant number of particles, volume and energy) ensemble at 100 K for 2.5 picoseconds (ps) and for solid Ar the system was equilibrated at 30 K for 10 ps.

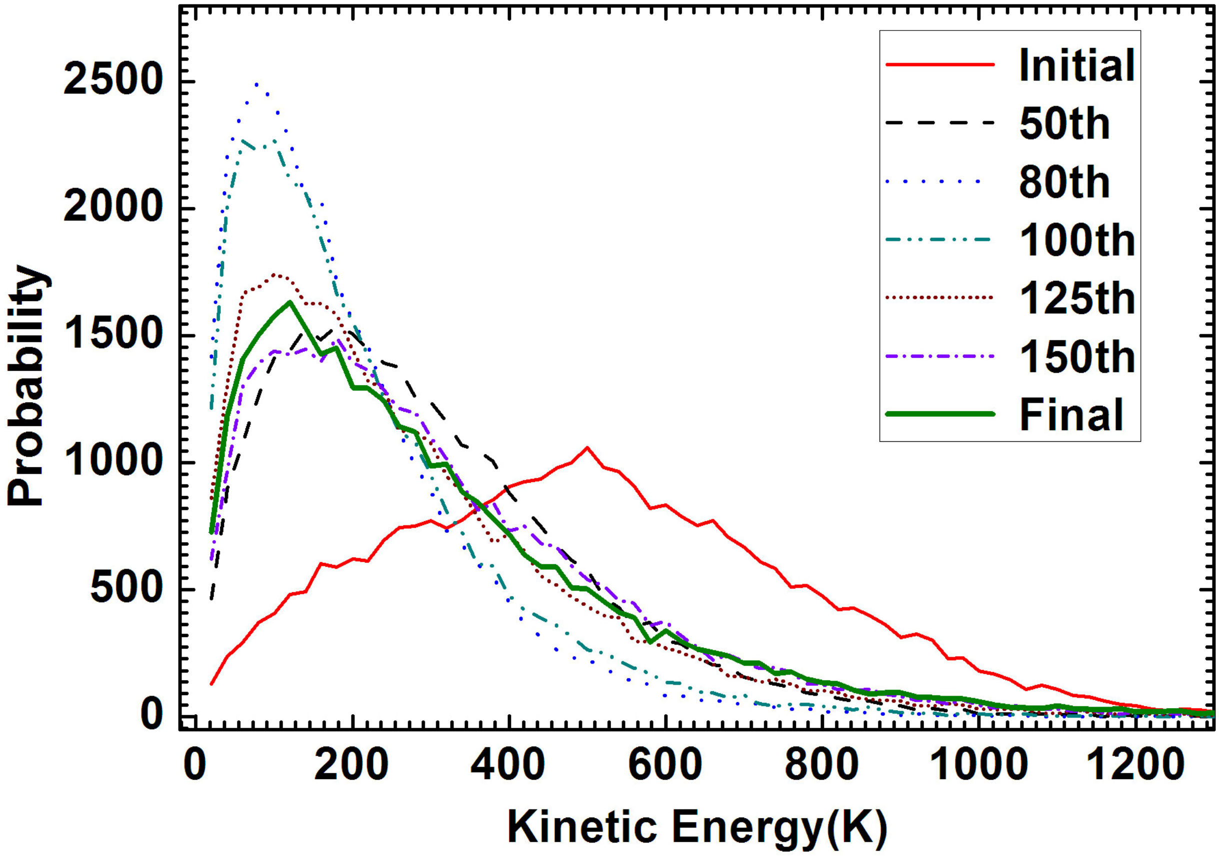

Figure 5.3: The probability distribution function of the kinetic energy (expressed in terms of temperature) of Cu atoms at initial, final and at five different time steps.

To generate the non-equilibrium state the velocities of the individual atoms in the simulation cell are changed to random values maintaining the average temperature at 500 K (70 K for solid Ar). The typical initial distribution function of KE for the Cu atoms in the

Table 5.1: The parameters used in the MD simulations.

Material	**Al**	**Cu**	**Fe**	**Solid Ar**	**Si-500**	**Ge-500**	**Si-800**	**Ge-800**	**Mo**
Simulation cell size (in unit cell)	20^3	20^3	25^3	20^3	25^3	15^3	15^3	15^3	25^3
Number of atoms in simulation cell	32000	32000	31250	32000	125000	27000	27000	27000	31250
Simulation time step (fs)	0.5	0.5	0.5	2.0	0.25	0.5	0.5	0.5	0.5
Inter-atomic potential used	GLUE[a]	EAM[b]	FS[c]	LJ[d]	SW[e]	SW	SW	SW	FS
Total number of data taken	3000	3000	3000	10000	6000	3000	3000	3000	3000
No. of bins used to define PDF	225	200	200	130	325	325	325	325	200
Bin size(in Kelvin)	20	20	20	5	20	20	20	20	20

---

[a] GLUE[7]
[b] EAM (Embedded Atom Model)[8, 9]
[c] FS (Finnis-Sinclair)[10]
[d] LJ (Lennard-Jones)[11]
[e] SW (Stillinger-Weber)[12]

non-equilibrium state is shown in Fig. 5.3. The atoms in the simulation cell are then allowed to equilibrate. The KE of all the atoms are calculated in subsequent time steps to evaluate the PDF. The PDF of KE for some discrete time steps are shown in Fig. 5.3. After sufficient period of time the system is observed to attain an equilibrium temperature of 300 K (50 K for solid Ar). The corresponding final equilibrium PDF is also shown in Fig. 5.3 by thick solid line. To understand the effect of the average temperature of the non-equilibrium state on the process of equilibration, velocity of the atoms in Si and Ge cases are also randomized making the average temperature to 800K. The details of the parameters used in the MD simulations[13] are given in the Table 5.1.

5.5 Data preparation for system identification

The variation of the KE of an atom is dictated by the force field experienced by it. The primary force field experiences by an atom arises from the nearest neighbor interaction potential whereas the interaction arising from the distant atoms generates a random force field. Thus the dynamics of the individual atom can be represented by the Langevin type equation[14]. Because of the existence of these force fields the KE of an atom and its reflection to the PDF of the ensemble at any instant of time will certainly have a deterministic and a random components. The calculated PDF of KE at different instant of time from the MD simulation is in the form of the distribution of KE in the bins and is identified as a vector $|X_i\rangle$ of dimension n in the i^{th} time step. The covariance matrix $\Sigma_x = \frac{1}{N}\sum_{i=1}^{N}|X_i\rangle\langle X_i| - |\bar{X}\rangle\langle\bar{X}|$ of all such vectors for a particular element is calculated. Where, $|\bar{X}\rangle = \frac{1}{N}\sum_{i=1}^{N}|X_i\rangle$ is the mean vector and N is the total number of time steps required for equilibration. Thus, each component of the data vector $|X_i\rangle$ consists of a deterministic component $|V_i\rangle$ and a random noise component $|\xi_i\rangle$. As $|\xi_i\rangle$ is uncorrelated with $|V_i\rangle$ and with another component of the random noise, the covariance matrix can be written as $\Sigma_x = \bar{\Sigma}_x + \langle\xi^2\rangle I_n$. Where, $\bar{\Sigma}_x$ is the covariance matrix formed by the deterministic components $|V_i\rangle$ and I_n is the unit matrix of dimension n. Thus λ_j, the eigenvalue of Σ_x, will be related with the corresponding eigenvalue $\bar{\lambda}_j$ of $\bar{\Sigma}_x$ by the relation $\lambda_j = \bar{\lambda}_j + \langle \xi^2 \rangle$, where j=1 to n. Hence, the noise causes all the eigenvalues of the covariance matrix Σ_x to be non-zero. Thus, when the data vectors are reconstructed with the eigenfunctions corresponding to the eigenvalues of significant magnitude they are devoid of random noise. Typical eigen values or the principal

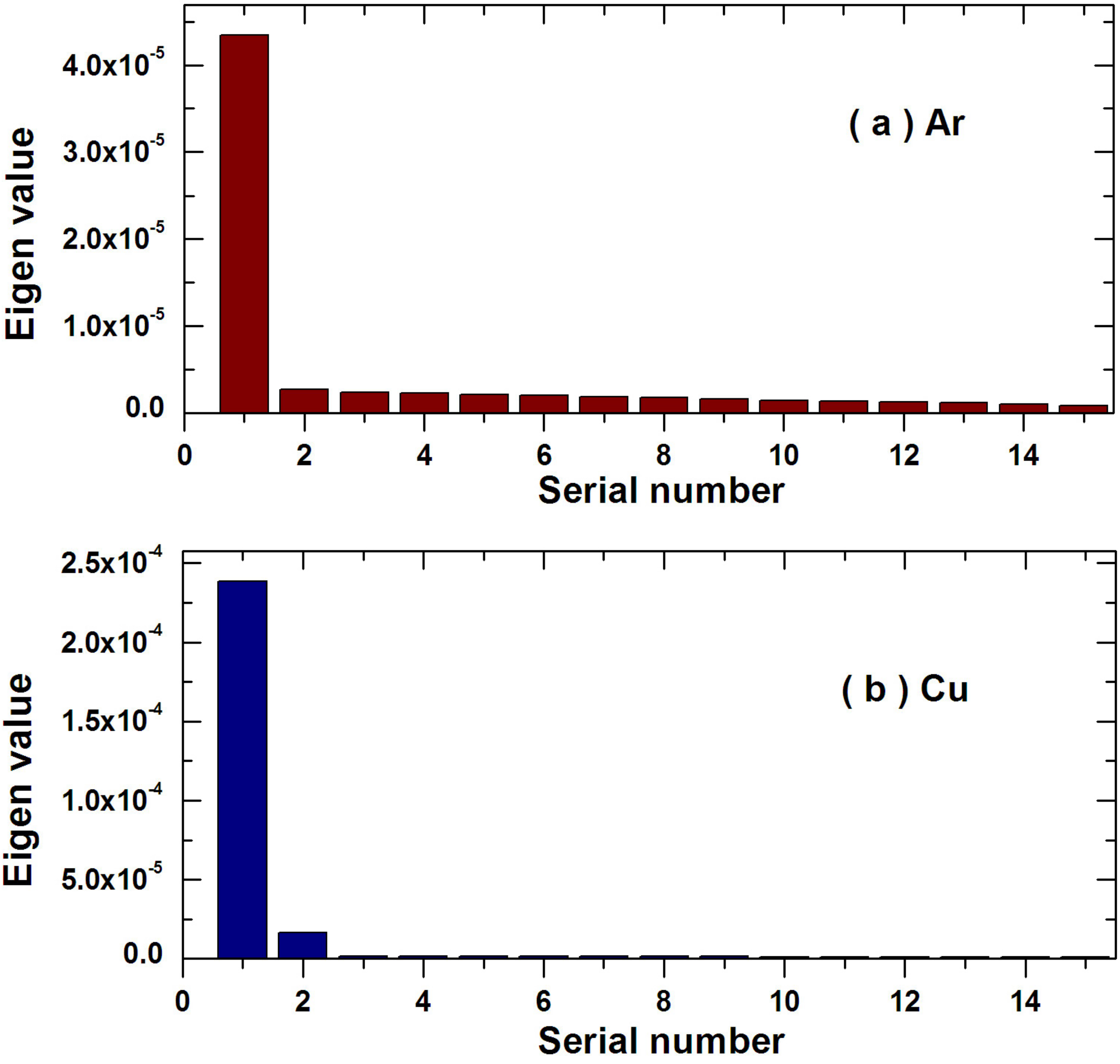

Figure 5.4: Eigen value spectra of the covariance matrix of (a) Ar and (b) Cu.

component spectra of Σ_x, for solid Ar and Cu are shown in Fig. 5.4. The prominent principal components for all the cases studied are found to be only two or three except for solid Ar where it is more than 20(Fig. 5.4). This is because, solid Ar being an inert gas crystal, the deterministic force field is reasonably weak compared to that of other studied elements. The trajectory of the evolution of the PDF in the subspace spanned by the eigen-functions corresponding to the primary principal components and the variation of the first principal component with time for Cu is shown in Fig. 5.5. The time evolution of these principal components for all the crystalline elements have a distinct oscillatory signature and a typical representation is shown in Fig. 5.5b.

5.6 Results and discussions

During the process of equilibration the PDF of KE oscillates about the equilibrium distribution as shown in Fig. 5.3. The amplitude of this oscillation reduces with time as the system approaches towards the equilibrium. Any system left of its own will certainly approach the final equilibrium distribution irrespective of the nature of the interaction among its constituents. Thus the dynamics of equilibration of this study is ultimately related to the nature of the coupled oscillation of the bins of PDF around their respective mean positions, determined by the equilibrium distribution. The existence of only 2 or 3 prominent eigen values of the covariance matrix Σ_x suggests that the oscillations are highly correlated. This modality of transforming the dynamics in reduced dimensional space helped us to analyze the complex dynamics in a more elegant way. The oscillation of the most significant eigen value (containing 82% to 95% of the trace of Σ_x in the respective cases) shows a decayed oscillation (Fig. 5.5b) as the system approaches equilibrium. This suggests that at equilibrium the deterministic component of PDF goes to zero. However, it is observed that for all studied cases the noise component remains the same. The observed nature of this oscillation is caused by the concerned system. So the prime interest will be to identify the nature of the system that is responsible for this oscillation by system identification technique[5]. This technique uses statistical methods to generate mathematical models of dynamical systems linking the observed data from the system.

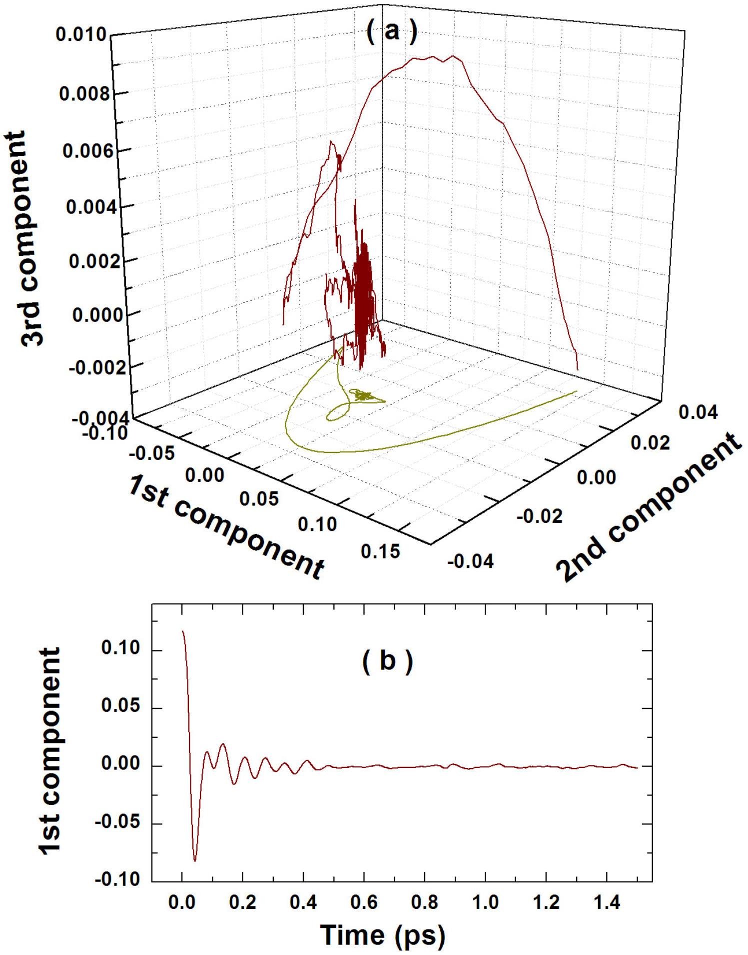

Figure 5.5: (a) Time evolution of the PDF of kinetic energy in the subspace spanned by the three eigen functions corresponding to the three largest eigen values of the covariance matrix Σ_x. The curve in the bottom plane is its projection. (b) Time evolution of the primary principal component of Cu.

In the MD simulation the equilibrium distribution of KE of the ensemble of atoms is purposely disturbed at time $t = 0$. Therefore the time evolution of the PDF can be considered as an outcome of the finite impulse response to the KE distribution in the system. Response of a system to a finite impulse can be used to estimate the characteristics of the system. From this observed impulse response the system responsible for this manifestation is identified. In system identification technique, the impulse response of a dynamical system is modeled from the response data and the system is estimated non-parametrically by time domain correlation analysis[5]. Correlation analysis presupposes a linear system and it does not require any explicit model structure.

The response to a finite impulse $u(t)$ is equal to the convolution of the impulse response and the transfer function $h(t)$ of the system and is given as $y(t) = \int_{\tau=0}^{+\infty} h(\tau)u(t-\tau)\,d\tau$.

The identified transfer function of the system is in Laplace domain which is given by $H(s) = \beta \frac{\Pi_i(s-z_i)}{\Pi_j(s-p_j)}$, where β is the gain constant. $H(s)$ is a rational function of the complex variable $s = \sigma + j\omega$. It provides the response characteristics of the system in the continuous domain without solving the necessary differential equation, governing the dynamics. The z_i's are the zeros and p_j's are the poles of $H(s)$, since $H(p_j) = \infty$ provided $z_i \neq p_j$. The poles and zeros of $H(s)$ together with β provide a complete description of the system. The partial fraction extension of $H(s)$ can be written as $H(s) = \sum_{j=1}^{P} K_j \frac{1}{(s-p_j)}$. Where, K_j's are the residues of the particular pole p_j and P is the number of poles in $H(s)$. From the inverse Laplace transformation of $H(s)$ one can obtain the natural response of the system as $\sum_{j=1}^{P} K_j \exp(p_j t)$, where the poles p_j's are the natural frequencies[15] of the system. The expression of $H(s)$ for Cu is given as

$$H(s) = 0.0022\frac{(s+1.018)(s+0.0296)((s+0.0078)^2+0.0842^2)}{(s+0.3178)(s+0.1044)((s+0.0048)^2+0.0930^2)((s+0.0250)^2+0.0420^2)} \tag{5.2}$$

For the present systems, the transfer functions have 2 to 3 complex conjugate pole pairs that are located to the left plane of the $j\omega$ axis as shown in Fig. 5.6 and the corresponding frequencies are given in Table 5.2. This guarantees that the denominator of $H(s)$ is never zero for any non-negative σ. As a consequence the system can not generate a sustained sine wave oscillation of the principal component but it will always be a decaying wave as shown in Fig. 5.5b. The poles of solid Ar are nearer to the origin directing the system to equilibrate over a longer period of time. This is the manifestation of the weak interaction of the atoms of the inert gas system. The poles and the corresponding frequencies of $H(s)$ for Si-500

Table 5.2: The frequencies at the poles of the transfer functions for different elements and their corresponding Debye frequencies at 298K.

	Al	**Cu**	**Fe**	**Solid Ar**	**Si-500**	**Ge-500**	**Si-800**	**Ge-800**	**Mo**
1st frequency (THz)	7.13	6.68	8.11	1.74	11.59	8.11	11.33	8.34	9.96
2nd frequency (THz)	12.03	14.80	14.20	4.19	30.67	14.35	29.11	14.48	15.91
3rd frequency (THz)	17.21				33.60	18.96	33.60	18.84	
Debye frequency at 298K (THz)[16]	8.13	6.46	7.76	1.92 [a]	14.4	8.4			7.86

---

[a] At 0K[17]

and Si-800 and for Ge-500 and Ge-800 are almost identical[Table 5.2], although their initial non-equilibrium states are different.

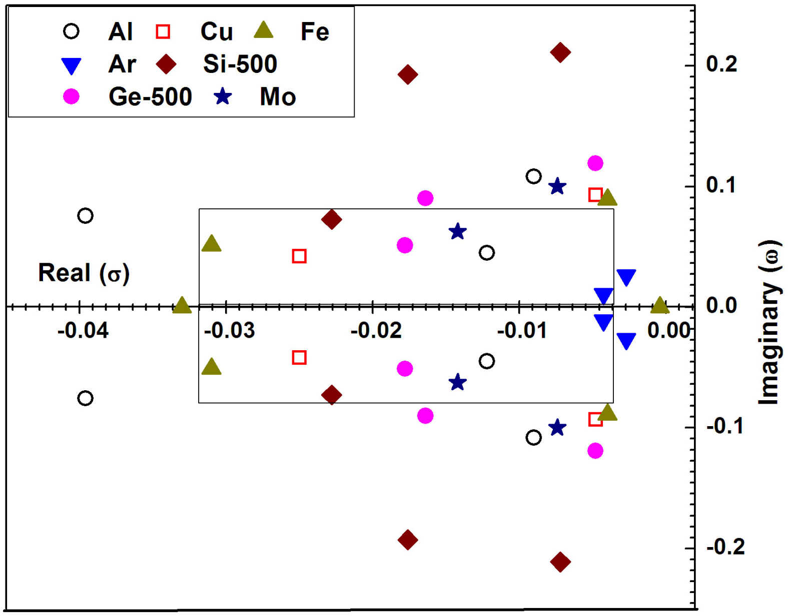

Figure 5.6: Real and imaginary part of the poles of the transfer functions for different elements. The points inside the box represents lower frequency. The poles of Si-800 and Ge-800 are not shown as they are almost identical to those of Si-500 and Ge-500 respectively.

5.7 Conclusions

The system in the process of equilibration redistributes its KE among the atoms. This in turn changes the spatial configuration of the atoms and the PE of the system. The impetus of the oscillation of PDF arises because the system is being compelled to attain the equilibrium distribution. The lowest frequencies of the poles of $H(s)$ for different elements are very near to the Debye frequencies[16, 17]. Other observed frequencies are much higher compared to the frequency of the lattice vibration. The lowest frequency having higher σ value signifies that it attenuates faster and helps the process of equilibration to the maximum extent. At the frequencies of the poles, the transfer function blows up and then only energy can be exchanged freely back and forth between KE and PE.

Equilibrium state of a system is uniquely defined. Non-equilibrium state of a system can be generated by various means and it is possible to bring it to any state far away from its equilibrium state. Thus, it is not realistic to adopt a proper definition for a non-equilibrium system. Consequently a question can arise whether there exists a unique way through which a non-equilibrium system equilibrates irrespective of how far it is away from equilibrium. This chapter tries to answer this question for certain crystalline systems. For this particular reason not only non-equilibrium states of various elements have been generated but also different non-equilibrium states for the same element are considered and then they are allowed it to equilibrate. The ensemble taken, is the simplest of all i.e. NVE or the micro-canonical ensemble. This statistical analysis of the time evolution of the PDF of KE shows that all the systems equilibrate in a unique way irrespective of the nature of the system and how far it is away from equilibrium.

Bibliography

[1] L. Onsager, Phys. Rev., 37 (1931) 405; 38 (1931) 2265.

[2] M. S. Green, J. Chem. Phys., 19 (1951) 1036.

[3] R. Kubo, J. Phys. Soc. Jpn., 12 570 (1957)

[4] Udo Seifert, Rep. Prog. Phys., 75 (2012) 126001 and the references therein.

[5] Lennart Ljung, *System Identification: Theory for the User* (second edition), Prentice Hall PTR (1999).

[6] http//micro.stanford.edu

[7] F. Ercolessi and J. B. Adams, Europhys. Lett., 26 (1994) 583.

[8] M. S. Daw and M. I. Baskes, Phys. Rev. B, 29 (1984) 6443.

[9] M. S. Daw, S. M. Foiles, and M. I. Baskes, Mat. Sci. Rep., 9 (1993) 251.

[10] M. Finnis and E. Sinclair, Phil. Mag. A., 50 (1984) 45.

[11] J. E. Lennard-Jones, Proc. R. Soc. Lond. A, 106 (1924) 463.

[12] F. Stillinger and T. A. Weber, Phys. Rev. B, 31 (1985) 5262.

[13] P. Barat, A. Giri, M. Bhattacharya, Nilangshu K. Das, and A. Dutta, Europhys. Lett., 104 (2013) 50003.

[14] Hideo Hasegawa, Phys. Rev. E, 83 (2011) 021104 and the references therein.

[15] Adel S. Sedra and Kenneth Carless Smith, *Microelectronic Circuits*, 4th ed, New York:Oxford University Press, 1998

[16] C. Y. Ho, R. W. Powell, and P. E. Liley, Journal of Physical and Chemical Reference Data, Volume 3, Supplement no. 1 (1975).

[17] G. R. Stewart, Rev. Sci. Instrum., 54 (1983) 1.

5.8 Appendix

5.8.1 Matlab procedure to obtain transfer function of a system from its output time series data

Time series data(real/complex) is read by matlab. Time-series data can not be directly used for transfer function model identification in system identification tool. Data preparation is required for the conversion of time series data into single /multiple output time domain data.

Read time series data in matlab workspace :: imported into the 'System Identification Tool' in the form of a column matrix . This data works as the time domain output data and an unit impulse (a column matrix having same dimension as that of output column matrix and the values of its elements are zeros except the initial one which is unity) is used as the input to the system. The output column matrix and the impulse input column matrix together are time domain data which the transfer function model supports. Perform any required data preprocessing operations(if required) :: select 'Estimate' > 'Transfer Function Models' :: 'Transfer Functions' window comes which requires the number of poles and zeros. Manually these numbers are changed to find out best fit (seen by clicking the 'Model output' in the 'System Identification Tool' window) of the output of time domain data. The corresponding polynomials of the denominator and numerator of transfer function are obtained by a double click on 'tf1' in 'System Identification Tool' window. Thereafter the values of poles and zeros are calculated.

Chapter 6

Role of Repulsive force in the Equilibration of Solid Argon

6.1 Introduction

In the previous three Chapters (3, 4 and 5) the time series evolution of kinetic energy of the constituents atoms of the systems undergoing equilibration is primarily the mainstay of analysis. The emphasis was entirely confined in the microscopic range since the time series data of kinetic energy of constituent atoms falls in the atomic scale. In the present chapter we would spread our observation into the macroscopic scale as well. Also, so far in the last three Chapters afew materials have been used for the MD simulation with appropriate interaction potential models. The used interaction potentials are appropriate in the sense that those models are being extensively used in the research community and successfully the results affirm and corroborate with experimental outcomes. It has been discussed in Section 2.3 of Chapter 2 that MD simulation assumes a cut off radius in the simulation supercell beyond which the affect of interaction potential is effectively considered as zero and the integrator, velocity verlet algorithm[1], integrates the equation of motion of the atomic trajectories of the atoms which are belongs to the sphere with radius having that cut off value to produce satisfying results. The central aim of this chapter would be, although the extensively potentials are worth enough to generate results to a certain degree of satiety, what would be the affect on the simulation results if the potential models are, keeping the nature of the interaction almost intact, slightly modified in order to incorporate a change in the value cut off radius.

Actually the famous review paper of S. Chandrasekhar[2] discusses in chapter 4 about the stellar dynamics of gravitational field arising from the random distribution of the stars. The fundamental problems of the stellar dynamics is concerned with the analysis of the nature of force acting on a given particular star which is one of the member of the solar system. Chandrasekhar suggested that there should be distinguishably two forces: first one is smoothly varying function of position and time due to the whole system and the second part is subjected to relatively rapid fluctuations due to the influence of intermediate local neighborhood. Analogous to the stellar system an atomic system may be, whatever be the nature of the incorporated potential model, thought of acted upon by a smoothly varying force field(deterministic part) and also by a randomly fluctuating force field(stochastic part) because of the random change in the atomic density in the intermediate neighborhood. This fact is very nicely depicted by the radial distribution function or pair correlation function of the system constituents by the fig. 7.7 in the next Chapter 7. Here on let us see what would be the association between those force fields and the equilibration process as the slight modification of potential model affects the cut off radius. For this purpose we would keep our attention, as has been mentioned earlier in this section, on the evolution of average system temperature which is a macroscopic thermodynamic entity of the system.

6.2 Modified form of the potential and molecular dynamics simulation

Let us consider the simplest inert gas crystal of solid Argon having face centered cubic crystal structure. Alike the previous three chapters(3, 4, 5), here also the system is initially set up in non-equilibrium state following the similar procedure. Atoms in solid Argon crystal have van der Waals bonding and are governed by Lennard-Jones potential. In the present study two separate non-equilibrium states of solid Argon crystal are considered by incorporating two forms of Lennard-Jones potentials. One of them is the original 12-6 potential[3] ($V_{12-6} = 4\epsilon[(\sigma/r)^{12} - (\sigma/r)^{6}]$) and the other is the variant of the original one, the 9-6 potential [4] ($V_{9-6} = 4\epsilon[(\sigma/r)^{9} - (\sigma/r)^{6}]$) with $\epsilon = 125K$ and $\sigma = 3.4A$. The size of the simulation cell for both the cases are 30 × 30 × 30 unit cells containing 108000 atoms. Periodic boundary conditions are imposed along all three directions (x, y, and z) in the simulation cells. Initially the systems are equilibrated using constant energy, number of particles and volume ensemble (NVE) at 30K for 100 ps. The period of time for equilibration is chosen to be sufficient to bring the total energy of the system to divide approximately equally between kinetic energy (KE) and potential energy (PE). To generate the non-equilibrium state, the three components of velocities of each of the individual atoms in the simulation cells were changed to random values such that the instantaneous KE of the atom increases, however the average temperature of the systems corresponds to T =70K. The atoms in the simulation cells are then allowed to equilibrate. After a sufficiently long period of time (20 ps), the systems are observed to attain an equilibrium temperature of 50K and the average KE becomes equal to the average PE of the systems. Average system temperature is estimated at each time step of 2 fs. A total 10000 steps were required for the equilibration. The variations of average temperatures with time of the systems leading to equilibration are shown in Fig. 6.1. The MD simulations are carried out using the LAMMPS [5] simulation package.

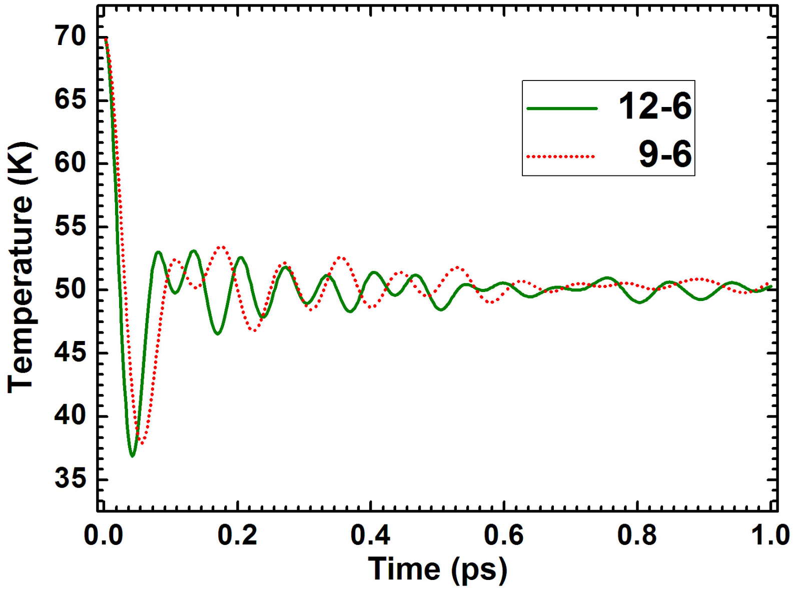

Figure 6.1: Temperature profiles of solid Argon crystals during the course of equilibration. Profile with solid line is corresponds to 12-6 crystal and dotted profile is corresponds to 9-6 crystal.

6.3 Impact on modified potential on the macroscopic entity: Evolution of average system temperature

Fig. 6.1 depicts how the two crystals equilibrate. The temperature profiles have oscillatory decaying nature as they proceed towards equilibrium. Apparently it is difficult to judge which system equilibrated faster relative to the other by just observing the profile of the two curves. By velocity rescaling when the KE energy of the simulating systems are enhanced to 70K, the configurations of constituent atoms remain intact. The configuration of atoms is correspond to 30K. This is the origin of unbalanced state. At higher temperature of the system the velocity of the constituent atoms are larger. As a consequence the constituents change their configuration according to the velocity such that the PE of the system increases. Because of the inertia of the transfer of KE initially exact amount of KE is not converted into PE. It make the system PE larger than the system KE and conversion occurs in opposite direction. This phenomena leads to the oscillatory temperature profile. How fast the oscillations are taking place in the transfer of KE into PE and PE into KE at different stages of equilibration and how long they sustain can not be predicted. Thus it requires further analysis. Before we proceed for the analysis part it is important to judge the radial variation of the two potential functions used in the simulations and the associated forces. Fig. 6.2 and Fig. 6.3 show the variation of the potential function and the force between the two Argon atoms for the two types of potential used. It is evident from the figures that the magnitude of negative potential and the force are always greater for the case of 12-6 potential than that of 9-6 one. Thus, the uses of 12-6 potential and 9-6 potential are quite relevant to introduce the variation in the magnitude of the force field in a solid Argon crystal. With out any quantitative analysis, the difference of the temperature profiles in the Fig. 6.1 address that the variation in the force field in the two cases has a significant impact on the equilibration process. The frequencies responsible for the energy transfer and the sustainability of the amplitudes correspond to these frequencies are are substantially affected due to the change in force field.

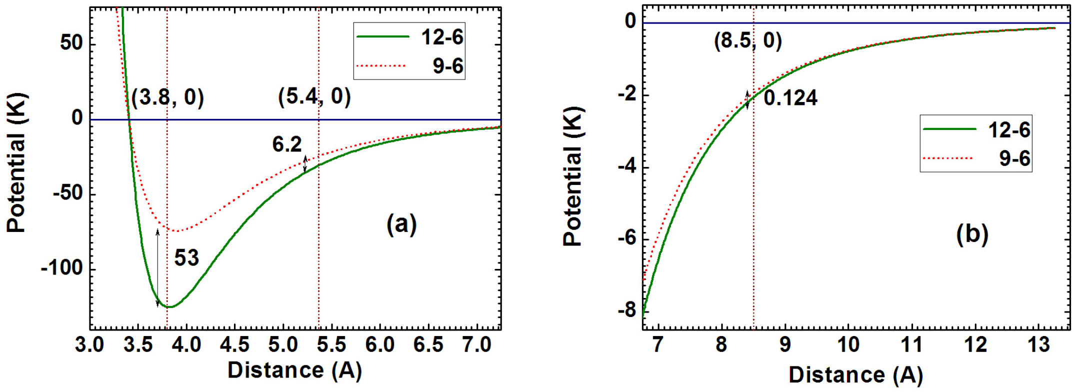

Figure 6.2: Lennard-Jones potentials as the function of inter-atomic distance for solid Argon crystal : (a) around a distance of lattice constant of solid Argon and (b) for larger distance..

6.4 System identification and results

The modality of equilibration is a very complex dynamical process. It is impossible to understand this dynamics analytically. The randomized state at 70K of two systems of solid

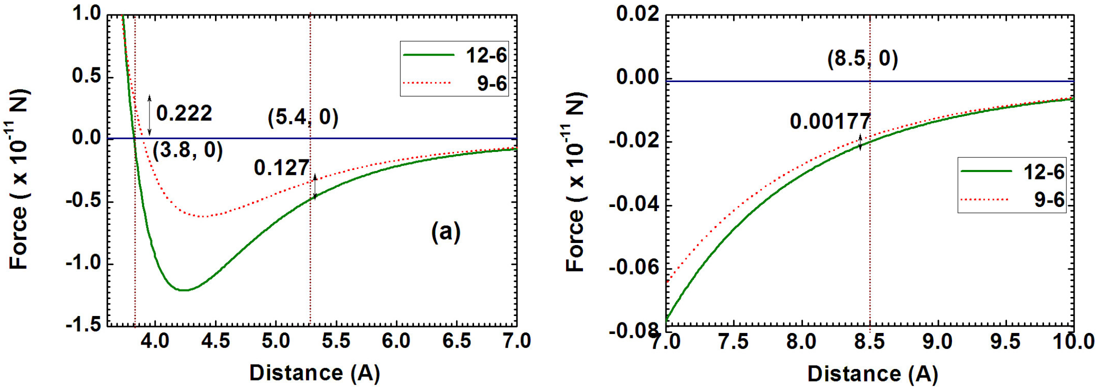

Figure 6.3: Lennard-Jones forces as the function of inter-atomic distance for solid Argon crystal : (a) around a distance of lattice constant of solid Argon and (b) for larger distance.

Argon crystal undergoing the equilibration acts as the sort of excitation and the response of the system to this finite impulse is the manifestation in the change of the average temperature at every time step. So if we take both the systems as a black box then at every instant of time the input to the box is the average temperature of the system and the output is the average temperature in the next step. Thus to understand the dynamics of the dynamical system we have to model the observed variation of the average temperature with time by system identification technique[6]. In the previous chapter(5) in details we have come across the working principle and the utility of system identification technique.

The poles of the transfer function$H(s)$ of temperature profiles of two different solid Argon systems are presented graphically in Fig. 6.4. For the studied systems of the present chapter, the transfer functions have three complex conjugate pole pairs(Table 6.1) that are located to the left plane of the $j\omega$ axis as shown in Fig. 6.4. This guarantees that the denominator of $H(s)$ is never zero for any non-negative σ which compels the non-equilibrium systems to equilibrate in a steady equilibrium state.

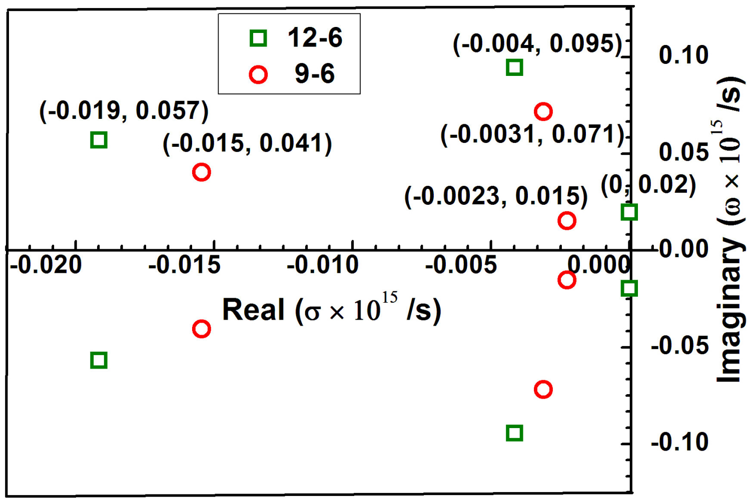

Figure 6.4: Graphical representation of the poles of the transfer functions of 12-6 crystal(squares) and 9-6 crystal(circles).

Table 6.1: The frequencies and the corresponding decay constants at the poles of the transfer functions for 12-6 and 9-6 solid Argon crystal.

Ar crystal	pole I		pole II		pole III	
	frequency (THz)	decay constant ($10^{15}/s$)	frequency (THz)	decay constant ($10^{15}/s$)	frequency (THz)	decay constant ($10^{15}/s$)
12-6	15.11	0.019	9.07	0.004	3.18	0
9-6	11.30	0.015	6.52	0.003	2.39	0.0023

6.5 Conclusions

The existence of complex conjugate pole pairs ensures quantitatively that the temperature profile is associated with oscillatory decaying nature. The 12-6 crystal which has larger magnitude of the force field converges to the equilibrium point faster since the decay constants(the real parts of the transfer function, see Table 6.1) are larger than those of its counterpart, the 9-6 crystal. Fig. 6.4 and fig. 6.5 ensures quantitatively that the force associated with 12-6 potential has the larger magnitude than that of 9-6 potential in the range between first nearest neighbor and forth nearest neighbor. Forth nearest neighbor and onwards they

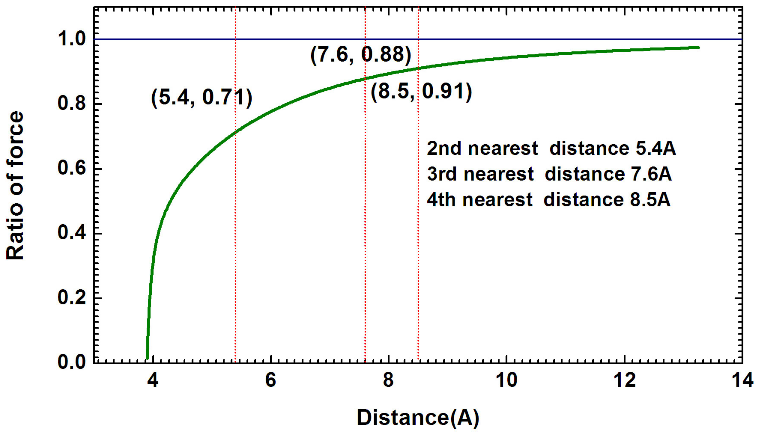

Figure 6.5: Ratio of the forces corresponds to 9-6 and 12-6 potential.

the force fields are more or less equal to each other. All these observation concludes that force in the region between first nearest neighbor and fourth nearest neighbor is mostly responsible for equilibration and the equilibration driven by a force having larger magnitude (12-6 potential) is faster and the sharing of kinetic energy and potential energy occurs more frequently(frequency, the real imaginary part is larger 12-6 potential, see Table 6.1) than those of the system driven by a force having smaller magnitude (9-6 potential).

Bibliography

[1] W. C. Swope, H. C. Andersen, P. H. Berens, and K. R. Wilson, J. Chem. Phys. **76**, 7 (1982).

[2] S. Chandrasekhar, Rev. M. Phys. **15**, 1 (1943).

[3] J. E. Lennard-Jones, Proc. R. Soc. Lond. A **106**, 4 (1924).

[4] A. Warshel and S. Lifson, J. Chem. Phys. **53**, 582 (1970).

[5] http://lammps.sandia.gov.

[6] Lennart Ljung, *System Identification: Theory for the User* (second edition), Prentice Hall PTR (1999).

Chapter 7

Measure of Complexity in Equilibrium Solid Argon System

7.1 Introduction

As the scale of human activity expands, our interaction with and dependence on Complex Systems is increasing rapidly. Continuing failure to deal appropriately with such systems poses a real threat whereas understanding their behavior offers the possibility of spectacular and unforeseen advances in many areas of science and its application.

Complex Systems research is the study of collective systems and their impact on their environment. Complex systems have emergent, non-linear properties and are able to adapt to changing environments; their traits can be observed in man made systems such as the Internet or the world's stock markets, as well as more organic structures such as ant colonies or collections of atoms and molecules.

The study of complexity is set to become a major area of interest for academia, society, industry and commerce in the 21st Century, as the world's political, economic, social and scientific arenas undergo change at an unprecedented rate. The science behind it is still in its infancy and is set to introduce a paradigm shift in our understanding of our natural, physical and social environment. However, the goal is not just to understand these systems but, ultimately, to manipulate them for the benefit of society and the economy.

Most of the systems observed in nature are complex in nature. Examples of complex systems are the flow of water in a river, metabolic activities in our body, the dynamic behavior of body cells etc. The manifestation of the dynamics of these complex systems are in the time and spatial scale. They are complex to us as because we can not predict their behavior or model them by a proper mathematical formalism. Modern science of this century are aiming to understand macroscopically the complex behavior of these systems by various statistical tools. The time series data, associated to an output variable, generated by such complex systems generally contain deterministic and stochastic components. Stochastic component represents the fluctuation in the output variable. The presence of this fluctuation is not simply due to contaminated noise. Rather a signature of the underlying dynamics of the system is reflected in the fluctuation of such uncontaminated stochastic component. Generally for time series analysis two classical approaches are used and these are related to deterministic and stochastic mechanism [1]. Both of them can explain the underlying dynamics of the system in a complementary manner. Instead of using any particular mechanism let us emphasize on a method which can quantify the degree of complexity of the time series. The measured complexity can be used to discriminate different time series generated by different dynamical systems or by same dynamical system having different physical conditions. In this context it is most important to mention that the first of its kind to define a dynamical system in terms of its complexity by Costa *et al.* [2]. Subsequently several works have been reported mostly on biological systems in several journals [3, 4, 5, 6, 7, 8, 9, 10] to measure the complexity of the dynamical systems.

The crystalline system is a very order structure as revealed by X-ray diffraction technique. In equilibrium at a fixed temperature the velocity of its constituents obey a stable Boltzmann distribution. Apparently one may think that such a system is one of the simplest one. However, if we go in deep and try to understand the dynamics of the system in terms of its constituent atoms, i.e. if the length scale is reduced and the dynamics of individual constituents atoms is observed it will obviously be complex. The atoms in crystalline systems can be of various types forming a cluster around a lattice point in the form of basis atoms. Interaction among these atoms is nevertheless highly non-linear. The atoms in a crystal at equilibrium are not static. They vibrate about their mean positions and the vibration frequencies are different for different atoms even though they follow a distribution of frequency. In addition the KE possessed by an atom of the system can have different values with finite probability. In spite of the fact that the system is in thermodynamic equilibrium the atoms at every moment acquire fresh KE value. The atoms vibrate about their mean position since they posses KE but don't have adequate space to move on in the solid structure although and also their vibration are not independent [11]. Thus, these apparent-simple systems are not as simple as it comes in ones thought. Moreover, for higher equilibrium temperatures the constituent atoms vibrate with higher amplitude about their mean making the atom dynamics much more complicated. In crystalline system the interaction with nearer neighbors leads to deterministic component and stochastic component of the force field turns up from the interaction with the distant atoms. This chapter deals with solid Ar systems at different equilibrium temperatures and with the help of molecular dynamics [12] simulation the temperature dependence and multiple scale factor dependence of the complexity of such simplest system are discussed.

7.2 Traditional entropy and complexity

For every system certain amount of information is required to describe it. In case of complex system this information is represented by the quantity complexity. By calculating complexity from the time series of a dynamical variable of physical system some conclusion can be drawn about the dynamics of the physical process. As per as information of a system is concerned physicists are accustomed with traditional entropy representation of the system which provides the randomness or disorderedness of the system. It merely evaluates the appearance of repetitive patterns of a time series and also no straightforward relationship exists between the repetitive pattern of a time series and its complexity. Complexity is related to "meaningful structural richness"[16] of the time series whereas the entropy based measurement looks for the randomness or the absence of regularity in a time series. Thus, for uncorrelated random noise entropy based method generates the highest value although the time series is not complex. Neither a completely predictable nor a completely unpredictable signal is structurally rich and both of them are not complex. In contrast, the assigned entropy to predictable signal is minimum and it monotonically increases with randomness of the signal to reach the maximum value for uncorrelated random signal(white noise). Thus, in time series analysis, entropy calculation doesn't lead to the proper understanding about the complex nature of the time series. For instance, entropy based methods assign higher entropy values to certain pathologic biological processes that generate irregular outputs than to healthy biological that are acutely regulated by multiple interacting control processes[2, 3] although the loss of complexity is a generic feature of pathologic dynamics and the biological complexity monotonically degrades with aging and disease. This contrast indicates the need for a thematically faithful formalism, instead of traditional entropy based measurements, for general applications so that visual intuition matches numerical results, for broad classes of stochastic processes as well as for dynamical systems.

7.3 Evolution of the irregularity and complexity measurement methods and introduction of the idea of multi-scale factor

Structural richness of a time series is associated to the inherent multiple spatio-temporal scale of the complex system. Generally one tries to distinguish a chaotic complex system via parameter estimation. The parameters typically associated with chaotic complex systems are the measures of dimension, rate of information generated(entropy), and the Lyapunov spectrum. The classification of dynamical systems via entropy and the Lyapunov spectra stems from work of Kolmogorov[13], Sinai[14], and Oseledets[15], though these works rely on ergodic theorems, and the results are applicable to probabilistic settings. Dimension formulas are motivated by a construction in the entropy calculation and generally resemble Hausdorff dimension calculations. The mentioned theoretical works above was not intended as a means to effectively and appropriately discriminate dynamical systems, given the data is finite and noisy. Pincus [16, 17] came with a solution by proposing a family of system parameters called approximate entropy(ApEn). It can potentially distinguish low-dimensional deterministic systems, periodic and multiply periodic systems, high-dimensional chaotic systems, stochastic, and mixed systems.

Construction of ApEn:

For any finite time series $\{\xi_i\} = [\xi_1, \xi_2, .., \xi_i, ...\xi_N]$ of N data points a vector sequences $u(1)$ through $u(N-m+1)$, defined by $u(j) = [\xi_j, \xi_{j+1}, .., \xi_{j+m-1}]$ with $1 \leq j \leq (N-m+1)$ can be constructed. These vectors represent m consecutive ξ values, commencing with the jth point. Define the distance $d[u(j), u(k)]$ between vectors $u(j)$ and $u(k)$ as the maximum difference in their respective scalar components. The vector sequence u(1),u(2), ... ,u(N-m+ 1) can be used to construct, for each $j \leq (N-m+1)$, $P_j'^m(r) =$ (number of $j \leq (N-m+1)$ such that $d[u(j), u(k)] \leq r)/(N-m+1)$. The $P_j'^m(r)$'s measure within a tolerance r the regularity, or frequency, of patterns similar to a given pattern of window length m. Define $U^m(r) = (N-m+1)^{-1} \sum_{j=1}^{N-m+1} \ln P_j'^m(r)$, where ln is the natural logarithm, then define the parameter ApEn(m,r,N)=$U^m(r) - U^{m+1}(r)$.

Mathematically, ApEn is the part of a general development as the rate of entropy for an approximating Markov chain to a process[18]. In applications to heart rate, findings have discriminated groups of subjects via ApEn, in instances where classical [mean, standard deviation (SD)] statistics did not show clear group distinctions [19, 20, 21, 22, 23]. In applications to endocrine hormone secretion data based on as few as N =72 points, ApEn has provided vivid distinctions between actively diseased subjects and normals, with nearly 100% specificity and sensitivity[24].

Informally, for N points, the family of parameters ApEn(m, r, N) is approximately equal to the negative average natural logarithm of the conditional probability that two sequences that are similar for m points remain similar, that is, within a tolerance r, at the next point. Thus a low value of ApEn reflects a high degree of regularity. Importantly, the ApEn algorithm counts each sequence as matching itself, in the calculations to skip the occurrence of ln(0) a practice is carried over following the work of Eckmann and Ruelle [25]. In practice, it is found that ApEn lacks two important expected properties. First, ApEn is heavily dependent on the record length and is uniformly lower than expected for short records. Second, it lacks relative consistency. That is, if ApEn of one data set is higher than that of another, it should, but does not, remain higher for all conditions tested [17]. This shortcoming is particularly important, because ApEn has been repeatedly recommended as a relative measure for comparing data sets [17, 21].

Following the approach of Grassberger and co-researchers[26, 27, 28, 29], Richman and Moorman[30] developed sample entropy (SampEn(m, r, N)) which is precisely the negative natural logarithm of the conditional probability that two sequences similar for m points remain similar at the next point, where self-matches are excluded during the calculation of the probability. Thus a lower value of SampEn also indicates more self-similarity in the time series. In addition to eliminating self-matches, the SampEn algorithm is simpler than the ApEn algorithm, requiring approximately one-half as much time to calculate. SampEn is largely independent of record length and displays relative consistency under circumstances where ApEn does not.

Construction of SampEn: If $n_j^m(r)$ be the number of vectors $u(k)$ with in the distance r of any particular vector $u(j)(j \neq k)$ the probability of that any $u(k)$ is within r of $u(j)$ is $P_j^m(r) = n_j^m(r)/(N-m)$. $P^m(r)$ is defined by

$$P^m(r) = 1/(N-m) \sum_{j=1}^{N-m} P_j^m(r) \tag{7.1}$$

and the SampEn is defined as

$$\begin{aligned} SampEn(m,r,N) &= \ln \frac{P^m(r)}{P^{m+1}(r)} \\ &= \ln \frac{\sum_{j=1}^{N-m} n_j^m(r)}{\sum_{j=1}^{N-m} n_j^{m+1}(r)} \end{aligned} \tag{7.2}$$

whereas,

$$\begin{aligned} ApEn(m,r,N) &= U^m(r) - U^{m+1}(r) \\ &\approx \frac{1}{N-m} \sum_{j=1}^{N-m} \ln \frac{P_j'^m(r)}{P_j'^{(m+1)}(r)} \\ &= \frac{1}{N-m} \sum_{j=1}^{N-m} \ln \frac{n_j'^m(r)}{n_j'^{(m+1)}(r)} \end{aligned} \tag{7.3}$$

where n_j^m differs from $n_j'^m$ to the extend that for SampEn self-matches are not counted $(j \neq k)$ and $1 \leq j \leq N-m$. A typical example of the procedure for calculating SampEn (m=2 and r is a arbitrarily chosen positive number) is illustrated in FIG. 7.1.

Application of both the ApEn and SampEn algorithms assign higher entropy for certain pathologic time series data than free running healthy physiological data which is a bit confounding. Intuitively a pathologic time series represents less complex system and do not comply with numerical results. The reason behind this unphysical result is that all these algorithms are based on single scale and only the uncertainty associated to the next new point is reflected in the entropy. As already stated that the structural richness and the complex behavior of a time series is significantly tied with inherent multiple spatio-temporal scale ApEn and SampEn algorithms do not account the features related to multiple scales other

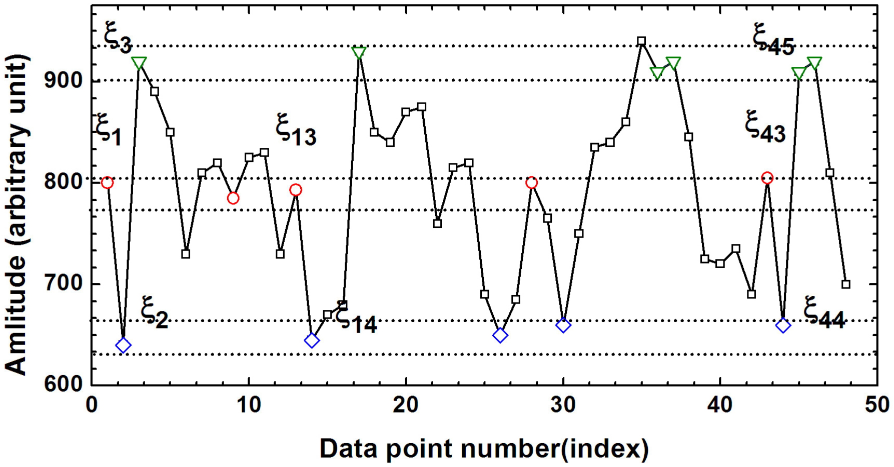

Figure 7.1: A typical time series of 48 data points $[\xi_1, \xi_2, ..., \xi_{48}]$ is considered for the illustration of the SampEn calculation procedure for $m = 2$ and for a real positive r value. This simulated time series provides 47 and 46 two component and three component vector sequences respectively. The dotted horizontal lines around data points ξ_1, ξ_2, ξ_3 are $\xi_1 \pm r$, $\xi_2 \pm r$, $\xi_3 \pm r$ lines respectively. The data points which match with first three data points(ξ_1, ξ_2, ξ_3) are represented by symbols ◦, ⋄, and ▽ respectively. For first two-component ◦-⋄ vector[ξ_1, ξ_2] we find only two other matching ◦-⋄ sequences [ξ_{13}, ξ_{14}] and [ξ_{43}, ξ_{44}]. This procedure is repeated for all the 47 two-component vectors and the matching counts for each two-component vectors are added up. Similarly for first three-component ◦-⋄-▽ vector[ξ_1, ξ_2, ξ_3] we find only one matching ◦-⋄-▽ sequence [ξ_{43}, ξ_{44}, ξ_{45}]. For all the 46 three-component vectors the matching procedure is repeated and the matching counts for each three-component vectors are added up. The natural logarithm of the ratio of total number of two-component matching and three-component matching provides the SampEn(m=2, r) for that particular simulated time series.

than the original scale. Zhang [31] proposed an approach to take into account the multi-scale information for large noise free data. Obviously physiological and physical signals are bounded and are not noise free.

SampEn algorithm is free from these two limitations whereas Zhang's method takes into account the multi-scale effect. Thus, collective use of Pincus's, Richman's, and Zhang's approach provides(treated as MSE analysis) the exact behavior of complex systems. Costa and co-workers used this approach, for the first time, to biological and physiological signals[2, 3, 4, 5, 6, 7, 8, 9, 10]. Afterwards, MSE analysis has been applied to metallurgical systems [32, 33] to calculate the complexity. In the present chapter, for the first time, the aforesaid method is used in the time series data of KE (FIG. 7.2) of individual atoms of solid Ar at various equilibrium temperatures.

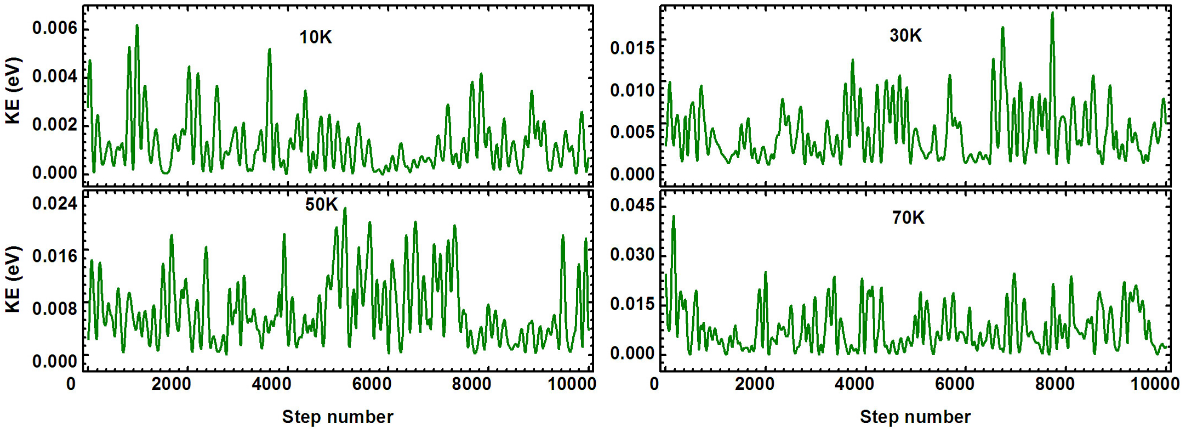

Figure 7.2: Time series data of KE of single Ar atom at temperatures 10K, 30K, 50K, and 70K. Each series contains 10^4 data points.

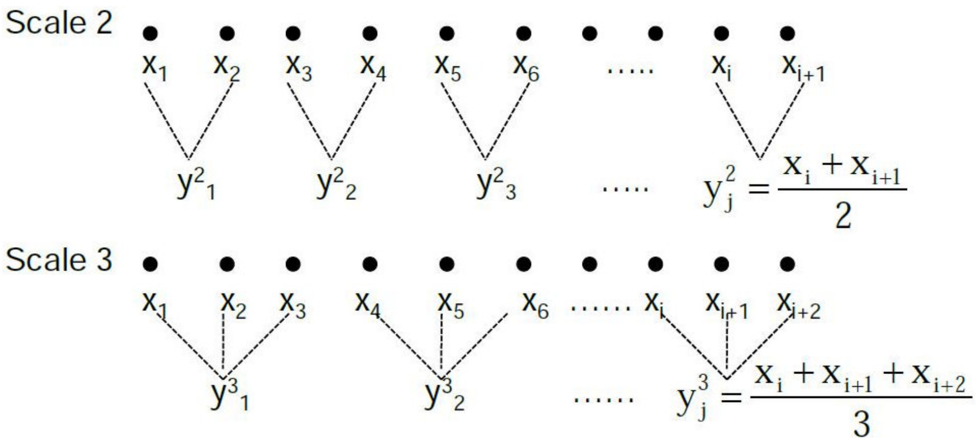

Figure 7.3: Procedure to generate new coarse-grained time series of scale factor two and three from the original time series($\{x_i\} = [x_1, x_2, ..., x_N]$) which is also a coarse-grained time series with scale factor one.

Construction of coarse-grained time series for different scale factors : Consider a finite time series data of N points given by $\{x_i\} = [x_1, x_2, ..., x_N]$. The algorithm for the coarse-grained time series corresponding to scale factor τ can be written as:

$$y_j^{\tau} = \frac{1}{\tau} \sum_{i=(j-1)\tau+1}^{j\tau} x_i \tag{7.4}$$

where y_j^τ is the j_{th} component of coarse-grained time series ($\{y_j^\tau\}$=[y_1^τ,y_2^τ,...,y_{jmax}^τ]) with scale factor τ and $1 \leq j \leq N/\tau$. Thus the coarse-grained series for scale factor $\tau = 1$ is the original time series. FIG. 7.3 is a schematic representation of coarse-graining procedure for scale factor two and three. Application of SampEn to each of these coarse-grained time series provides the MSE. This method is applied to white noise (FIG. 7.4a) and $1/f$ (FIG. 7.4b) noise (with 10^5 data points) to reproduce the result(inset of FIG. 7.5) which was reported by Costa and co-researchers [2, 3]. FIG. 7.5 shows a congruity between numerical results and our intuition about regularity and complexity of these two types of noise. White noise contains all the frequencies with equal probability. Hence no constraint will be there on the similarity of the frequency of data points of white noise. This regularity is reflected in the lower values of multi-scale entropy. On the contrary for 1/f noise lower frequencies are most likely compared to the higher frequencies (FIG. 7.6). This particular restriction makes the 1/f noise to lose the regularity in the data points. The higher values of SampEn justifies this idea. The linear nature of SampEn against scale factor(in *log* scale) indicates logarithmic relation between SampEn and scale factor for both the noises.

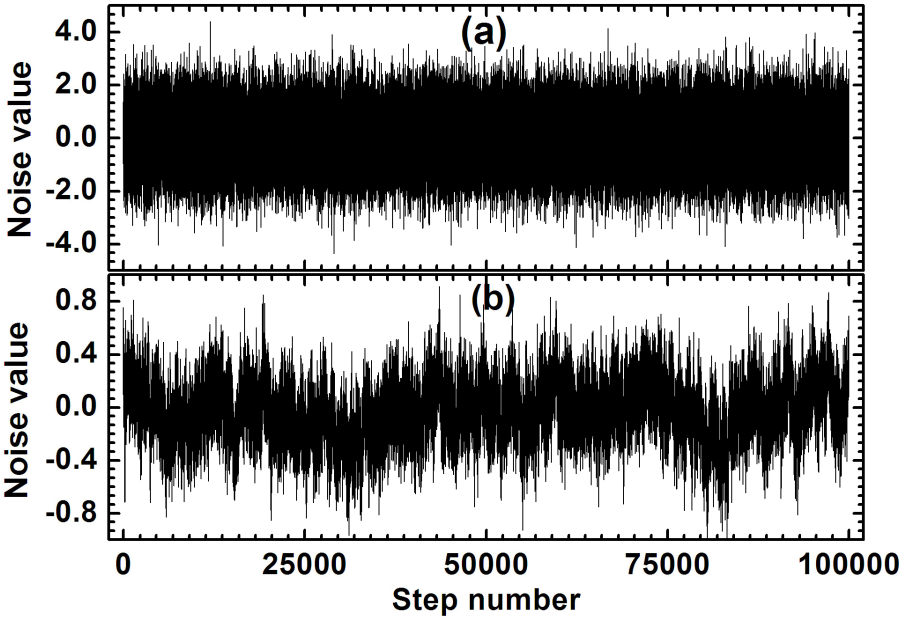

Figure 7.4: Time series of (a) white noise and (b) 1/f noise with 10^5 data points.

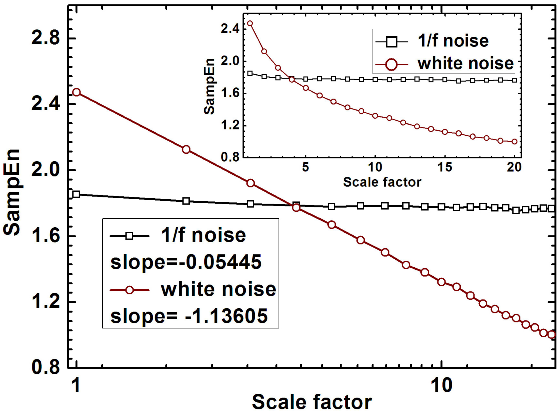

Figure 7.5: MSE analysis($m = 2$, $r = 15\%$ of the standard deviation of the respective original time series) of white noise (circular) and 1/f noise (square) with 10^5 data points showing the logarithmic relation between SampEn and scale factor and the inset is exactly the result showed by Costa *et al.* [2, 3]

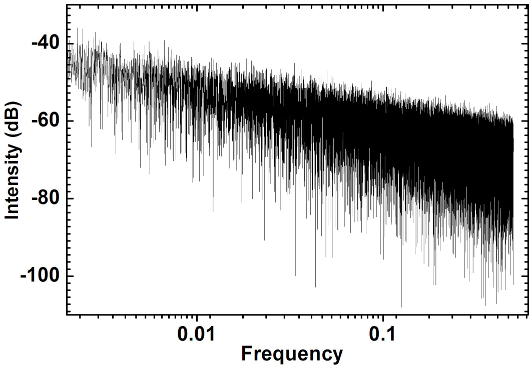

Figure 7.6: Frequency spectrum of 1/f noise.

7.4 Simulation procedure

The required time series data, for the measurement of complexity of crystalline systems, are generated with the help of molecular dynamics simulation technique. Molecular dynamics provides the time series data of KE of the individual constituent atoms in the time interval of the order of femtosecond(fs). A cubic system of solid Ar of dimension of 30 unit cells(uc) in each of the three directions is taken as simulation cell. The crystalline solid Ar has face centered cubic structure and the simulation cell contains 108000 atoms. Periodic boundary condition is imposed in all the three directions of the cell to avoid any surface effect. At every 2fs time interval the Newtonian equations of motion of each constituent atom of the system are solved with the help of widely used Lennard-Jones(12-6) potential [34]. Initially,

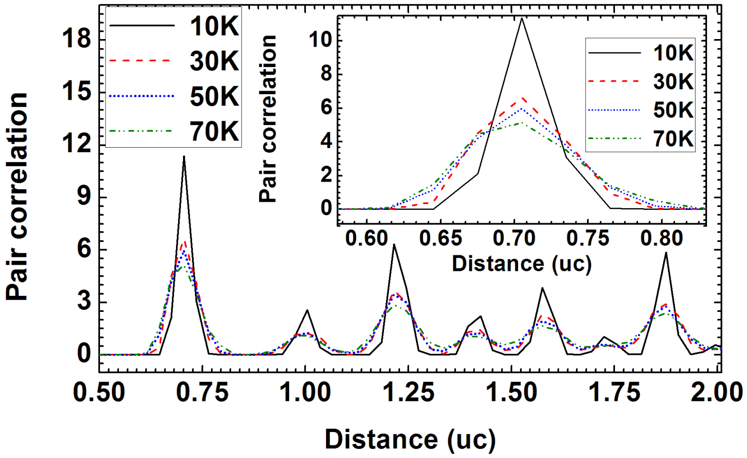

Figure 7.7: Variation of pair correlation function of solid Ar at different equilibrium temperatures. The figure in the inset represents the enlarged view of the first peak.

the velocity components of all the constituent atoms of the simulation cell are defined by random numbers such that the initial average KE of the system becomes double of the value what is expected in equilibrium and the average potential energy(PE) is zero. Thereafter, using constant energy and volume ensemble (NVE) the crystalline solid Ar system is left of its own for long time(50000 steps, 100ps) to reach the equilibrium distribution. Under equilibrium, the final average KE is equal to the average PE and because of this transfer of KE into PE, the final average KE value reaches the desired value (half of the initial average KE). After the system reaches the equilibrium, the simulation run is continued for another 20ps and atomistic simulation data are recorded at each time step of that 20ps(10000 steps) interval to study the complex dynamics of the equilibrium crystalline system. For different equilibrium temperatures(10, 30, 50 and 70K) of crystalline solid Ar system this procedure is repeated.

7.5 Computation of MSE of crystalline solid Ar

In FIG. 7.7 the pair correlation function (sometimes called radial distribution function) of the Ar atoms is portrayed for different equilibrium temperatures. Pair correlation function describes how the normalized particle density varies as a function of distance from a reference particle. The atom residing at the center of the simulation cell is considered as the reference particle. For closer distance it exhibits peaks at first, second, third nearest neighbor etc. and gradually flattens to unity for larger distance. An increment in temperature enhances the KE of individual atoms and hence the amplitude of vibration about their respective mean positions. Gradual flattening of the first peak at the cost of peak height (in the inset of FIG. 7.7) consolidate the concept of larger KE and larger vibration of atoms for increasing temperatures. Thus, rise of temperature introduces more randomness and irregularity to the dynamics of system particles. Temperature dependence of the standard deviation and the height of the first peak of pair correlation function are shown in FIG. 7.8a and FIG. 7.8b respectively.

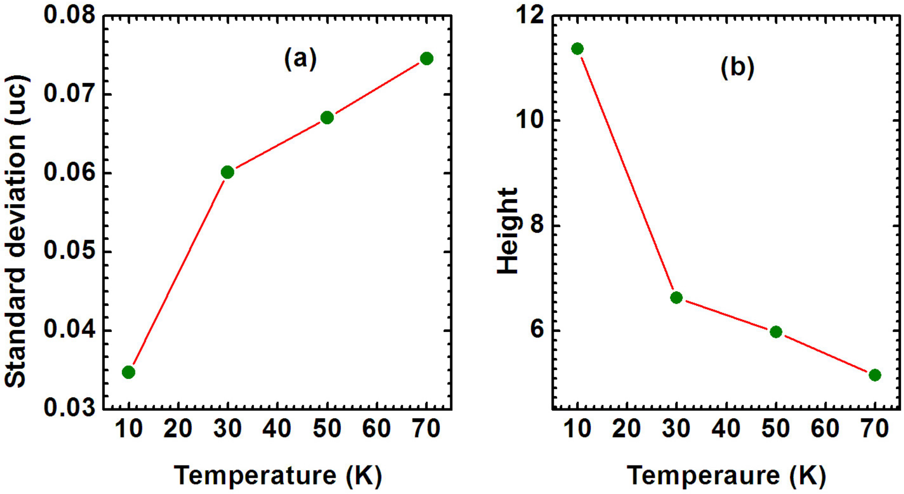

Figure 7.8: Temperature variation of (a) standard deviation and (b) height of the first peak.

Few atoms (around 70) in the simulation cell are identified with in a sphere of radius 1.6uc whose center is chosen to be almost at the middle of the cell, far away from the surface. The time series data (10^4 data points) of KE of the identified atoms are used for the analysis. Throughout the analysis the values of SampEn are estimated with $m = 2$ and the r value equals to 15% of the standard deviation of original time series data. Subsequently the average of SampEn over the identified atoms is considered for the quantification of the complex behavior of the particle dynamics. The dependence of average SampEn on scale factor is shown in FIG. 7.9. The corresponding figure in the inset of FIG. 7.9b provides an idea about the temperature variation of complex nature of the system for scale factors 16-25. It is observed that for a particular scale factor SampEn increases linearly with temperature.

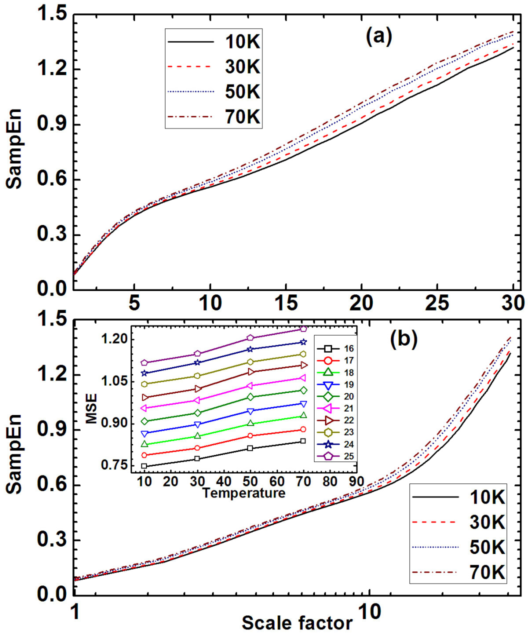

Figure 7.9: Calculated SampEn for different equilibrium temperatures of solid Ar in (a) *linear* scale and in (b) *log* scale. Dependence of SampEn on temperature for different scale factors are shown in the inset of (b).

7.6 Result and conclusions

The pair correlation function (FIG. 7.7) and the calculated SampEn (FIG. 7.9) corroborate each other. Pair correlation function reflects the idea what our intuition tells about the complex dynamics of the system. Whereas, MSE is the method to quantify the irregularity of uncorrelated noise of a complex system. Flattening of pair correlation peak (inset of FIG. 7.7) with the enhancement of temperature and the linear dependence of SampEn on temperature (inset of FIG. 7.9b) both are the signature of analogous fact that temperature makes the system dynamics more uncorrelated, noisy and irregular. Another important outcome of the current MSE analysis is the peculiar random nature of time series data of KE. Continuous coarse-graining procedure can not eliminate the uncorrelated random component of the time series which is originally uncorrelated and irregular. Rather the procedure progressively makes the correlation of the time series even worse. The inherent multiple spatio-temporal scale dependence is exposed for higher scale factors. Undoubtedly, only the asymptotic value of SampEn (scale factor one) does not make any sense about the complexity and the introduction of multi-scale factor in the analysis of complexity affirms its utility.

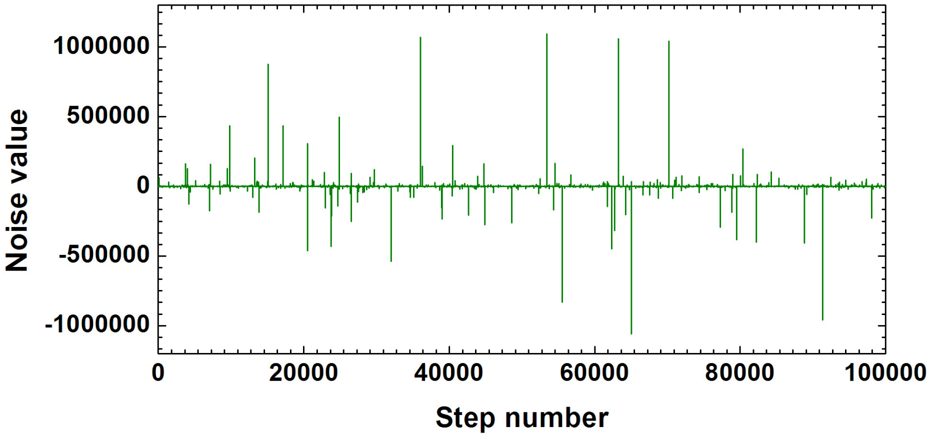

Figure 7.10: A typical Levy noise with 10^5 data points. Hurst exponent, $\alpha = 0.7$

Recently P. Barat *et al.* have shown that in crystalline solid systems the time series data of the KE of individual atoms exhibits Levy walk property [35]. On the other hand using Ford-Kac model [36] and Caldeira-Leggett model [37, 38] Hideo Hasegawa has shown that the individual particles of a classical small system coupled to finite bath [39] follow Langevin equation [40]. In this context, synthetically Levy noise and Langevin solution are generated and an exercise has been carried out on the complex behavior of these noisy signals. The

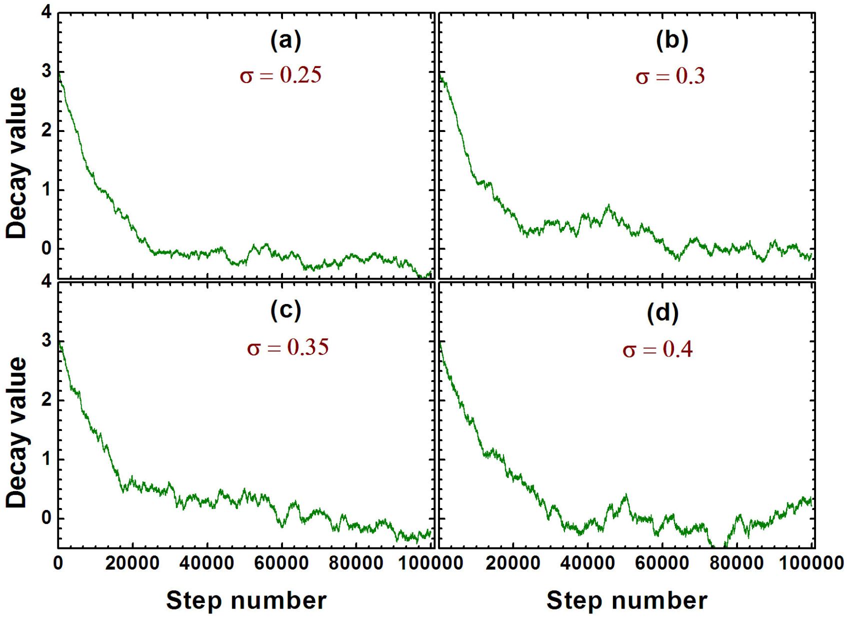

Figure 7.11: Exponential decay series with different amplitude of the noise component. (a) $\sigma = 0.25$, (b) $\sigma = 0.3$, (c) $\sigma = 0.35$, (d) $\sigma = 0.4$. Each series starts at initial value 3.

Levy noise is the time series of 10^5 data points having Hurst exponent 0.7 (FIG. 7.10). The time series of Langevin solution represents an exponential decay with noise given by the equation:

$$dx(t) = -x(t)\, dt + \sigma\, dB(t)$$

In discrete form

$$x(i+1) = x(i) - x(i)\Delta t + \sigma\sqrt{\Delta t} \times \text{(a random number)}$$

where, the σ value introduce the noise component to the decay series and Δt is the dimensionless time interval. The decay constant being dimensionless unity. Eight exponential decay series with varying σ values (0.05, 0.1, 0.15, 0.2, 0.25, 0.3, 0.35, 0.4) are generated (FIG. 7.11). At time $t = 0$ the decay starts with initial value 3 and data points are stored at every $\Delta t = 8 \times 10^{-5}$ time interval.

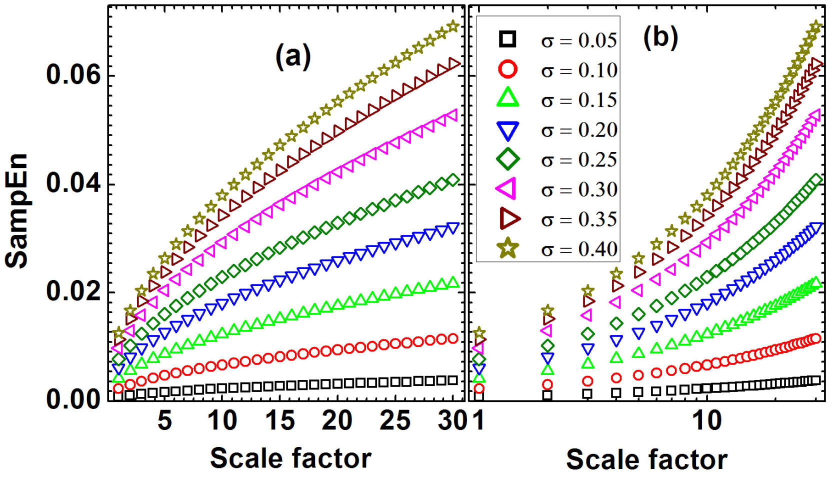

Figure 7.12: MSE analysis of exponential decay series with noise(Langevin solution) in (a) *linear* scale and in (b) *log* scale.

For MSE analysis of Langevin solutions only the flat tail parts of decay series (containing final 5×10^4 data points) are considered. The quantified SampEn values for Langevin solutions are illustrated in FIG. 7.12. Similar to the temperature effect (enhancement of the amplitude of atomic vibrations) in solid Ar crystal the SampEn of decay series with larger σ values quantifies higher degree of uncorrelated randomness. The scale dependence of SampEn for both Levy noise (FIG. 7.13) and Langevin solutions exhibit similar sort of tendency as that of the time series data of KE of individual atoms in solid Ar system. Unlike

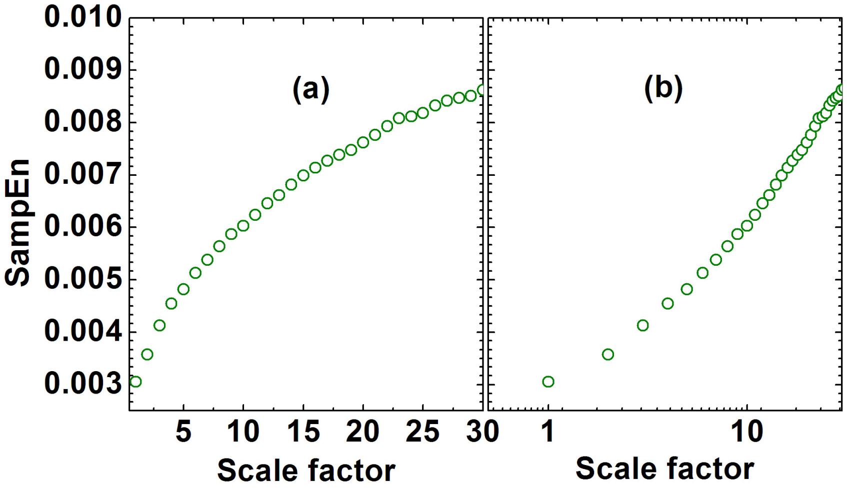

Figure 7.13: MSE analysis of Levy noise in (a) *linear* scale and in (b) *log* scale.

the white noise and 1/f noise, in case of time series data associated to molecular dynamics generated of KE of Ar atoms, Levy noise, and Langvin solution the SampEn is not related to scale factor by logarithmic function. With scale factor, in all these three cases, SampEn increases with decreasing slope. Thus, the complexity analysis of time series data of KE strengthen the remarks of references [35] and [40].

Bibliography

[1] F. Takens, *Dynamical Systems and Turbulence*, edited by D. A. Rand and L. S. Young. Lecture Notes in Mathematics Vol. **898** Springer, Berlin, 1981, p. 366.

[2] M. Costa, Ary L. Goldberger, and C.-K. Peng, Phys. Rev. Lett. **89**, 068102 (2002).

[3] M. Costa, Ary L. Goldberger, and C.-K. Peng, Phys. Rev. E **71**, 021906 (2005).

[4] M. Costa, Ary L. Goldberger, and C.-K. Peng, Physica A **330**, 53 (2003).

[5] M. Costa, C.-K. Peng, and Ary L. Goldberger, Cardiovascular Engineering **8**, 88 (2008).

[6] M. Costa, A. A. Priplata , L. A. Lipsitz, Z. Wu, N. E. Huang, Ary L. Goldberger, and C.-K. Peng, Europhys. Lett. **77**, 68008 (2007).

[7] MM. Costa, I. Ghiran, C.-K. Peng, A. Nicholson-Weller, and Ary L. Goldberger, Phys. Rev. E **78**, 020901 (2008)(R).

[8] H. G. Kang, M. Costa, A. A. Priplata, O.V. Starobinets, Ary L. Goldberger, C.-K. Peng, D. K. Kiely, L. A. Cupples, L. A. Lipsitz, The Journals of Gerontology Series A: Biological Sciences and Medical Sciences **64A(12)**, 1304 (2009).

[9] B. Manor, M Costa, K. Hu, E. Newton, O. Starobinets, H. G. Kang, C.-K. Peng, V. Novak, L. A. Lipsitz, Journal of Applied Physiology **109(6)** 1786 2010.

[10] S. J-J. Leistedt, P. Linkowski, J-P. Lanquart, J. E. Mietus, R. B. Davis, Ary L. Goldberger, M. Costa, Translational Psychiatry **1(7)**, e27 (2011).

[11] Peter Debye, Annalen der Physik (Leipzig) **39(4)**, 789 (1912).

[12] *http//micro.stanford.edu.*

[13] A. N. Kolmogorov, Doklady of Russian Academy of Sciences **119**, 861 (1958).

[14] Ya. G. Sinai, Doklady of Russian Academy of Sciences **124**, 768 (1959).

[15] V. I. Oseledets, Trans. Moscow Math. Soc. **19**, 197 (1968).

[16] S. M. Pincus, Proc. Natl. Acad. Sci. **88**, 2297 (1991).

[17] S. M. Pincus, Chaos **5**, 110 (1995).

[18] S. M. Pincus, Proc. Natl. Acad. Sci. **89**, 4432 (1992).

[19] L, A. Fleisher, S. M, Pincus, and S. H, Rosenbaum, Anesthesiology **78**, 683 (1993).

[20] D, T. Kaplan, M. 1. Furman, S. M. Pincus, S. M. Ryan, L. A. Lipsitz, and A. L. Goldberger, Biophys. J. **59**, 945 (1991).

[21] S. M. Pincus, T. R. Cummins, and G. G. Haddad, Am. J. Physiol. Regulatory Integrative Comp Physiol **264**, R638 (1993).

[22] S. M. Pincus, I. M. Gladstone, and R. A. Ehrenkranz, J. Clin. Monit. **7**, 335 (1991).

[23] S, M. Pincus and R. R. Viscarello, Obstet. Gynecol. **79**, 249 (1992).

[24] M. L. Hartman, S. M. Pincus, M, L. Johnson, D, H. Matthews, L. M. Faunt, M. L. Vance, M. O. Thorner, and J. D. Veldhuis, J. Clin.Invest. **94**, 1277 (1994).

[25] JP Eckmann and D. Ruelle, Rev. Modern Phys. **57**, 617 (1985).

[26] A. Ben-Mizrachi, I. Procaccia, and P. Grassberger, Phys. Rev. A **29A**, 975 (1984).

[27] P. Grassberger, Phys. Lett A **128**, 369 (1988).

[28] P. Grassberger and I. Procaccia, Phys Rev A **28**, 2591 (1983).

[29] P. Grassberger, T. Schreiber and C. Schaffrath, Int J Bifur Chaos **1**, 547 (1991).

[30] J. S. Richmann, and J. R. Moorman, Am. J. Physiol. **278**, H2039 (2000).

[31] Yi-Cheng Zhang, J. Phys. I. **1**, 971 (1991).

[32] A. Sarkar, and P. Barat, Mod. Phys. Lett. B **20**, 1075 (2006).

[33] A. Sarkar, P. Barat, and P. Mukherjee, Fractals **18**, 319 (2010).

[34] J. E. Lennard-Jones, Proc. R. Soc. Lond. A **106**, 463 (1924).

[35] P. Barat, A. Giri, M. Bhattacharya, Nilangshu K. Das and A. Dutta, Europhysics Lett **104**, 50003 (2013).

[36] G. W. Ford and M. Kac, J. Stat. Phys. **46**, 803 (1987).

[37] A. O. Caldeira and A. J. Leggett,Phys. Rev. Lett. **46**, 211 (1981).

[38] A. O. Caldeira and A. J. Leggett, Ann. Phys. **149**, 374 (1983).

[39] *Every atom of crystalline solid Ar inside the simulation cell similarly can be thought as coupled with rest of the system particles through the Lennard-Jones potential. Here rest of the system acts the role of finite bath.*

[40] H. Hasegawa, Phys. Rev. E **83**, 021104 (2011).

Chapter 8

Summary and Prospects

In the previous chapters repeatedly it has been mentioned that equilibration process is inevitable in a system when it is in non-equilibrium state. On the other hand, practically, an equilibrium state can not retain its stable state until suitable experimental arrangement is there to make the system thermodynamically isolated from its surroundings. Thus, in nature most of the natural phenomena are on the way to achieve the equilibrium state but yet to reach it due to its interaction with surroundings. In this context the happenings of a equilibration process can not be observed with the help of experiment in atomistic scale both spatially and temporally. Even the analytical methods become rigorously complicated to solve the huge number(of the order of Avogadro number) of coupled differential equations. As per as atomistic scale of the physical phenomena is concerned the advent of modern techniques of computational methods have put up the research in the field of material science, solid state physics, nuclear physics, biophysics etc in more prolific and fertile stage. In the context of equilibration process, molecular dynamics simulation is the one of the most appropriate and economical computational method at the atomistic scales of length and time. The studies covered in this thesis make extensive use of the molecular dynamics simulations. As this method inherently provide the numerical data at the atomistic scale, they are extremely useful in unearthing the fundamental physics of equilibration. In addition to that, in future, the simulation outcome can provide newer insight of an existing theory and compel us to revisit our understanding of equilibration phenomena. In general, the atomistic simulations also cater to the need of obtaining some fundamental data, which are used as inputs to other forms of simulation. For example, the size effect is quantified with the help of one simulation and is incorporated in the other simulation for the proper quantification of a macroscopic physical quantity, thereby forming the basis of multi scale modeling.

All the studies included in this dissertation rely heavily upon the molecular dynamics simulation. The basic aim has been to demonstrate how these simulation tools are capable of discovering and explaining new fundamental physics of equilibration. For this purpose, a set of five different problems has been selected. A particular feature common to these four problems is the scale of the involved phenomena. In all these studies, the underlying physics associated with the explored issue is always at the atomistic scale, both temporally and spatially. Moreover, all of these five studies are typical examples of the cases where the experimental techniques and analytical methods are not appropriate or unavailable to capture and measure the essential physical parameters so that the atomistic simulation becomes the only tool, which can furnish an insight into the otherwise inaccessible aspects of these phenomena. The studies documented in the present thesis are as follows:

■ Atoms in the simulation cell, when brought to a non-equilibrium state by enhancing their kinetic energy, try to redistribute their excess kinetic energy by the process of diffusion. This process of redistribution of kinetic energy among the atoms changes their mean positions of vibration and consequently their potential energy. In the process of diffusion all the atoms in the cell participate together. The variation of the kinetic energy with time for each atom are random since it is associated to the diffusion process. The analysis of the time series of the kinetic energy with time for a single atom in the simulation cell provides an account for the modality of this diffusion process and the nature of the equilibration. Few queries, like, whether there exist any self similarity property in this random time series data and whether the time series data is associated with a universality class, are answered by scaling analysis of the time series data. The scaling property of the time series of kinetic energy of individual particles are studied using two complementary scaling analysis methods: Diffusion Entropy Analysis (DEA) and Finite Variance Scaling Method (FVSM). Application of these scaling analyses reveals that the fluctuations in the time series of kinetic energy follow similar kind of dynamics irrespective structures and non-equilibrium temperatures of the systems under study. Several crystal structures diamond cubic, face centered cubic and body centered cubic structure with suitable potential functions were used. The results of the scaling analyses conform that for all cases the time series of the kinetic energy of system particles exhibits an anomalous diffusion and it belongs to Levy walk process. In Levy walk a time series has a probability distribution function having a long tail. Most of the natural phenomena like food foraging in hungry animals, spreading of vector mediated disease in animals and human are examples of Levy walk with few but effective long hops. Thus the time series of kinetic energy of non-equilibrium system particles confirms the existence of a universality class.

■ Probability distribution function is the global representation of a system(in contrast to the previous paragraph where emphasis was on single atom). Evolution of the probability distribution function of kinetic energy of the constituent atoms of the equilibrating system is oscillatory and subsequently the oscillation dies down after a long time. Shannon entropy is a measure of uncertainty or unpredictability of information contained in a probability distribution. The time variation of global information of the equilibrating system are studied by calculating the Shannon entropy from their time evolution of probability distribution. For more random information the uncertainty in its prediction is higher and the corresponding value of Shannon entropy will be more. In case of tossing coin or rolling n-sided die outcomes lead to maximum Shannon entropy given that that the coin or the die is fair. For unfair coin or die predictability of the outcomes becomes easy and value of Shannon entropy drops down. For a two headed/tailed coin or for a die with all the sides identical the outcomes become completely predictable and the entropy goes to zero. For a physical equilibrium/non-equilibrium system the distribution of constituent particles among energy eigen states is not as simple as the outcomes of tossing coin or rolling die. Except the combinations among particles, occurrence of the energy eigen states follow some restriction in this case. Unlike the situation for fair coin or fair die where the all the outcomes are equally probable the equilibrium physical system does not generate a probability distribution with equal population in each energy eigen state. Thus the variation of Shannon entropy for completely unfair and partially unfair coin/die should be monotonically increasing and ultimately reaches a constant maximum value for fair coin/die. On the other hand due to adopted non-equilibrium nature of the system where the system kinetic energy and the system potential energy are not equal, in the initial phase of equilibration there will be transfer of kinetic energy into potential energy by changing the configuration of constituent atoms. Since this process is very fast the system cannot estimate exactly how much kinetic energy should be transferred into potential energy to make them equal. The inertia of the process transfers more kinetic energy and a reverse situation appears with potential energy more than the kinetic energy. This mechanism leads to an oscillatory transfer of energy during equilibration and the oscillation gradually dies down with time. Such variation of energy and restriction in the energy states do not allow the Shannon entropy to follow monotonic increasing behavior but is oscillatory and at equilibrium it becomes constant of time.

■ The force field in crystalline system is the sum of deterministic part due to nearer atoms and random part due to distant atoms. The affects of these two parts of the force are reflected on the probability distribution function. The random part of the force introduces a noise component to the system response. Hence in the study of equilibration mechanism from the time variation of probability distribution function it is desirable to eliminate the noise part. Use of principal component analysis helps to eliminate the noise part and reduces the histograms of probability distribution functions into 2-3 principal dimensions and it becomes easier to study the evolution of probability distribution function in terms of those two or three components. The component which has highest egien value is most important (more than 75% of total eigen value except for solid Argon where it is around 60%) and is used for the analysis. The existence of 2-3 major eigen values ensure that the probability distribution functions are highly correlated. A statistical method called system identification technique is used to analyze the evolution of most significant component. This method relates the system input and output by a rational function called transfer function. The analysis reveals that the dynamical process of equilibration takes place through two or three modes and the mode associated to lowest frequency which is very close to Debye frequency of the corresponding element. These modes are calculated from the denominator of the transfer function of the system obtained from the system identification.

■ Another important aspect of non-equilibrium system is simultaneous impact of deterministic and random force together on the process of equilibration. How the process of equilibration depends on the magnitude of the force has been studied by slightly changing the magnitude of the force. For this study two separate crystalline solid Argon systems driven by original 12-6 Lennard Jones potential ($V_{12-6} = 4\epsilon[(\sigma/r)^{12} - (\sigma/r)^{6}]$) and the variant of original one, the 9-6 Lennard Jones potential ($V_{9-6} = 4\epsilon[(\sigma/r)^{9} - (\sigma/r)^{6}]$) are taken. The nature of the non-equilibrium state is same as defined initially. It is seen that the force associated with 12-6 potential has the larger magnitude than that of 9-6 potential in the range between first nearest neighbor and forth nearest neighbor. The observed temperature profiles, leading to the equilibration for the two cases, indicate that the process of equilibration is significantly affected by the modified force field. This observation concludes that force in the region between first nearest neighbor and fourth nearest neighbor is mostly responsible for equilibration. The system identification of the temperature profiles of the two equilibrating systems show that the equilibration driven by a force having larger magnitude (12-6 potential) is faster and the sharing of kinetic energy and potential energy occurs more frequently than those of the system driven by a force having smaller magnitude (9-6 potential).

■ A system which consists of a large number of parts and the parts are connected to each other in a non-linear fashion is a complex system. A crystalline system is composed of large number atoms and the constituent atoms interact with each other through a non-linear potential. The presence of non-linear interaction makes the crystalline system complex. Besides the non-linear behavior of the interaction if the system temperature is increased the constituent atoms vibrate about their mean positions with larger amplitudes making the system much more complex. Crystalline solid Argon systems at different equilibrium temperatures (10K, 30K, 50K and 70K) are generated from non-equilibrium state and temperature dependence of complex nature of the crystalline solid Argon are studied by measuring complexity at different equilibrium temperatures. Complexity of a system is associated with meaningful structural richness that gives an idea of correlation between the multiple spatio-temporal scales. Traditional entropy measurement of a time series data only quantifies the regularity and predictability of the time series. Complexity cannot be defined in a straightforward way from the regularity of the time series data. This is because neither completely predictable (e.g., periodic) data, which have minimum entropy, nor completely unpredictable (e.g., uncorrelated random) data, which have maximum entropy, are truly complex and they can be described very compactly. The time variations of the kinetic energy of single atoms at each equilibrium temperature are considered for complexity measurement. Sample entropy for increasing scale factors (multiscale entropy) are calculated from the time series data of the kinetic energy of individual constituent atoms instead of traditional entropy calculation. It is observed that with the increment of system temperature the complexity of the system also increases. The scale variation of complexity is found to follow the same nature as that of synthetically generated time series data of Levy process and Langevin solution. This result confirms that the diffusion kinetic energy among the constituent atoms is a Levy process and the atoms in crystal follow Langevin dynamics.

So far, in most of the cases, people are interested in the study of various sort of physical properties of matter using atomistic simulations. This dissertation tells us not only about physics behind physical properties of matter but also the dynamics, kinetics and statistics of the constituents of the system can be explored successfully with the help atomistic simulation. In a nutshell, the present thesis discusses only the equilibration process of a particular non-equilibrium system generated using an innovative trick and efficacy of atomistic simulation in unraveling the hidden dynamics of such process. This is another fascinating and pompous dimension of physics and this discourse is the commencement of the proceeding to unwrap this particular field of science. Hopefully in coming future physicists around the globe will be passionate to work on such a beautiful branch of science to make it more and more affluent and opulent. Keeping in mind that computer merely understands and works in its own way to stirred out some raw data, it is the responsibility of our human society to assimilate those numbers and elicit comprehensive scientific interpretation of physical phenomena.